Generating Obligate Heterodimeric Transcription Activator-Like Effector Nucleases to Inactive Hepatitis B Viral Replication

Tiffany Shenay Smith

A dissertation submitted to the Faculty of Health Sciences, University of the Witwatersrand, in fulfilment of the requirements for the degree

of

Master of Science in Medicine

Johannesburg, 2018

Declaration

I, Tiffany Shenay Smith declare that this Dissertation is my own, unaided work. It is being submitted for the Degree of Master of Science in Medicine at the University of the Witwatersrand, Johannesburg. It has not been submitted before for any degree or examination at any other University.

....

Signature Date

Dedication

To my parents

Ernest and Faiza Smith.

Thank you for your unconditional love and support.

Conference presentations

1. 17th National Congress of South African Society of Medical Oncology (SASMO) and South African Society of Clinical and Radiation Oncology (SASCRO). 07th-09th August 2015.Cape Town International Convention Centre. [**Poster presentation**: Smith, T.S, Francies, F. Z, Herd, O, Cairns, A, Slabbert, J. P and Baeyens, A. The influence of age on chromosomal radiosensitivity of breast cancer patients.

2. 53rd National Congress of the South African Association of Physicists in Medicine and Biology (SAAPMB). 23rd-27th September 2015. University of the Free State, Bloemfontein. [**Oral poster presentation:** Smith, T.S, Francies, F. Z, Herd, O, Cairns, A, Slabbert, J. P and Baeyens, A. The influence of age on chromosomal radiosensitivity of South African breast cancer patients

3. African Centre for Gene Technologies (ACGT). 07th July 2017, Plant Sciences complex, University of Pretoria. [**Oral presentation**: Smith T.S, Singh P.S, Ely A and Arbuthnot P. Targeted inactivation of hepatitis B Viral Replication using Obligate Heterodimeric Transcription Activator-Like Effector Nucleases.]

4. Molecular Biosciences research Thrust (MBRT) Postgraduate Research Day. 30th November 2017, Wits club, West Campus University of the Witwatersrand. [**Poster presentation**: Smith T.S, Ely A, Maepa B and Arbuthnot P. Generating Obligate Heterodimeric Transcription Activator-Like Effector Nucleases to Inactive Hepatitis B Viral Replication.]

Abstract

The hepatitis B virus (HBV) remains a global health concern as chronic infection can lead to cirrhosis and hepatocellular carcinoma. Current therapies are only partially effective and do not target the HBV covalently closed circular DNA (cccDNA). cccDNA serves as a replication intermediate for the transcription of viral RNA, resulting in the persistence of infection. Several designer nucleases have therefore been developed to target cccDNA. Their mutagenic effect is mediated by causing double-strand breaks at target sites, consequently disrupting translation of viral proteins. Previous studies observed successful inhibition of HBV, with the use of homodimeric transcription activator-like effector nucleases (TALENs). TALENs are designed in pairs (left and right monomers) to cleave complementary strands of targeted DNA. They consist of a DNA-binding domain which is attached to the wildtype nuclease domain of *Fok*I. TALENs have exhibited considerable predictable interaction with their target sites and have shown diminished toxicity *in vitro* and *in vivo*. Despite this success, TALENs containing wildtype *Fok*I nuclease domains may be prone to off-target effects as two of the same domains (two left or two right) in close proximity on opposite strands of DNA can result in cleavage at unintended sites. To establish a more clinically applicable therapy, obligate heterodimeric TALENs targeted against the *core* (*C*) and *surface* (*S*) open reading frames (ORFs) of cccDNA were generated and referred to as C or S Variant TALENs. Variant TALENs contain mutant *Fok*I nuclease domains. This allows for cleavage only when two different domains (one left and one right) are in close proximity on opposite strands of DNA thus reducing off-target effects. Overall the variant TALENs demonstrated significant knockdown of the HBV replication marker, hepatitis B surface antigen (HBsAg). Additionally variant TALEN-mediated targeted disruption occurred in ≥5.7% of total HBV DNA *in vitro* and ≥13% of total HBV DNA *in vivo*. Finally variant TALEN-treated mice also demonstrated significant knockdown of pregenomic RNA and *surface* mRNA levels as well as markedly reduced circulating viral particle equivalents. Together these results show that obligate heterodimeric TALENs are capable of HBV knockdown and serve as an advanced gene editing tool against chronic HBV infection.

Acknowledgements

I would like to sincerely thank my supervisors, Prof. Patrick Arbuthnot, Prof. Abdullah Ely and Dr Betty Maepa for their endless support and assistance in all aspects of my research.

I would like to thank the following individuals for their much needed materials in the use of my research, Dr Kristie Bloom for supplying me with TALEN plasmids as well as Dr Wolfgang Prinz for providing me with celI enzyme.

I am immensely grateful for every member in the Antiviral Gene Therapy Research Unit (AGTRU) that is always ready to assist in any manner. A very big thank you goes to Ms Prashika Singh, who has motivated me throughout my research.

I am eternally grateful for the support system from my family. A Special mention goes out to my parents, Ernest and Faiza, my sister Asheline and my boyfriend Decclan Lawrence. Your prayers, guidance and support have been the biggest encouragement in every part of my academic journey.

Enormous gratitude goes towards all my funding bodies for their financial support: Witwatersrand Post Graduate Merit Award bursary, National Research Fund and the Poliomyelitis Research fund.

Most importantly, all glory goes to our Heavenly Father who has given me the knowledge, faith and endurance to accomplish my goals.

Proverbs 1:7 “To have knowledge, you must first have reverence for the Lord.”

Matthew 6:33 “But seek ye first the kingdom of God, and His righteousness; and all these things shall be added unto you”.

Table of contents

Declaration....ii

Dedication....iii

Conference presentations....iv

Abstract....v

Acknowledgements....vi

List of Tables....xiii

List of Abbreviations....xiv

Chapter 1....1

1. Introduction....1

1.1 Epidemiology of and infection by the hepatitis B virus....1

1.2 HBV structure and replication....3

1.2.1 cccDNA persistence....10

1.3 Current anti-HBV treatment....11

1.4 Designer nucleases....13

1.4.1 ZFNs and CRISPR/Cas9 structure....14

1.4.2 TALEN structure and design....15

1.5 Designer nucleases targeted against the HBV genome....18

1.5.1 ZFNs and CRISPR/Cas9 used to target HBV genome....18

1.5.2 TALENs targeted against the HBV genome....18

1.6 Heterodimeric TALEN design....19

1.7 Aim....23

Chapter 2....24

2. Materials and Methods....24

2.1 Plasmids....24

2.1.1 pCH-9/3091....24

2.1.2 pCI-neo eGFP....24

2.1.3 pCI-neo FLuc....24

2.1.4 pUC118....24

2.1.5 Anti-HBV TALEN plasmids....25

2.2 Generation of obligate heterodimeric TALEN plasmids....28

2.2.1 Preparation of TALE- and nuclease-encoding DNA fragments for ligation 30
2.2.2 Ligation of variant nuclease domain-encoding fragments into anti-HBV TALE backbones 30
2.2.3 Cloning of ligated products and subsequent positive clone selection 32
2.3 Bulk plasmid preparation 32
2.4 *In vitro* characterisation of heterodimeric TALENs 33
2.4.1 Culture conditions for liver and kidney derived cells 33
2.4.2 Immunofluorescence microscopy 34
2.4.3 HBsAg enzyme-linked immunosorbent assays (ELISA) 35
2.4.4 *In vitro* celI endonuclease assay 36
2.4.5 Cell viability assay 40
2.5 *In vivo* characterisation of heterodimeric TALENs 41
2.5.1 Hydrodynamic injection of NMRI mice with TALEN-expressing plasmids 41
2.5.2 Bioluminescence imaging 42
2.5.3 ELISA 42
2.5.4 Quantification of HBV VPEs 42
2.5.5 Assessing HBV gene expression 43
2.5.6 Assessment of *in vivo* targeted cleavage 44
2.5.7 Assessing liver toxicity 45
2.6 Data analysis 45
Chapter 3 46
3 Results 46
3.1 Successful generation of obligate heterodimeric TALEN vectors 46
3.2 Obligate heterodimeric TALENs are efficiently expressed in liver-derived cells 52
3.3 Obligate heterodimeric TALENs mediate efficient inhibition of HBsAg expression in Huh7 cells 54
3.4 *In vitro* TALEN-mediated targeted disruption 56
3.5 Assessing potential TALEN-mediated cellular toxicity 59
3.6 TALEN-mediated silencing of viral gene expression *in vivo* 61
3.6.1 Hydrodynamic injections of TALEN-expressing plasmids in NMRI mice 61
3.6.2 Bioluminescence imaging 62
3.6.3 Obligate heterodimeric TALENs mediate efficient inhibition of HBsAg expression *in vivo* 63
3.6.4 TALEN-mediated inhibition of HBV replication *in vivo* 65
3.6.5 *In vivo* TALEN-mediated repression of HBV *core* and *surface* transcripts 67
3.6.6 *In vivo* TALEN-mediated targeted disruption 69

3.6.7 *In vivo* liver toxicity analysis 71
Chapter 4 73
4. Discussion 73
4.1 Wildtype TALENs are prone to off-target effects 73
4.2 Successful generation of obligate heterodimeric TALENs 73
4.2.1 Obligate heterodimeric TALENs inhibit HBV replication 74
4.2.2 Obligate heterodimeric TALENs mediate targeted cleavage of HBV DNA 75
4.2.3 Obligate heterodimeric TALENs do not illicit cytotoxic effects 76
4.3 Obligate heterodimeric TALENs represents a safe and efficient tool for disabling HBV replication 77
4.4 Current challenges hindering successful HBV therapy 77
4.5 Conclusion 79
4.6 Future studies 79
Chapter 5 80
5. Appendix 80
5.1 Generation of anti-HBV obligate heterodimeric TALENs 80
5.1.1 Agarose gel electrophoresis protocol 80
5.1.2 pCMV TALEN (WT) and pAC AAVS1 plasmid maps 81
5.1.3 Gel electrophoresis images of TALE and nuclease generation 83
5.1.5 Gel extraction protocol 87
5.1.6 Ligation molar ratios 88
5.1.7 Preparation and transformation of $CaCl_2$competentbacterial cells 89
5.1.8 Small scale plasmid preparation 91
5.1.9 Large scale plasmid preparation 92
5.2 *In vitro* experiments 93
5.2.1 Mycoplasma detection 93
5.2.2 Transfection mixes 94
5.2.3 Immunocytochemistry 96
5.2.4 Immunofluorescence images from Huh7 cells 97
5.2.5 Immunofluorescence images from HepG2.2.15 cells 98
5.2.6 PCR carried out on samples from HepG2.2.15 cells 99
5.2.7 CelI assay carried out on PCR products from HepG2.2.15 cells 100
5.2.8 CelI targeted disruption calculation 101
5.2.9 Immunofluorescence images from HEK293 cells 102
5.3 *In vivo* experiments 103

5.3.1 Ethics certificate 103
5.3.2 Endotoxin-free large scale plasmid preparation 105
5.3.3 PCR carried out on samples from murine hepatocytes 106
5.3.4 CelI assay carried out on PCR products from murine hepatocytes 107
6. References 108

List of Figures

Figure 1.1: The HBV genome 6

Figure 1.2: The HBV replication cycle 9

Figure 1.3: TALE structure and RVD nucleotide base recognition 17

Figure 1.4: Obligate heterodimeric design improves TALEN specificity and reduces off-target cleavage 22

Figure 1.5: Obligate heterodimeric TALEN binding sites 23

Figure 2.1: Generation of obligate heterodimeric TALENs. 31

Figure 2.2: HepG2.2.15 transfections for the CelI assay 37

Figure 3.1.1: Verification of WT and Variant TALEN assembly 48

Figure 3.1.2: Verification of TALEN DNA bindng domain (DBD)-encoding sequences. 49

Figure 3.1.3: Verification of vectors carrying Variant nuclease domain sequences 51

Figure 3.2: Immunofluorescence detection of TALEN monomers in Huh7 cells 53

Figure 3.3: TALEN-mediated HBsAg knockdown in Huh7 cells 55

Figure 3.4.1:Gel electrophoresis after CelI treatment 57

Figure 3.4.2: TALEN-mediated site-directed targeted mutagenesis in HepG2.2.15 cells 58

Figure 3.5: Absence of TALEN-associated cellular toxicity 60

Figure 3.6.1: Timeline representing the experimental procedure of TALEN-treated mice 61

Figure 3.6.2: Bioluminescence imaging of NMRI mice 62

Figure 3.6.3: TALEN-mediated HBsAg knockdown in NMRI mice 64

Figure 3.6.4: TALEN-mediated viral replication inhibition.....66

Figure 3.6.5: *In vivo* TALEN-mediated knockdown of HBV mRNA 68

Figure 3.6.6: TALEN-mediated targeted disruption of HBV-encoding DNA in murine liver samples 70

Figure 3.6.7: Absence of hepatic toxicity in TALEN-treated NMRI mice 71

Figure 5.1: p CMV TALEN (WT) plasmid map.....81

Figure 5.2: pAC AAVS1 left and right TALEN Variant 82

Figure 5.3: One percent agarose gel electrophoresis of core and surface wildtype TALENs..83

Figure 5.4: One percent agarose gel electrophoresis of plasmids encoding heterodimeric *Fok*I nuclease 84

Figure 5.5: Heterodimeric left *Fok*I multiple sequence alignment.....85

Figure 5.6: Heterodimeric right *Fok*I multiple sequence alignment 86

Figure 5.7: GFP visualisation in transiently transfected Huh7 cells from the enzyme-linked immunosorbent assay 97

Figure 5.8: Transient co-transfections in HepG2.2.15 cells.....98

Figure 5.9: Agarose gel electrophoresis of PCR products obtained from treated HepG2.2.15 cells.....99

Figure 5.10: TALEN-induced site directed targeted mutagenesis in HepG2.2.15 cells 100

Figure 5.11: GFP efficiency in transiently transfected HEK293 cells from the cell viability assay 102

Figure 5.12: Agarose gel electrophoresis of PCR products obtained from NMRI treated mice 106

Figure 5.13:TALEN-induced site directed targeted mutagenesis in murine hepatocytes 107

List of Tables

Table 1: The interactions between the left and right monomers of *Fok*I 20

Table 2.1: The TALEN DBD and DNA base recognition sequences for core TALEs (from 2319-2370 bp relative to the HBV genome) 26

Table 2.2: The TALEN DBD and DNA base recognition sequences for surface TALEs (from 411-462 bp relative to the HBV genome) 27

Table 2.3: TALEN plasmids nomenclature 29

Table 2.4: Primer sequences used to amplify putative TALE binding and cleavage sites for *C* and *S* ORFs 39

Table 2.5: Primer sequences used to amplify the HBV *surface* gene 42

Table 2.6: Primer sequences used to amplify HBV and mGAPDH genes 44

Table 5.1: Ligation of *Fok*I insert: TALE backbone 88

Table 5.2: Lipofectamine® 3000 Transfection mix 95

List of Abbreviations

A1AT	-	Alpha-1 Antitrypsin
AAV	-	adeno-associated virus
ALT	-	alanine aminotransferase
bp	-	basepair
BCP	-	basic core promoter
BSA	-	bovine serum albumin
Cas9	-	CRISPR associated 9
cccDNA	-	covalently closed circular DNA
CL Variant TALEN	-	core left Variant TALEN
CL WT TALEN	-	core left wildtype TALEN
CM	-	conditioned medium
CMV	-	cytomegalovirus
CR Variant TALEN	-	core right Variant TALEN
CR WT TALEN	-	core right wildtype TALEN
CRISPR	-	clustered regularly interspaced short palindromic repeats
Cys2His2	-	cysteine2-histidine2
DAPI	-	4,6-diamidine-2-phenylindole chloride
DBD	-	DNA-binding domain
DMEM	-	Dulbecco’s Modified Eagle’s Medium
DMSO	-	dimethyl sulphoxide
DR1/DR2	-	direct repeats1/2
DSBs	-	double-strand breaks
eGFP	-	enhanced green fluorescent protein
ELISA	-	enzyme-linked immunosorbent assay
EnhI	-	enhancer I
EnhII	-	enhancer II
ER	-	endoplasmic reticulum
FBS	-	foetal bovine serum
FDA	-	Food and Drug Administration
FITC	-	fluorescein isothiocyanate

FLASH	-	fast ligation based automatable solid phase high-throughput
GRE	-	glucocorticoid-responsive element
gRNA	-	guide RNA
HA	-	haemagglutinin
HAART	-	highly active antiretroviral therapy
HBcAg	-	hepatitis B virus core antigen
HBeAg	-	hepatitis B virus e antigen
HBsAg	-	hepatitis B virus surface antigen
HBV	-	hepatitis B virus
HBx	-	hepatitis B virus X protein
HCC	-	hepatocellular carcinoma
HDI	-	hydrodynamic injection
HDR	-	homology directed repair
HEK293	-	human embryonic kidney 293
hESCs	-	human embryonic stem cells
HIV	-	human immunodeficiency virus
Huh7	-	human hepatoma 7
IE	-	immediate early
IFN-α	-	interferon-α
Indel	-	insertion/deletion
iPSCs	-	induced pluripotent stem cells
KanR	-	kanamycin resistance
m*GAPDH*	-	murine *glyceraldehydes-3-phosphate dehydrogenase*
MTT	-	3-(4,5-dimethylthiazol-2-yl)-2,5-diphenyltetrazolium bromide
mTTR	-	modified transthyretin
MWM	-	molecular weight marker
NAs	-	nucleoside/nucleotide analogues
NeoR	-	neomycin resistance
NGS	-	next-generation sequencing
NHEJ	-	non-homologous end joining
NLS	-	nuclear localisation signal
NMRI	-	Naval Medical Research Institute
nt	-	nucleotide

NTCP	-	sodium taurocholate co-transporting polypeptide
ORF	-	open reading frame
PAM	-	protospacer adjacent motif
PBS	-	phosphate buffered saline
PEI	-	polyethylenimine
PEPCK	-	phosphoenolpyruvate carboxykinase
PFA	-	paraformaldehyde
PF-rcDNA	-	protein-free rcDNA
pgRNA	-	pregenomic
PROGNOS	-	Predicted Report of Genome-wide Nuclease Off-target Sites
PSADT	-	plasmid safe ATP-dependent DNase treatment
qPCR	-	quantitative PCR
rcDNA	-	relaxed circular DNA
RNase H	-	ribonuclease H
RVDs	-	repeat variable diresidues
SL Variant TALEN	-	surface left Variant TALEN
SL WT TALEN	-	surface left wildtype TALEN
Smc	-	structural maintenance of chromosomes
SR Variant TALEN	-	surface right Variant TALEN
SR WT TALEN	-	surface right wildtype TALEN
T7E1	-	T7 endonuclease 1
TAE	-	Tris Acetate EDTA
TALEN	-	transcription activator-like effector nuclease
VPE	-	viral particle equivalent
ZFN	-	zinc finger nuclease

Chapter 1

1. Introduction

1.1 Epidemiology of and infection by the hepatitis B virus

The hepatitis B virus (HBV) belongs to the family *Hepadnaviridae* (Marion and Robinson, 1983). HBV infects hepatocytes which can either lead to acute or chronic infection. Infected hepatocytes continuously shed virus into the bloodstream, making HBV highly infectious [reviewed in (Seeger and Mason, 2000)]. One of the first vaccination programmes against HBV took place in Taiwan as early as 1984 (D-S et al., 1988). Chronic HBV infection remains a worldwide health concern despite universal vaccination that was implemented in 1991, covering many hyperendemic areas (Meireles et al., 2015).

To date HBV has been differentiated into 10 genotypes with A-H being well characterised and I-J being newly identified (Kramvis and Kew, 2007, Sunbul, 2014). Furthermore some genotypes are classified into sub-genotypes. The nucleotide difference between each genotype is approximately 8% whereas the nucleotide difference between sub-genotypes is between 4-8% (McMahon, 2009). Epidemiological studies have revealed that genotypes and sub-genotypes are geographically distributed (Kurbanov et al., 2010, Liaw et al., 2010, Croagh et al., 2015). The highest rates of infection occur in sub-Saharan Africa and Asia (Luo et al., 2012). Genotypes A and E are predominantly found in sub-Saharan and western Africa respectively whereas Genotype D is mainly found in northern Africa (Kramvis and Kew, 2007, Forbi et al., 2013). Genotypes B and C are found in Asia with genotype C being particularly widespread in South East Asia (Jutavijittum et al., 2008). It is important to distinguish between HBV genotypes as infection and disease progression differs significantly between them (Kiesslich et al., 2009).

Infection in young children and adults differ quite notably as children are often more immune compromised compared to adults. In children younger than 1 year, infection is generally asymptomatic and almost always progresses to chronicity while most unvaccinated adults are capable of clearing acute infection (Liang, 2009, Seeger and Mason, 2000). In most cases, acute infection has an incubation period of about 2-3 months (Kappus and Sterling, 2013). In adults this incubation period is generally followed by a transient preicteric phase of symptoms such as nausea, anorexia, body aches and fatigue (McMahon et al., 1985, Liang, 2009, Kappus and Sterling, 2013). The preicteric phase is followed by jaundice which is often

cleared in a few weeks and acute liver failure occurs in as few as 1% of infected individuals (Bernal et al., 2010).

The route of transmission differs between Asian and African populations due to the differences between the virus populations. Perinatal (vertical) transmission occurs mainly in Asia whereas horizontal transmission among young children occurs mainly in Africa (Mendy et al., 2010). In the case of vertical infections, mothers can transmit infection to their infant by percutaneous exposure during child birth. This demonstrates the highest rates of infectivity with a 90% chance of transmitting infection to the infant (Kelly, 2006, Yi et al., 2016).

Chronic HBV infection is the major contributor to liver damage (Suhail et al., 2014). Many infected individuals will develop cirrhosis and/or hepatocellular carcinoma (HCC). The survival rate of chronically infected individuals depends on the severity of the disease. Currently 2.5 million people are chronically infected in South Africa alone. Furthermore it has been globally estimated that 1 million chronically infected individuals die annually (Spearman and Sonderup, 2014, Meireles et al., 2015). The effects of chronicity have been shown to differ between different HBV genotypes as well as host characteristics such as gender, where males are more likely to develop chronic infection (Yang et al., 2009). Chronic HBV infection remains a global concern which requires novel therapeutics to eradicate infection and disease.

1.2 HBV structure and replication

HBV is an enveloped virus with a diameter of 42 nm. Viral particles exist as infectious (Dane) and non-infectious particles (Hruska et al., 1977). The Dane particle consists of viral surface antigens embedded within the lipid bilayer which surrounds an inner nucleocapsid. The nucleocapsid comprises the hepatitis B core antigen (HBcAg), the viral polymerase and the viral genome which is double-stranded relaxed circular DNA (rcDNA) (Dane et al., 1970). Non-infectious particles lack the nucleocapsid (Gavilanes et al., 1982).

The virus replicates through an RNA intermediate, known as pregenomic RNA (pgRNA), yielding rcDNA. rcDNA comprises a full length minus strand and an incomplete plus strand (Rieger and Nassal, 1996, Seeger and Mason, 2000) (Figure 1.1). In the nucleus the rcDNA is repaired to covalently closed circular DNA (cccDNA) which serves as a template for the transcription of viral genes and plays an important role in HBV replication (Beck and Nassal, 2007).

The HBV genome is approximately 3.2 kilobase pairs in size, and encodes four overlapping open reading frames (ORFs) known as the *surface* (*S*), *polymerase* (*P*), *precore/core* (*C*) and *X* ORFs [reviewed in (Seeger and Mason, 2000)] (Figure 1.1). The *S* ORF is divided into three sections based on structure and functionality, namely *Pre-S1*, *Pre-S*2 and *S*. *Pre-S1* codes for the large (L) HBV surface antigen (HBsAg) while *Pre*-S2 mRNA codes for the middle (M) and small (S) HBsAgs (Churin et al., 2015). All surface proteins share the same C terminal domain and also contain a glycosylation site in the S domain. Additional modifications includes an N-linked oligosaccharide at the M domain as well as a myristic acid at the L domain (Lepère-Douard et al., 2009, Dandri and Locarnini, 2012). The L domain is responsible for viral entry as it is involved in attachment to hepatocytes. In the non-infectious virus there is very little to no L and M protein present but significantly more L protein is present in the Dane particles (Lamontagne et al., 2016).

The *C* gene contains the *precore* as well as *core* regions (Jean-Jean et al., 1989). The *S* and *C* genes are similar in that they both comprise codons from which multiple in-frame translation takes place (Liang, 2009). This results in the production of structurally related but functionally different proteins. The *C* ORF encodes both the HBV e antigen (HBeAg) and the HBcAg. Transcription of the *C* ORF yields pgRNA as well as the *precore* RNA which is longer than the pgRNA at its 5'-end. Translation of the pgRNA from the core start site yields the HBcAg while translation of the *precore* RNA from the precore start site yields precore protein (Datta et al., 2012). The precore protein will ultimately be processed to HBeAg.

The function of the HBe protein is not well defined but it has been suggested to play a role in immune tolerance because it maintains persistent infection (Alexopoulou and Karayiannis, 2014). The HBcAg is 185 amino acids in length. The first 149 amino acids are resilient to proteolytic cleavage and can therefore remain stable upon infection resulting in nucleocapsid assembly (Gallina et al., 1989, Hatton et al., 1992). The viral genome is surrounded by 240 copies of the HBcAg which forms the viral capsid (Yu et al., 2013). Each HBcAg consists of four arginine-rich clusters at its C terminus, which contains nucleotide binding motifs capable of RNA binding (Hatton et al., 1992).

The *P* ORF encodes viral polymerase which is the largest HBV protein, approximately 800 amino acids in length (Bavand et al., 1989). Translation of the viral polymerase takes place from the second start codon of the pgRNA. The viral polymerase is composed of three domains, a terminal protein domain, a polymerase/reverse transcriptase domain and a ribonuclease H (RNase H) domain (Nassal, 2008, Hamadalnil and Bakheit, 2017). The terminal protein domain is involved with encapsidation as well as priming of the minus strand synthesis of the virus (Clark and Hu, 2015). The polymerase/reverse transcriptase domain acts as both an RNA-dependent DNA polymerase to make the minus strand from the pgRNA and a DNA-dependent DNA polymerase to initiate plus strand synthesis from the minus strand. The RNase H domain degrades the pgRNA once it has been reverse transcribed to the minus strand thereby allowing plus strand synthesis to begin.

The *X* ORF encodes the hepatitis B virus X protein (HBx), which is important for HBV infection *in vivo* and is associated with hepatocarcinogenesis (Doria et al., 1995). Translation of HBx takes place from the *HBx* mRNA. Recently, HBx was found to target structural maintenance of chromosomes (Smc) complex Smc5/6 for ubiquitin-mediated degradation. Smc5/6 is a restrictive factor capable of suppressing the expression from episomal HBV DNA (Decorsière et al., 2016).

The HBV genome also contains several functionally important *cis*-acting elements. These include three direct repeats, namely DR1, DR2 and DR1*, which play an important role in plus strand DNA synthesis (Habig and Loeb, 2006). Other elements such as enhancer elements, namely enhancer I (EnhI), located upstream of the *X* promoter, and enhancer II (EnhII), located upstream of the basic core promoter (BCP), are responsible for liver specific viral gene expression (Doitsh and Shaul, 2004).

EnhI has been shown to play an extremely important role in HBV transcription. In the absence of EnhI in HBV transgenic mice, viral gene expression is low which results in inadequate virion production (Guidotti et al., 1995). EnhII, in addition to regulating its own transcription, has been shown to regulate the transcription of the Pre-S1 and Pre-S2 promoters (Yuh and Ting, 1990). The need for two enhancer elements suggests that HBV gene expression is regulated temporally (Doitsh and Shaul, 2004). EnhI is activated relatively early upon infection, followed by EnhII activation associated with simultaneous EnhI silencing (Doitsh and Shaul, 2004). Temporal gene expression is a characteristic of DNA viruses. In the case of HBV these elements control the expression of different HBV genes with respect to the viral replication cycle which expresses early and late genes (Doitsh and Shaul, 2004). Several other elements such as glucocorticoid-responsive element (GRE) located within the *S* ORF, polyadenylation signal within the *C* ORF and a post-transcriptional regulatory element overlapping EnhI and the *HBx* ORF have all been shown to play important roles in HBV gene expression (Tur-Kaspa et al., 1988).

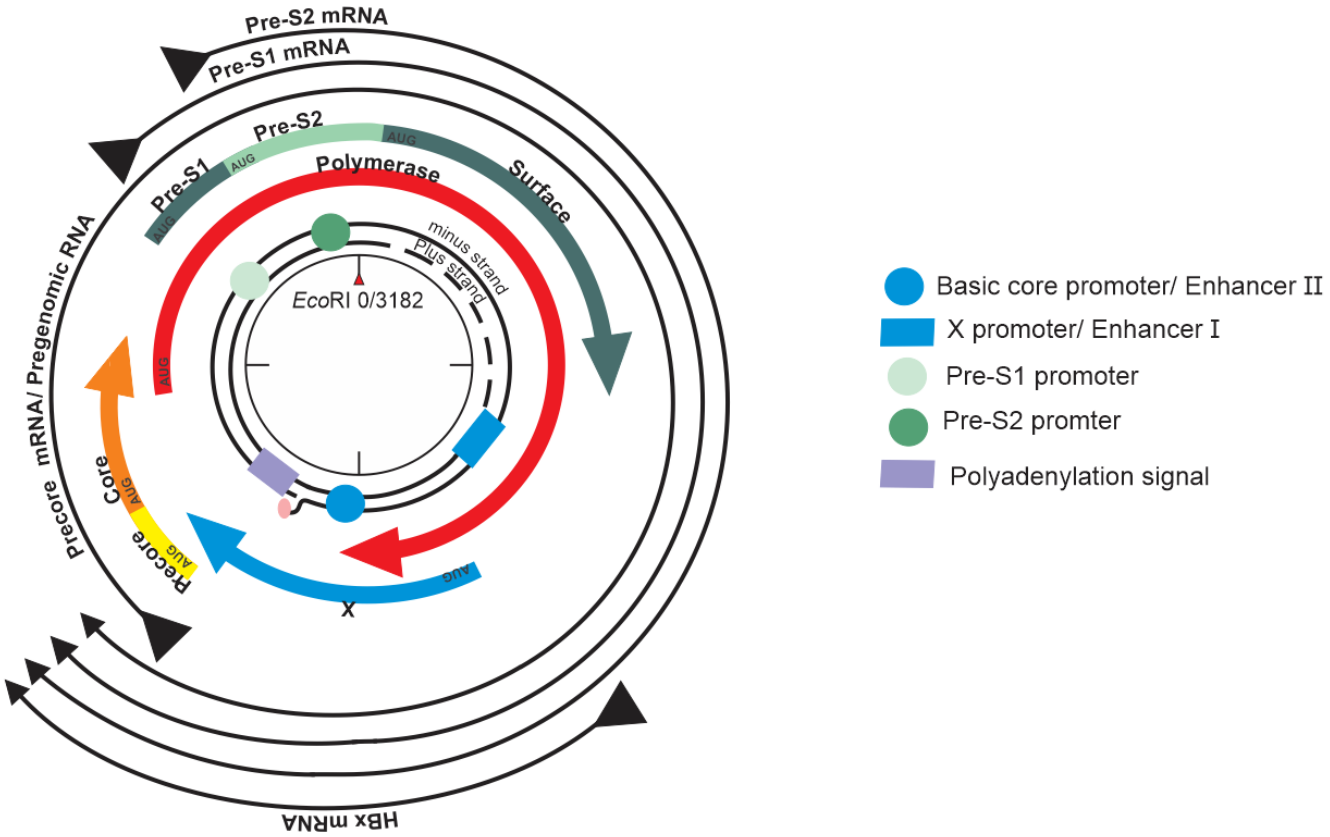

Figure 1.1: The HBV genome.

The rcDNA is shown at the centre of the genome which has a partially double-stranded plus and minus strand. The genome is approximately 3.2 kb in length comprising four overlapping open reading frames depicted by *Surface* (*S*), *Polymerase* (P), *Precore/Core* (*C*) and *X*. The Enhancer I and II elements are located directly upstream of the *X* promoter and basic core promoter respectively. A polyadenylation signal is on the plus strand within the *core* ORF. Nucleotide co-ordinates are read in the order from the unique *Eco*RI site within the genome [Adapted from (Seeger and Mason, 2015)].

HBV replication is initiated upon infecting hepatocytes. HBV surface proteins play an important role in cell entry (Figure 1.2). Glycosaminoglycan-mediated clustering of viral particles results on the surface of hepatocytes (Ely et al., 2016). This is important for entry as the virions enter the cell through the interaction of the myristoylated L HBsAg with the sodium taurocholate co-transporting polypeptide (NTCP). This interaction was only discovered recently (Yan et al., 2012).

Host factors may play a role in viral attachment and uptake of virions into cells (Glebe and Urban, 2007, Rehman et al., 2015). The binding of the virus to the receptor becomes irreversible (Dandri and Petersen, 2016). Internalisation mechanisms have been partly described for several genotypes (Schmitz et al., 2010). Briefly, once the virus enters the cell, the nucleocapsid (rcDNA surrounded by the capsid) is released into the cytoplasm. The nucleocapsid accumulates at the nuclear membrane of the cell where it can interact with the nuclear pore complex. The nucleocapsid is subsequently released into the nucleus, where it disassembles (Kann et al., 2007).

Upon disassembly of the nucleocapsid repair of the rcDNA is initiated. The viral polymerase is covalently attached to the 5' end of the minus strand and needs to be removed before repair can be completed. Removal of the polymerase is mediated by host machinery and plus strand synthesis is completed thus forming cccDNA (Beck and Nassal, 2007). cccDNA becomes associated with histone and non-histone proteins where it resides in the cell as a minichromosome (Newbold et al., 1995). HBV viral transcripts are unspliced and polyadenylated from a single common polyadenylation signal and capped at the 5' end (Schreiner and Nassal, 2017).

Virion assembly is initiated when the viral polymerase interacts with a *cis*-acting element, epsilon (Ɛ), on the 5' end of the pgRNA to initiate encapsidation (Hu and Boyer, 2006). Reverse transcription is initiated through protein priming whereby the first nucleotide is covalently attached to a tyrosine residue within the terminal protein domain of the viral polymerase. Initially a 3-4 nucleotide (nt) sequence is reverse transcribed which will serve as a primer for minus strand synthesis. The pgRNA contains 3 direct repeats DR1, DR2 and DR1*. At its 5' end it has DR1 and at its 3' end it has DR2 and DR1*. The viral polymerase translocates to the 3'-end of the pgRNA where the 3-4 nt primer binds to DR1*. Reverse transcription of the pgRNA proceeds to produce the minus strand of the viral genome.

Only part of DR1* is reverse transcribed so the minus strand will have DR1 at its 3' end and DR2 and the partial DR1* at its 5' end. The RNase H activity of the viral polymerase will degrade most of the pgRNA only leaving behind a small RNA sequence that will serve as the primer for plus strand synthesis. The RNA primer covers DR1 and as a consequence is also complementary to DR2 at the 5'-end of the pgRNA allowing it to be moved to DR2. This is referred to as primer translocation (Habig and Loeb, 2006, Wang et al., 2014). Plus strand synthesis can then begin and will extend from DR2 to the partial DR1*. At this point the plus strand switches from using the partial DR1* as template to using DR1. The minus strand has to circularise to bring its 3'-end close to its 5'-end and allow template switching to occur. Synthesis continues to form the incomplete plus strand. This results in newly synthesised rcDNA.

Surface protein synthesis takes place on the surface of the endoplasmic reticulum (ER) and once the surface proteins are translated they will embed themselves in the ER membrane. The nucleocapsid buds into the ER and gains a lipid bilayer with the already embedded surface proteins thus forming the mature virion which is secreted into the extracellular milieu. Alternatively the mature nucleocapsid can be recycled to the nucleus to produce cccDNA (Mhamdi et al., 2007).

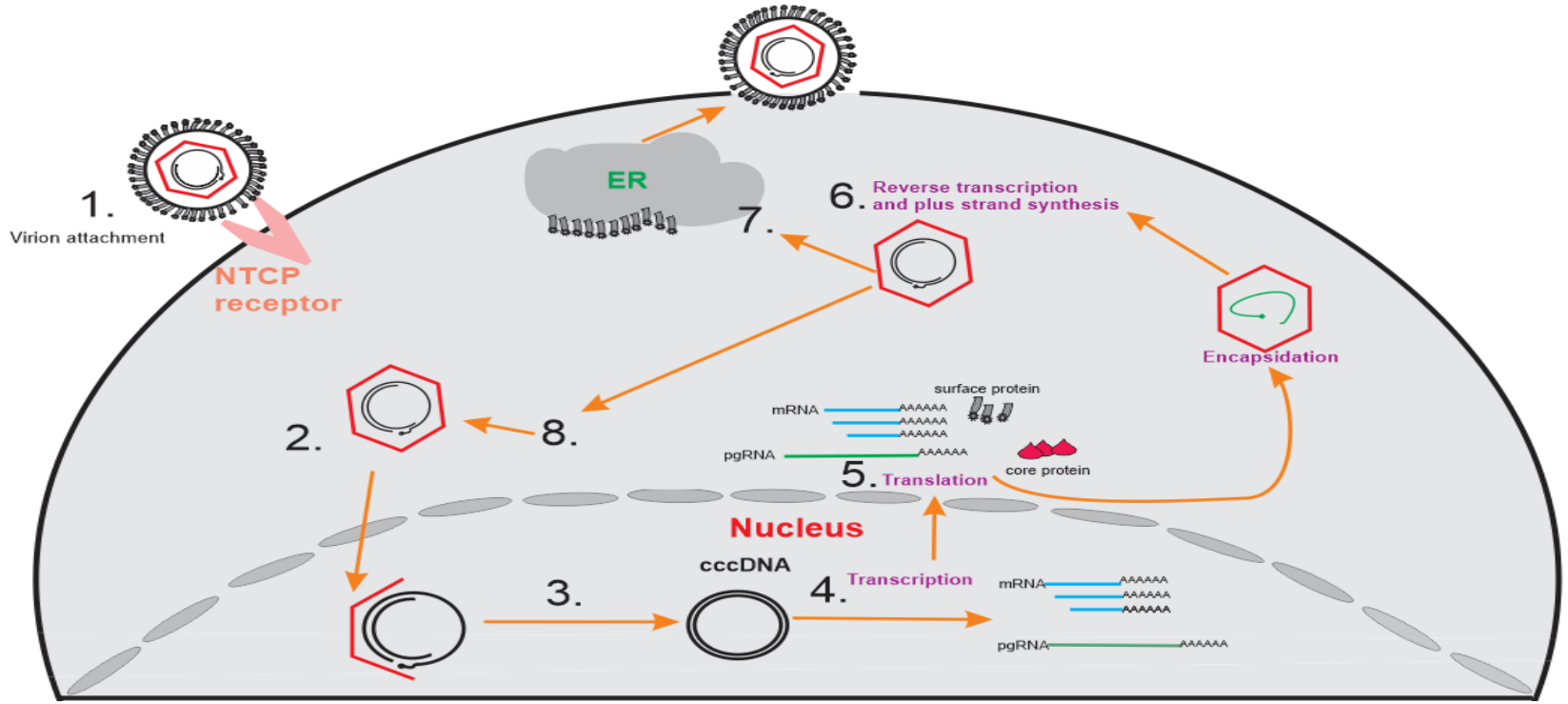

Figure 1.2: The HBV replication cycle.

1.) The virion attaches to the cell surface through glycosaminoglycan-mediated clustering of viral particles on the surface of hepatocytes whereby surface proteins recognise and binds to the NTCP receptor. **2.)** Once in the cell the nucleocapsid enters the nucleus where disassembly occurs to release the rcDNA genome. **3.)** The capsid disassembles and the viral genome is repaired to cccDNA. **4.)** cccDNA serves as a template for the transcription of viral RNAs. **5.**) The viral RNAs are then translated into proteins in the cytoplasm. Once translated, the viral polymerase binds to the pgRNA, initiating encapsidation to yield the nucleocapsid. **6.**) The pgRNA will then be reverse transcribed. Reverse transcription leads to minus strand synthesis followed by plus strand synthesis leading to rcDNA**. 7.)** This newly synthesised capsid can either obtain viral envelope proteins in the endoplasmic reticulum after which it exits the cell ready to infect another cell or **8.)** re-enter the nucleus to produce more cccDNA [Adapted from (Liu et al., 2013)].

1.2.1 cccDNA persistence

The exact mechanism of partially double-stranded circular DNA conversion to cccDNA is still unclear (Cai et al., 2012). Briefly, cccDNA formation requires the removal of covalently attached viral polymerase from the 5' end of the minus strand. This results in a protein-free rcDNA (PF-rcDNA) intermediate, capable of persisting in infected cells [reviewed in (Seeger and Mason, 2000)]. cccDNA formation also requires the removal of the RNA primer at the 5' end of the plus strand. Finally the repair of the plus strand by cellular replicative machinery followed by the subsequent ligation of the DNA results in cccDNA (Levrero et al., 2009).

cccDNA rarely integrates into the host genome and therefore exists as an episomal minichromosome in the nucleus, however in the event of such integration, HBV DNA sequences are generally truncated (Ozkal-Baydin, 2014). Because cccDNA exists as a minichromosome it becomes undetectable to host immune responses (Allweiss and Dandri, 2017). Furthermore, cccDNA is continuously formed, either from incoming virions or newly synthesised nucleocapsid upon cell entry [reviewed in (Chang et al., 2014)] (Figure 1.2). Once cccDNA is established in the nucleus it is regulated by two enhancer elements, EnhI and EnhII as well as four promoters, namely the basic core promoter (BCP) and pre-S1, pre-S2 and X promoters (Levrero et al., 2009). These rely on the co-operation of transcription factors as well as signalling factors such as co-activators and co-repressors.

cccDNA is robust and owes its minimal sequence plasticity to the four overlapping ORFs of the HBV genome. Partially double-stranded circular DNA to cccDNA conversion has been detected *in vitro* within 48 hours of infection and each infected hepatocyte has been found to contain 1-50 copies of cccDNA (Zhang et al., 2003, Guo et al., 2016). Chronic infection is a result of persistence of the cccDNA. In addition, cccDNA remains relatively stable in quiescent hepatocytes. The exceptionally resilient and replicative properties of cccDNA have made it exceedingly difficult to eradicate. Therefore the need for a curative therapy that disables cccDNA is highly sought after.

1.3 Current anti-HBV treatment

Currently vaccination against HBV is the leading strategy to prevent infection. The active ingredient in the hepatitis b vaccine is the HBsAg. Anti-HBs antibodies are used as a replicative marker of HBV and therefore determine immunity against the virus. The first vaccinations contained HBsAg purified from the plasma of chronically infected patients, however these vaccinations have been replaced by recombinant vaccines which became available in the early 1980s to increase the safety and immunogenicity of the vaccine (Szmuness et al., 1980, Thomssen et al., 1982). Importantly antibody response occurs in >90% of the population and in addition, stimulates a long-term immune response (Liao et al., 1999). Protection against HBV is defined as an anti-HBs titre >10 IU/L whereas individuals with titres <10 IU/L are defined as "non-responders" (Wiedmann et al., 2000). Factors such as age, obesity, type I diabetes or smoking can result in non-responsiveness (Andy et al., 2006). Despite these regimes, vaccination remains ineffective against already established infection.

There are currently two main therapeutic strategies that have been approved by the U.S Food and Drug Administration (FDA) for treating chronic HBV infection (De Clercq et al., 2010). The first strategy consists of nucleoside/nucleotide analogues (NAs) where the nucleoside compounds are lamivudine, entecavir and telbivudine and the nucleotide compounds are adefovir dipivoxil and Tenofovir disoproxil (Fung et al., 2011). The second strategy consists of immune-based therapy such as interferon-α (IFN-α) [reviewed in (Jordheim et al., 2013)].

The NAs function primarily by inhibiting HBV DNA polymerase activity thus suppressing replication (Karayiannis, 2012). Oral NAs have become the favoured option of treatment against chronic infection for two reasons. Firstly they have been found to efficiently suppress replication and secondly, the oral method of administration makes it easier for compliance (Fung et al., 2011). The human immunodeficiency virus (HIV) is known to be highly mutagenic and exceedingly susceptible to drug resistance. Combinatorial therapy such as highly active antiretroviral therapy (HAART) has therefore become well established against HIV. The rationale behind combinatorial therapy was consequently adopted for combating HBV infection by combining different NA treatments. However in the case of chronic HBV, combinatorial therapy is yet to show any additional benefits against viral replication (Fung et al., 2011).

IFN-α functions as an anti-proliferative and antiviral immunoregulator (Maher et al., 2008) and can have its half-life extended with PEGylation (PEG-IFN-α) (Dozier and Distefano, 2015). IFN-α binds to specific receptors on the cell surface which results in a signalling cascade that regulates the transcription of genes that are involved in viral replication inhibition [reviewed in (Platanias, 2005)]. PEG-IFN-α treatment has been shown to decrease HBsAg with minimal drug resistance however treatment is very inefficient as only 30% of patients respond.

New drugs have been developed to target viral components such as MCC-478 which is a derivative of adefovir. MCC-478 functions by inhibiting protein priming. As mentioned before, the viral polymerase must bind to ε to initiate protein priming and signal encapsidation of pgRNA. The inhibition of protein priming therefore prevents the encapsidation of pgRNA thus reducing viral replication. This drug seems promising against lamivudine resistant mutants [reviewed in (Kang et al., 2015)].

As the entry receptor for HBV, the NTCP has become a promising therapeutic target. Myrcludex-B is a synthetic lipopetide, derived from the pre-S1 domain (Volz et al., 2013). The pre-S1 domain has been shown to be important for cell entry as it interacts with NTCP to enter the cell. Myrcludex-B has shown specific binding to NTCP, inhibiting its function and furthermore it has shown a reduction in HBV binding and intrahepatic viral entry (Nakabori et al., 2016).

Although there has been some success in viral synthesis inhibition with the use of these antiviral treatments, viral elimination was not established and current drugs have little or no effect on HBV cccDNA (Werle–Lapostolle et al., 2004). Therefore a new approach against cccDNA is needed.

1.4 Designer nucleases

While available treatment options for chronic HBV sufferers are aimed at curing infection and alleviating disease progression, they have no effect on established cccDNA pools (Revill and Locarnini, 2016). This has led researchers to the use of a class of genome editing tools referred to as designer nucleases. Research on genetic engineering began over half a century ago when it was discovered that bacteria and yeast were capable of using homologous recombination to replace DNA sequences within their genomes (Weeks et al., 2016). Since then scientists have been driven to study and develop novel gene editing tools. These tools have gained popularity as they can be designed to target any known sequence.

In recent years designer nucleases have taken precedence in the field of gene therapy. The ability to design a custom-made gene editing tool targeted to any known sequence has made the use of designer nucleases exceptionally attractive. Various designer nucleases have been used for studying complex diseases as well as inducing mutagenic effects to cure or alleviate the burden of disease (Amer, 2014). Some of the first successful uses of designer nucleases have been observed in human embryonic stem cells (hESCs), induced pluripotent stem cells (iPSCs) as well as in model organisms such as zebrafish, rats and plants (Hockemeyer et al., 2009, Merkert and Martin, 2016).

Designer nucleases have been developed to mutate cccDNA (Bloom et al., 2013, Weber et al., 2014, Kennedy et al., 2015). In general, their mutagenic effect is mediated by causing double strand breaks (DSBs) at target sites (Lee et al., 2016b). Nucleases are designed to cause DSBs and this stimulates error-prone repair mechanisms at target sites. The two main pathways used to repair DSBs in eukaryotes are the homology directed repair (HDR) and the non-homologous end joining (NHEJ) repair pathways [reviewed in (Lieber, 2010)].

DSBs are in fact a normal occurrence in eukaryotic cells. Once a DSB is detected, the cell will depend on NHEJ for repair. NHEJ occurs faster and more frequently than HDR (Mao et al., 2008). The rate-limiting step in HDR is that it requires undamaged homologous DNA as a template for repair (Zaboikin et al., 2017). In the case of HBV, the NHEJ repair mechanism is favoured because it is more efficient at knocking out cccDNA. Following induction of DSBs by nucleases, the NHEJ repair mechanism restores the DNA sequence. However after repeated target cleavage, NHEJ repair leads to insertion and deletion mutations (indels) which disables cccDNA, consequently disrupting viral gene expression. The most widely used nucleases used to target the HBV ORFs have been zinc finger nucleases (ZFNs), transcription activator-like effector nucleases (TALENs) and RNA-guided nucleases [i.e. the clustered

regularly interspaced short palindromic repeats (CRISPR)/CRISPR-associated 9 (Cas9) or the CRISPR/Cas9 system] (Cradick et al., 2010, Bloom et al., 2013, Lin et al., 2014).

1.4.1 ZFNs and CRISPR/Cas9 structure

ZFNs were among the first gene editing tools developed and later tested in animal models (Kim et al., 1996, Provasi et al., 2012). Naturally, zinc fingers are DNA-binding proteins that play an important role in gene regulation, in particular, regulating transcriptional activation. Initially discovered in the early 1980s, zinc fingers showed a novel principle of DNA recognition (Miller et al., 1985). Other DNA binding proteins relied on the two-fold symmetry of the double helix DNA structure for DNA recognition, whereas zinc fingers are linearly linked for DNA recognition [reviewed in (Klug, 2010)]. One of the first applications in studying zinc fingers showed that the fusion of zinc finger peptides to bind DNA can selectively repress or activate domains thus regulating gene expression (Miller et al., 1985).

Zinc fingers are best characterised by the Cysteine2-histidine2 (Cys2-His2) fold, which has the following sequence, X_2-Cys-$X_{2,4}$-Cys-X_{12}-His-$X_{3,4,5}$-His, where X represents any amino acid and the distance between the cysteine and histidine residues are variable (Miller et al., 1985). Each zinc finger consists of a short antiparallel β-sheet containing two cysteine residues and an α-helix containing two histidine residues that is held together by a zinc ion, hence the name zinc finger. In the event of DNA recognition, three fingers wrap around the DNA, whereby the α-helices interact with three nucleotides within the major groove of DNA (Elrod-Erickson et al., 1996). Engineered zinc finger proteins are typically made up of three zinc fingers and consequently bind to 9 basepair (bp) DNA sequences. By attaching a zinc finger DNA-binding domain to the nuclease domain of *Fok*I, an artificial nuclease capable of binding and cleaving targeted DNA is created.

Unlike ZFNs where protein domains recognise target DNA, the CRISPR/Cas9 system uses both RNA and protein to target DNA. The CRISPR/Cas9 system was the most recent tool to have been added to the repertoire of gene editing technologies. The CRISPR/Cas system was first discovered in Archaea, and later shown to also exist in Eubacteria (Jinek et al., 2012). The CRISPR/Cas system exhibited an intelligent immune response against invading bacteriophages (Barrangou et al., 2007, Jinek et al., 2012). Upon infection, the bacteriophage DNA is processed. This DNA is incorporated into the archaeal or bacterial genome at a region termed as the CRISPR locus. This equips the bacterium with an acquired immune response against future bacteriophage invasion.

In the natural system, transcripts from the CRISPR locus are processed into CRISPR RNAs (crRNAs) and transactivating CRISPR RNA (tracrRNAs) responsible for guiding the CRISPR associated (Cas) nuclease to complementary DNA sequence for cleavage (Wu et al., 2014). Cas proteins have been differentiated into two classes subdivided into 6 types based on differences in cleavage efficiency [reviewed in (Mohanraju et al., 2016)]. For the purpose of gene editing the crRNAs and tracrRNAs were fused to produce small guide RNAs (sgRNAs) (Jinek et al., 2012). The sgRNAs complex with a class II, type II Cas nuclease 9 from *Streptococcus pyogenes* referred to as Cas9 which gives rise to the complete CRISPR/Cas9 system (Shmakov et al., 2015). In the event of target sequence recognition, a protospacer adjacent motif (PAM) sequence upstream from the target sequence will direct Cas9 cleavage to result in desired mutagenic effects (Sander and Joung, 2014).

1.4.2 TALEN structure and design

Transcription activator like effectors (TALEs) were first discovered in the *Xanthomona*s genus of bacteria [reviewed in (Boch and Bonas, 2010)]. These bacteria infect crop plants which have devastating effects on agriculture and so motivated the study of TALEs. The molecular mechanisms of these bacteria revealed that effector proteins were secreted into the cells of host organisms (Nemudryi et al., 2014). Upon further investigation it was found that effector proteins bind to DNA and act as transcription factors, hence the name "transcription activator-like effector".

TALE proteins comprise three domains namely a central domain necessary for DNA binding, a gene transcription activation domain, and a nuclear localisation signal (Moore et al., 2014). The DNA binding properties of TALEs presented a potentially useful tool to engineer artificial nucleases. However propagating TALE sequences presented a challenge in terms of cloning repeat arrays (Gaj et al., 2013). This hampered the use of TALENs for a long time, but several methods have now been developed to rapidly assemble custom TALE arrays. These techniques include restriction enzyme and ligation methods (Morbitzer et al., 2011), the Golden Gate method (Cermak et al., 2011) and the fast ligation based automatable solid phase high-throughput (FLASH) method (Reyon et al., 2012).

Naturally occurring TALEs contain as few as 1.5 to 33.5 tandem repeats (Moscou and Bogdanove, 2009). For the purpose of gene editing TALEs are normally composed of 17.5 or 18.5 tandem repeats comprising 34 highly conserved amino acids (Deng et al., 2014) (Figure 1.3). The C-terminal repeat that binds to a nucleotide at its 3'-end only consists of 20 amino acids and this is referred to as a half-repeat (Zhang et al., 2014).

Positions 12 and 13 are referred to as the repeat variable diresidues (RVDs) which are responsible for single nucleotide recognition (Jankele and Svoboda, 2014).

Researchers deciphered the RVD code necessary to engineer specific DNA binding arrays, which was an important advance for TALEN design (Boch et al., 2009). Amino acids NG, NN, HD and NI bind to nucleotides T, G, C and A respectively. However some degeneracy occurs in the code as NN may also bind A. Researchers then explored increasing code specificity and it was observed that replacing NN with NH or NK increases specific binding to G (Cong et al., 2012). With the TALE code deciphered, custom-designed TALEs were attached to a nuclease domain for site-specific cleavage. To test this theory, the DNA binding domain of the TALE was placed into a vector that was previously used for producing ZFNs (Christian et al., 2010). This generated TALEs which contained the *Fok*I nuclease domain, giving rise to TALENs.

The *Fok*I endonuclease is only functional as a dimer and as a consequence TALENs are designed as two monomers that come together on target DNA to create a DSB. TALE DNA-binding domains bind one strand of the DNA helix necessitating a design where each TALEN monomer binds to opposite strands of DNA in a manner that leaves a 12-25 bp spacer region (Yan et al., 2013). Upon binding target DNA the *Fok*I nuclease domains of each monomer dimerise, cleaving the DNA backbone resulting in DSBs. One limitation of engineering TALEs is that the target sequence should start with a thymine base for optimal TALE interaction with DNA (Rogers et al., 2015). This limitation can however be overcome by designing TALENs with different spacer sequence lengths to ensure that the target sequence starts with a thymine (Booher and Bogdanove, 2014).

TALENs are more specific than ZFNs because single nucleotide recognition occurs as opposed to triple nucleotide recognition. This also makes TALENs more “flexible” to engineer against target sites. Importantly ZFs do not function independently of each other as the α-helix of one finger influences the orientation of the α-helix side chains in an adjacent finger. This complicates ZFN design, whereas TALENs do not have the problem of influencing neighbouring monomers. Studies have shown that nucleases result in successful inactivation of HBV replication, however each nuclease differs in specificity and efficacy (Bloom et al., 2013, Weber et al., 2014, Kennedy et al., 2015).

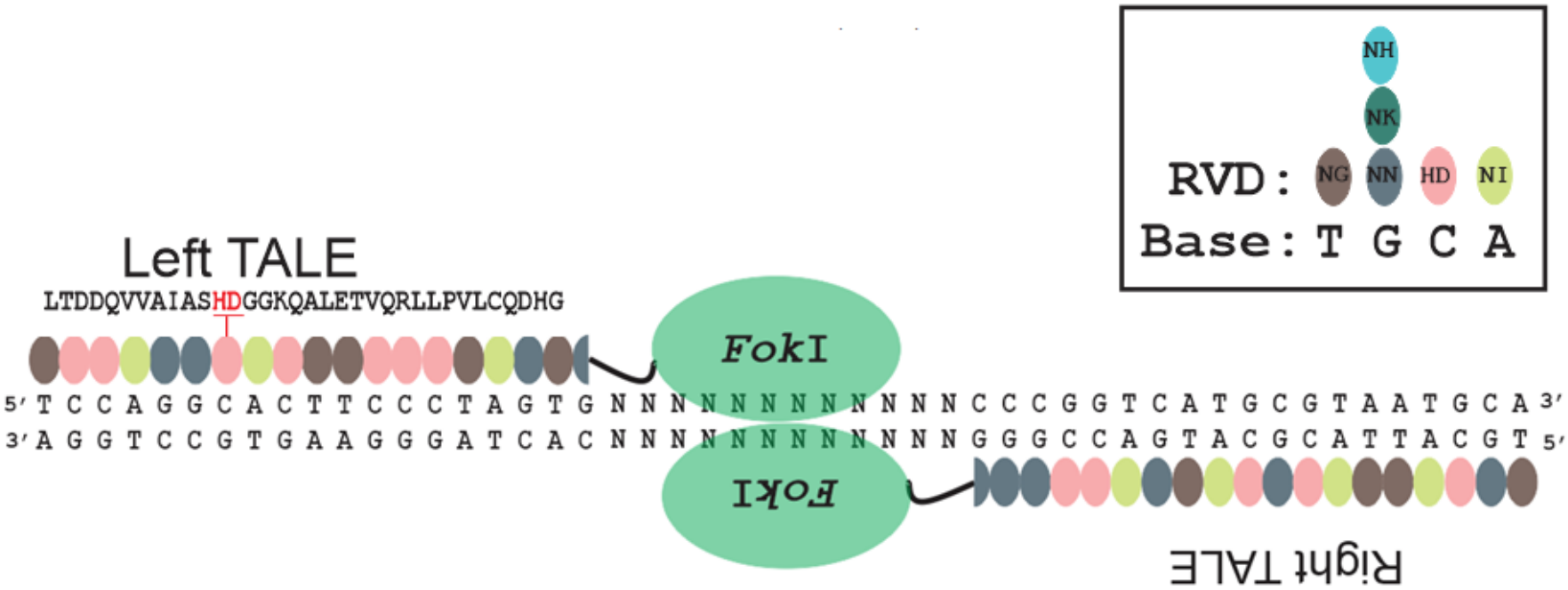

Figure 1.3: TALE structure and RVD nucleotide base recognition.

TALEs are usually comprised of 17.5 or 18.5 tandem repeats that bind to target DNA through its RVDs. The degenerate RVD code appears in the top right corner. One repeat consists of 34 amino acids with positions 12 and 13 being the RVD outlined as **HD**. *Fok*I nuclease domains are depicted as ovals and they cleave at non-specific sequences (N_{12-25}) [Adapted from (Kim and Kim, 2014)].

1.5 Designer nucleases targeted against the HBV genome

1.5.1 ZFNs and CRISPR/Cas9 used to target HBV genome

ZFNs were the first engineered nucleases used for the targeted disruption of HBV, however while viral DNA sequences were effectively targeted there was no evidence of an effect on cccDNA (Cradick et al., 2010). A more recent study used self-complementary adeno-associated virus (AAV) mediated delivery of ZFNs to improve antiviral activity, but ZF pairs proved to be inefficient and one pair was cytotoxic in HepAD38 cells (Weber et al., 2014). While the CRISPR/Cas9 system has achieved much acclaim, a study using these RNA-guided nucleases exhibited only 5% targeted mutagenesis in cccDNA (Fu et al., 2013). ZFNs and CRISPR/Cas9 have recently shown some promise as designer nucleases; however they have largely been associated with off-target effects (Pattanayak et al., 2011, Lee et al., 2016a). Assembly of zinc finger domains that are capable of binding extended stretches of DNA with high affinity has proven to be challenging (Ramirez et al., 2008). Although individual zinc fingers can easily bind to nucleotide triplets, the position of each finger within the domain can reduce binding affinity. Several studies using ZFNs for genome editing has exhibited off-target cleavage and substantial genotoxicity (Beumer et al., 2006). CRISPR/Cas9 is highly active even with imperfectly matched RNA-DNA interfaces in human cells as sgRNA can tolerate a number of mutations and this leads to off-target effects. A recent study identified potential off-targets which were mutagenised with frequencies higher than those observed at the intended on-target site (Fu et al., 2013).

1.5.2 TALENs targeted against the HBV genome

The first study to describe the use of TALENs against HBV demonstrated successful inhibition of the virus (Bloom et al., 2013). Four TALENs were designed to target *S, P* and *C* genes. Huh7 and HepG2.2.15 liver-derived cells were treated with S and C TALEN plasmids. Concentrations of HBsAg secreted by the cells into the culture supernatant were significantly decreased when treated with S TALENs and approximately 35% targeted mutagenesis was observed in cccDNA. *In vivo* experiments carried out in mice also revealed significantly decreased serum HBsAg and intrahepatic HBcAg levels when using the S and C TALENs respectively. Furthermore between 58-87% mutagenesis in HBV target plasmids was observed in mice.

Another study, designed TALENs to target regions around the RNase H domain of the viral polymerase as well as two sets of TALENs targeted against the *C* gene (Chen et al., 2014). Huh7 cells were co-transfected with TALEN plasmids targeted against the *P* and *C* ORF as well as the pCR.HBV.A.EcoRI HBV replication competent plasmid. This study demonstrated significant reductions in HBeAg as well as HBsAg both *in vitro* and *in vivo*. Furthermore, 32% targeted mutagenesis in cccDNA molecules was observed in Huh7 cells when using TALENs targeted against the HBV *C* ORF.

Taken together these experiments demonstrate that TALENs are active against HBV replication, exhibiting considerable predictable interaction with their target sites and have shown diminished toxicity *in vitro* and *in vivo* (Bloom et al., 2013, Miller et al., 2015). Despite the recent success with TALENs capable of cutting cccDNA, homodimeric *Fok*I nuclease domains may be prone to off-target effects (Grau et al., 2013).

1.6 Heterodimeric TALEN design

The specificity of TALEN technology is crucial to the success as a therapy. Targeted cleavage occurs when left (L) and right (R) monomers bind to DNA. However cleavage can still occur when homodimers (two L or two R monomers) bind non-specifically to DNA resulting in cleavage at unintended sites (Miller et al., 2007). To reduce off-target effects caused by cleavage at unintended sites, Miller and colleagues focused on generating *Fok*I variants that were more specific to site-directed cleavage. Miller et al designed a 4 cycle-step-wise mutational system to select variants with the least off-target effects (Miller et al., 2007). These variants retained their catalytic activity upon mutation. Importantly during each cycle of variant design, amino acid substitutions that were generated in one cleavage domain (L or R) were unmodified at that same position for the partner monomer. Modelling was based on published *Fok*I structures (Wah et al., 1997). The 4 cycle-step-wise mutational system led to Q486E and I499A substitutions in the left monomer as well as E490K and I538V in the right monomer (Miller et al., 2007). The Q486E variant interacts with E490K while the I499A variant interacts with I538V (Miller et al., 2007). The effects of these associations are described in Table 1.1.

Table 1.1: **The interactions between the left and right monomers of *Fok*I heterodimeric variants**

Left monomer variants	Right monomer variants	Interaction between left and right monomers
Q486E	E490K	Glutamic acid (E) is negatively charged whereas lysine (K) is positively charged, electrostatic interaction will occur between a left and a right monomer, however amino acid 490 on the left monomer is an E, so electrostatic repulsion will occur between two left monomers
I499A	I538V	Alanine (A) and valine (V) are hydrophobic, and therefore reduce hybridisation energy between L and R monomers. To strengthen the interaction, monomers will only hybridise after binding to intended target sequences

The 4 cycle-step-wise mutational system ultimately gave rise to obligate heterodimeric nucleases which also comprise L and R monomers. The mutations in the monomers of obligate heterodimeric nucleases disrupt dimerisation between homodimers while promoting dimerisation between heterodimers thus reducing off-target effects (Figure 1.4).

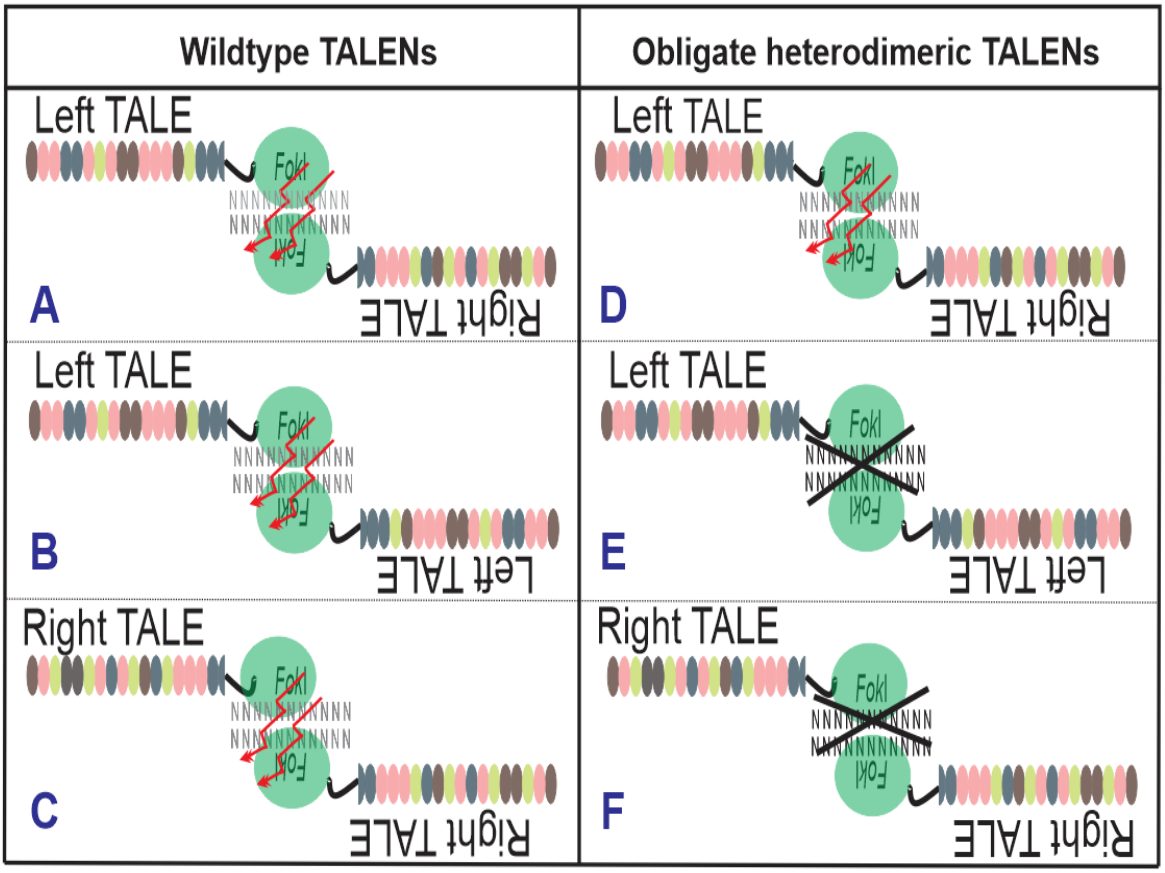

Figure 1.4: **Obligate heterodimeric design improves TALEN specificity and reduces off-target cleavage.**

A-C indicates wild type *Fok*I nuclease domains. **A** indicates heterodimeric TALENs where double-arrow lines show DNA cleavage. **B** and **C** indicate homodimeric TALENs where double-arrow lines show off-target DNA cleavage. **D-F** indicates mutated *Fok*I nuclease domains. **D** indicates heterodimeric TALENs where double-arrow lines show DNA cleavage. **E** and **F** indicate homodimeric TALENs where crosses show that homodimerisation is inhibited and cleavage does not occur. Target DNA is only cleaved when L and R monomers come together. Two of the same monomers result in electrostatic repulsion and do not cleave.

1.7 Aim

The aim of this study was to generate obligate heterodimeric TALENs by replacing the homodimeric *Fok*I nuclease domains of existing well-characterised anti-HBV TALENs with heterodimeric *Fok*I nuclease domains. The obligate heterodimeric TALENs were designed to target the *S* and *C* ORFs of HBV (Figure 1.5). The focus was on improving specificity of cccDNA cleavage and subsequently inactivating HBV viral replication. Surface protein inhibition, transcriptional repression, targeted mutagenesis and cytotoxicity were characterised in *in vitro* and *in vivo* models.

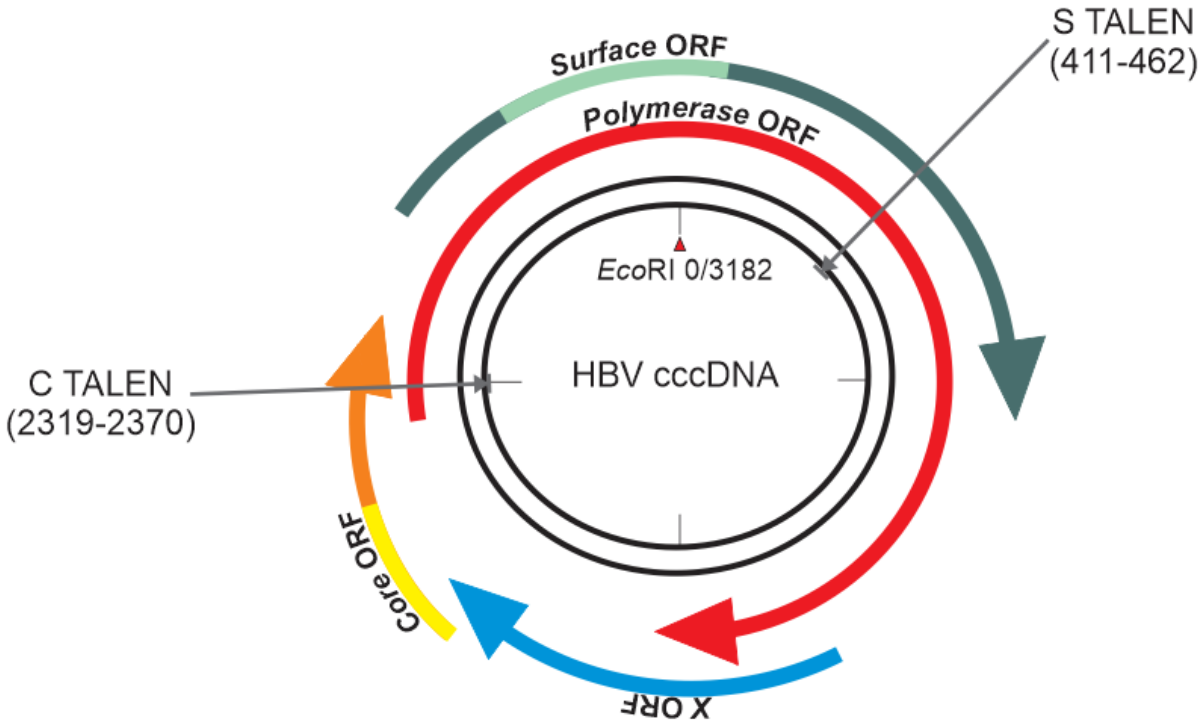

Figure 1.5: **Obligate heterodimeric TALEN binding sites.**

Two obligate heterodimeric TALENs were generated to target the *C* and *S* ORFs of the HBV cccDNA as depicted by arrows at sites illustrated in parentheses. Additionally the C and S TALENs also target the overlapping *P* ORF [Adapted from (Bloom et al., 2013)].

Chapter 2

2. Materials and Methods

2.1 Plasmids

2.1.1 pCH-9/3091

Established by Nassal and colleagues, pCH-9/3091 was designed as an HBV replication competent plasmid (Nassal et al., 1990). This plasmid comprises a full-length HBV sequence with terminal repeats that allows for the transcription of a greater-than-genome length pgRNA (imitating what would normally be transcribed from cccDNA). Furthermore the reverse transcription of pgRNA results in cccDNA formation. pCH-9/3091 is based on genotype D and transcription of the pgRNA is under the control of a cytomegalovirus immediate-early (CMV-IE) promoter. It was used in this study to mimic HBV replication both *in vitro* and *in vivo*.

2.1.2 pCI-neo eGFP

This is an enhanced green fluorescent protein (eGFP) reporter which is under the control of the CMV-IE promoter, generated by Passman and colleagues (Walter et al., 2000). pCI-neo eGFP served as an *in vitro* reporter useful for monitoring transfection efficiencies. Higher GFP expression correlates with greater transfection efficiency.

2.1.3 pCI-neo FLuc

This is a Firefly luciferase plasmid which served as an *in vivo* reporter used for monitoring hepatic delivery efficiency (Ely and Arbuthnot, 2010). Firefly luciferase oxygenates luciferin to oxyluciferin which is highly unstable and when it returns to its ground state it gives off energy in the form of light (von Degenfeld et al., 2009).

2.1.4 pUC118

This is a bacteriophage packaging plasmid. It is a high copy plasmid and does not contain any TALE nor HBV sequences thus serving as a mock control in all experiments to ensure that there is uniform DNA quantity in each transfection (Mussolino et al., 2014).

2.1.5 Anti-HBV TALEN plasmids

TALEs were derived from the TALE protein AvrBs4 scaffold (Mussolino et al., 2011), and were designed to target the *C* and *S* ORFs of the HBV genome (Bloom et al., 2013). TALE repeat arrays were generated by Golden Gate cloning. The amino acid sequences for the TALE DBDs and DNA base recognition are shown in Tables 2.1 and 2.2. The CMV promoter drives expression of the left and right TALEN monomers. Each TALE monomer comprises the haemagglutinin (HA) epitope followed by a nuclear localisation signal (NLS), a TALE DNA-binding domain (DBD) and finally the wildtype *Fok*I nuclease domain (Hus et al., 2004, Lange et al., 2007). This resulted in pVAX CMV TALEN plasmids and for simplicity these plasmids have been referred to as pCMV CL TALEN (WT), pCMV CR TALEN (WT), pCMV SL TALEN (WT) and pCMV SR TALEN (WT) (Table 2.3).

Table 2.1: The TALEN DBD and DNA base recognition sequences for core TALEs (from 2319-2370 bp relative to the HBV genome)

Core TALEs			
Left TALE DBD sequence	**DNA base**	**Right TALE DBD sequence**	**DNA base**
LTPDQVVAIAS**NI**GGKQALETVQRLLPVLCQAHG	A	LTPDQVVAIAS**NI**GGKQALETVQRLLPVLCQAHG	A
LIPQQVVAIAS**NG**GGKQALETVQRLLPVLCQDHG	T	LTPEQVVAIAS**NN**GGKQALETVQRLLPVLCQAHG	G
LTPEQVVAIAS**HD**GGKQALETVQALLPVLCQAHG	C	LTPEQVVAIAS**NN**GGKQALETVQRLLPVLCQAHG	G
LTPDQVVAIAS**NI**GGKQALETVQRLLPVLCQAHG	A	LTPEQVVAIAS**NN**GGKQALETVQRLLPVLCQAHG	G
LTPDQVVAIAS**NI**GGKQALETVQRLLPVLCQAHG	A	LTPEQVVAIAS**NN**GGKQALETVQRLLPVLCQAHG	G
LTPEQVVAIAS**HD**GGKQALETVQALLPVLCQAHG	C	LTPDQVVAIAS**NI**GGKQALETVQRLLPVLCQAHG	A
LTPDQVVAIAS**NI**GGKQALETVQRLLPVLCQAHG	A	LTPEQVVAIAS**HD**GGKQALETVQALLPVLCQAHG	C
LTPEQVVAIAS**HD**GGKQALETVQALLPVLCQAHG	C	LTPEQVVAIAS**HD**GGKQALETVQALLPVLCQAHG	C
LIPQQVVAIAS**NG**GGKQALETVQRLLPVLCQDHG	T	LIPQQVVAIAS**NG**GGKQALETVQRLLPVLCQDHG	T
LIPQQVVAIAS**NG**GGKQALETVQRLLPVLCQDHG	T	LTPEQVVAIAS**NN**GGKQALETVQRLLPVLCQAHG	G
LTPEQVVAIAS**HD**GGKQALETVQALLPVLCQAHG	C	LTPEQVVAIAS**HD**GGKQALETVQALLPVLCQAHG	C
LTPEQVVAIAS**HD**GGKQALETVQALLPVLCQAHG	C	LTPEQVVAIAS**HD**GGKQALETVQALLPVLCQAHG	C
LTPEQVVAIASN**NG**GKQALETVQRLLPVLCQAHG	G	LIPQQVVAIAS**NG**GGKQALETVQRLLPVLCQDHG	T
LTPEQVVAIASN**NG**GKQALETVQRLLPVLCQAHG	G	LTPEQVVAIAS**HD**GGKQALETVQALLPVLCQAHG	G
LTPDQVVAIAS**NI**GGKQALETVQRLLPVLCQAHG	A	LTPEQVVAIAS**NN**GGKQALETVQRLLPVLCQAHG	G
LTPEQVVAIAS**NN**GGKQALETVQRLLPVLCQAHG	G	LIPQQVVAIAS**NG**GGKQALETVQRLLPVLCQDHG	T
LTPDQVVAIAS**NI**GGKQALETVQRLLPVLCQAHG	A	LTPEQVVAIAS**HD**GGKQALETVQALLPVLCQAHG	C
LTPEQVVAIAS**HD**GGKQALETVQALLPVLCQAHG	C	LTPEQVVAIAS**NK**GGKQALETVQRLLPVLCQAHG	G

Table 2.2: The TALEN DBD and DNA base recognition sequences for surface TALEs (from 411-462 bp relative to the HBV genome)

Surface TALEs			
Left TALE DBD sequence	**DNA base**	**Right TALE DBD sequence**	**DNA base**
LTPEQVVAIAS**HD**GGKQALETVQALLPVLCQAHG	C	LTPDQVVAIAS**NI**GGKQALETVQRLLPVLCQAHG	A
LTPEQVVAIAS**HD**GGKQALETVQALLPVLCQAHG	C	LTPEQVVAIAS**HD**GGKQALETVQALLPVLCQAHG	C
LIPQQVVAIAS**NG**GGKQALETVQRLLPVLCQDHG	T	LTPEQVVAIAS**HD**GGKQALETVQALLPVLCQAHG	C
LTPEQVVAIAS**NK**GGKQALETVQRLLPVLCQAHG	G	LIPQQVVAIAS**NG**GGKQALETVQRLLPVLCQDHG	T
LTPEQVVAIAS**HD**GGKQALETVQALLPVLCQAHG	C	LIPQQVVAIAS**NG**GGKQALETVQRLLPVLCQDHG	T
LIPQQVVAIAS**NG**GGKQALETVQRLLPVLCQDHG	T	LTPEQVVAIAS**NK**GGKQALETVQRLLPVLCQAHG	G
LTPEQVVAIAS**NK**GGKQALETVQRLLPVLCQAHG	G	LTPDQVVAIAS**NI**GGKQALETVQRLLPVLCQAHG	A
LTPEQVVAIAS**HD**GGKQALETVQALLPVLCQAHG	C	LIPQQVVAIAS**NG**GGKQALETVQRLLPVLCQDHG	T
LIPQQVVAIAS**NG**GGKQALETVQRLLPVLCQDHG	T	LTPDQVVAIAS**NI**GGKQALETVQRLLPVLCQAHG	A
LTPDQVVAIAS**NI**GGKQALETVQRLLPVLCQAHG	A	LTPEQVVAIAS**NK**GGKQALETVQRLLPVLCQAHG	G
LIPQQVVAIAS**NG**GGKQALETVQRLLPVLCQDHG	T	LIPQQVVAIAS**NG**GGKQALETVQRLLPVLCQDHG	T
LTPEQVVAIAS**NK**GGKQALETVQRLLPVLCQAHG	G	LTPEQVVAIAS**HD**GGKQALETVQALLPVLCQAHG	C
LTPEQVVAIAS**HD**GGKQALETVQALLPVLCQAHG	C	LTPEQVVAIAS**HD**GGKQALETVQALLPVLCQAHG	C
LTPEQVVAIAS**HD**GGKQALETVQALLPVLCQAHG	C	LTPDQVVAIAS**NI**GGKQALETVQRLLPVLCQAHG	A
LIPQQVVAIAS**NG**GGKQALETVQRLLPVLCQDHG	T	LTPEQVVAIAS**NK**GGKQALETVQRLLPVLCQAHG	G
LTPEQVVAIAS**HD**GGKQALETVQALLPVLCQAHG	C	LTPDQVVAIAS**NI**GGKQALETVQRLLPVLCQAHG	A
LTPDQVVAIAS**NI**GGKQALETVQRLLPVLCQAHG	A	LTPDQVVAIAS**NI**GGKQALETVQRLLPVLCQAHG	A
LIPQQVVAIAS**NG**GGKQALETVQRLLPVLCQDHG	T	LTPEQVVAIAS**NK**GGKQALETVQRLLPVLCQAHG	G

2.2 Generation of obligate heterodimeric TALEN plasmids

The pCMV TALEN (WT) plasmids and plasmids encoding heterodimeric *Fok*I nuclease domains (pAC AAVS1 Left and pAC AAVS1 Right) were used to generate obligate heterodimeric TALENs. All heterodimeric TALEN nomenclature is described in Table 2.3. The left heterodimeric *Fok*I nuclease domain contained the Q486E and I499A mutations whereas the right heterodimeric *Fok*I nuclease domain contained the E490K and I538V mutations (Miller et al., 2007).

Table 2.3: TALEN plasmid nomenclature

TALEN description	Plasmid nomenclature	Plasmid Description
TALENs containing wildtype *Fok*I nuclease domain sequence	pCMV CL TALEN (WT)	Core left TALE with upstream nuclear localisation signal (NLS), haemagglutinin (HA) epitope, CMV promoter attached to the wildtype *Fok*I nuclease domain sequence
	pCMV CR TALEN (WT)	Core right TALE with upstream nuclear localisation signal (NLS), haemagglutinin (HA) epitope, CMV promoter attached to the wildtype *Fok*I nuclease domain sequence
	pCMV SL TALEN (WT)	Surface left TALE with upstream nuclear localisation signal (NLS), haemagglutinin (HA) epitope, CMV promoter attached to the wildtype *Fok*I nuclease domain sequence
	pCMV SR TALEN (WT)	Surface right TALE with upstream nuclear localisation signal (NLS), haemagglutinin (HA) epitope, CMV promoter attached to the wildtype *Fok*I nuclease domain sequence
TALENs containing variant *Fok*I nuclease domain sequence (obligate heterodimeric *Fok*I)	pCMV CL TALEN (Var)	Core left TALE with upstream nuclear localisation signal (NLS), haemagglutinin (HA) epitope, CMV promoter attached to the variant left *Fok*I nuclease domain sequence
	pCMV CR TALEN (Var)	Core right TALE with upstream nuclear localisation signal (NLS), haemagglutinin (HA) epitope, CMV promoter attached to the variant right *Fok*I nuclease domain sequence
	pCMV SL TALEN (Var)	Surface left TALE with upstream nuclear localisation signal (NLS), haemagglutinin (HA) epitope, CMV promoter attached to the variant left *Fok*I nuclease domain sequence
	pCMV SR TALEN (Var)	Surface right TALE with upstream nuclear localisation signal (NLS), haemagglutinin (HA) epitope, CMV promoter attached to the variant right *Fok*I nuclease domain sequence

2.2.1 Preparation of TALE- and nuclease-encoding DNA fragments for ligation

To generate obligate heterodimeric TALEN plasmids, all four pCMV TALEN (WT) plasmids and plasmids encoding heterodimeric *Fok*I nuclease domains were cleaved with *Apa*I and *Bam*HI restriction enzymes (Figure 2.1). All restriction digest reactions were carried out according to the manufacturer's instructions (Thermo Scientific, CA, USA). Briefly, the digest was carried out in a 20 µL reaction containing 1 µg of plasmid DNA, 1 U of *Apa*I followed by 1 U of *Bam*HI, 2µL of a 10× Buffer *Bam*HI and dH_2O up to 20 µL. The reaction was incubated at 37 °C for two hours. The restriction digests were subsequently resolved on a 1% agarose gel containing 0.3 µg/mL of ethidium bromide (Appendix 5.1.1). The gel was then viewed with a G:Box UV transilluminator (Syngene, Cambridge, UK) and the 5 284 bp bands (Appendix 5.1.2 and 5.1.3) were excised and purified using the QIAquick® Gel Extraction Kit (Qiagen, Hilden, Germany) (Appendix 5.1.5). The purity and concentration of the extracted DNA was determined by spectrophotometry. The plasmids encoding heterodimeric *Fok*I nuclease domains were digested as above and the 601 bp bands (Appendix 5.1.2 and 5.1.3) were excised then purified.

2.2.2 Ligation of variant nuclease domain-encoding fragments into anti-HBV TALE backbones

The TALE backbone fragments from pCMV TALEN (WT) plasmids and the insert fragments from either pAC AAVS1 Left variant or pAC AAVS1 Right *Fok*I nuclease-encoding plasmids were ligated and cloned to produce the final obligate heterodimeric TALEN plasmids, referred to as pCMV CL TALEN (Var), pCMV CR TALEN (Var), pCMV SL TALEN (Var), pCMV SR TALEN (Var) (Table 2.3). The ligation took place overnight at 14 °C with 1 U of T4 Ligase, 2 µL of 10× Ligation buffer and dH_2O up to 20 µL, according to the manufacturer's instructions (Thermo Scientific, CA, USA) (Appendix 5.1.6). In addition, negative controls containing TALE backbones without nuclease domain-encoding fragments were also ligated as mentioned above.

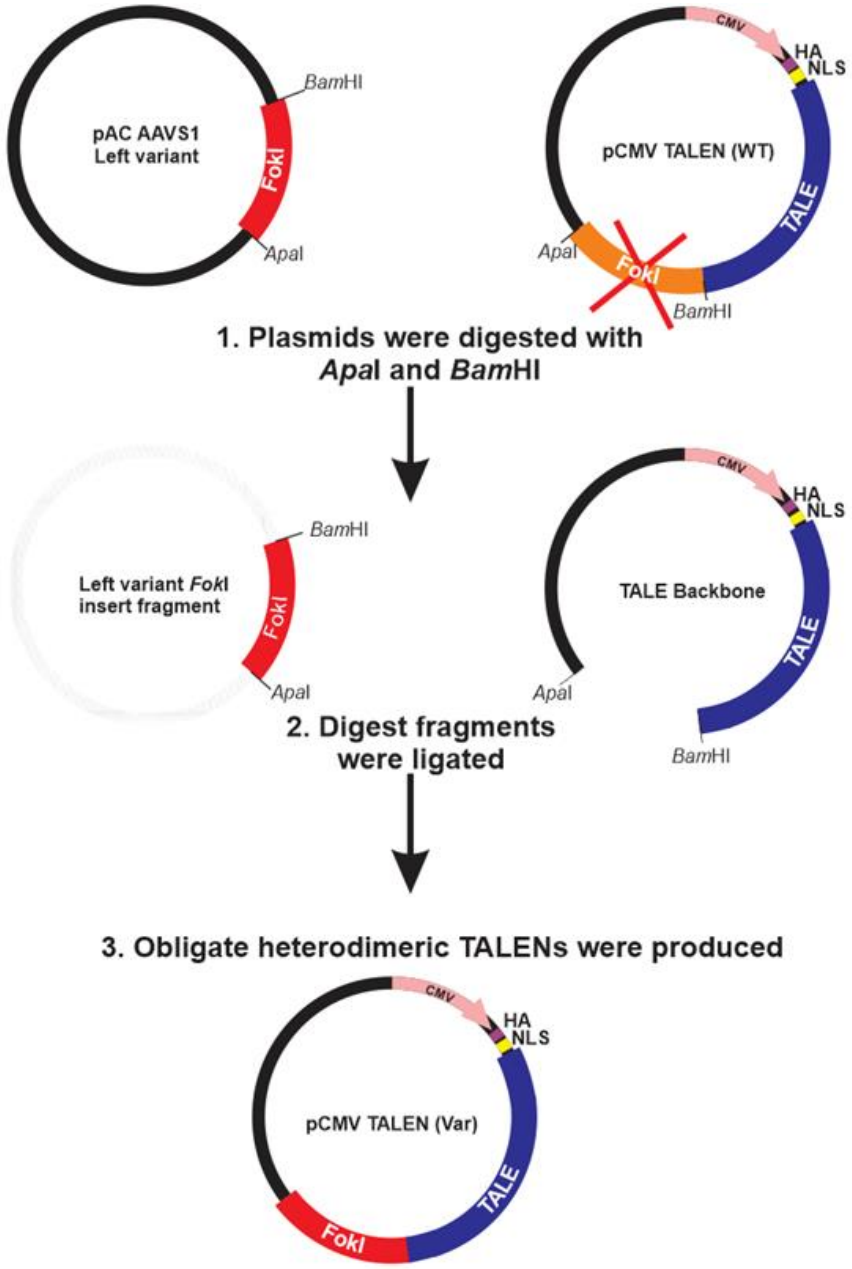

Figure 2.1: Generation of obligate heterodimeric TALENs.

1. pAC AAVS1 Left variant contains the sequence for the left obligate heterodimeric *Fok*I nuclease domain and this sequence was cleaved by *Apa*I and *Bam*HI restriction enzymes. pCMV TALEN (WT) contains the sequences for the left TALEs (either core or surface). The wildtype *Fok*I nuclease domain sequence was removed by *Apa*I and *Bam*HI restriction and then discarded. **2.** Products after cleavage. **3.** The left heterodimeric *Fok*I nuclease domain sequence was inserted into the vector containing the left TALE (either core or surface). The same steps (**1-3**) were used to generate the right obligate heterodimeric *Fok*I TALEN. pAC AAVS1 Right variant containing the sequence for the right obligate heterodimeric *Fok*I nuclease domain and pCMV TALEN (WT) containing the right TALEs were used.

2.2.3 Cloning of ligated products and subsequent positive clone selection

After the overnight incubation, 10 µL of each ligation reaction was used to transform 100 µL of chemically competent *Escherichia coli* (Appendix 5.1.7). In addition the negative controls (TALE backbone fragments without the insert) were transformed into *E. coli*. Single colonies from the overnight culture were picked and inoculated into 10 mL of Luria Bertani medium supplemented with kanamycin (40 µg/mL) which was left to incubate at 37 °C overnight with shaking. Plasmid DNA was extracted and purified from *E. coli* using Econospin™ All-in-One Mini Spin Columns according to the manufacturer's instructions (Epoch Life Science, TX, USA) (Appendix 5.1.8). The purity and concentration of DNA was determined using spectrophotometry. The clones were screened alongside pCMV TALEN (WT) plasmids using *Eco*RI and *Dra*I to distinguish between the wildtype and variant plasmids, clones were also screened alongside pCMV TALEN (WT) plasmids with *Bgl*I to determine TALE DBD patterns. Finally clones were screened with *Pdi*I to distinguish between the left and right variant *Fok*I domain sequences and their amino acid sequence alignment data is illustrated in Appendix 5.1.4.

2.3 Bulk plasmid preparation

All positive clones were prepared using the QIAGEN Plasmid Maxi Kit according to the manufacturer's instructions (Qiagen, Hilden, Germany). DNA was eluted in 100 µL of water and stored at -20 °C (Appendix 5.1.9).

2.4 *In vitro* characterisation of heterodimeric TALENs

2.4.1 Culture conditions for liver and kidney derived cells

Human hepatoma 7 (Huh7) and HepG2.2.15 cells were used to assess TALEN efficacy *in vitro.* Huh7 cells were cultured in a CellStar® 75cm^2 flask (Greiner Bio-One, Frickenhausen, Germany) using low glucose (1 g/L) Gibco™ Dulbecco's Modified Eagle's Medium (DMEM) (Thermo Scientific, CA, USA), supplemented with penicillin (100 000 U/mL), 10% foetal bovine serum (FBS) and streptomycin (100 μg/mL). Cells were incubated at 37 °C and 5% CO_2 until they reached a confluency of 80-90% which was observed under a light microscope (Olympus CKX31,Tokyo, Japan).

Upon reaching confluency approximately 50% of medium was removed and discarded while the remaining medium was removed and placed in a 50 mL tube with an equal volume of fresh medium. This mixture was filter sterilised and served as conditioned medium (CM). Cells were washed with 5 mL of saline containing 1× EDTA followed by a 5 minute incubation at 37 °C in 10 mL of saline. The saline was removed and the cells were treated with 3 mL of 1× TrypLE Express (Thermo Scientific, CA, USA) for 3 minutes to allow for cellular detachment. The flask was gently tapped and this was sufficient to dislodge the cells from the surface of the flask. Once the cells were in suspension, 7 mL of fresh low glucose medium was added and resuspended in the flask. The cell suspension was transferred to a 50 mL tube and centrifuged at 200 ×g for 3 minutes. The resulting pellet was resuspended in 1 mL of fresh low glucose medium and transferred to a new flask containing 14 mL of CM. These cells were incubated at 37°C and 5% CO_2 until the next passage.

HepG2.2.15 cells were cultured similarly to Huh7 cells. HepG2.2.15 cells were grown in a CellStar® 75cm^2 flask using high glucose (4.5 g/L) Gibco™ DMEM (Thermo Scientific, CA, USA), supplemented with penicillin (100 000 U/mL), 10% foetal bovine serum (FBS) and streptomycin (100 μg/mL). Upon reaching confluency, these cells were subjected to the same procedures as above; however the pellet was resuspended in normal glucose medium and then was transferred to a new flask containing 14 mL of fresh normal glucose medium only. Cells were maintained as above until the next passage.

Human embryonic kidney 293 (HEK293) cells were grown in the same medium and incubation conditions as HepG2.2.15 cells. Briefly, upon reaching confluency, cells were incubated with 10 mL of saline containing 1× EDTA for 3 minutes at 37 °C. At this point saline was carefully removed and 10 mL of fresh medium was added and used to resuspend

the cells. This suspension was transferred to a 50 mL tube and centrifuged at 200 ×g for 4 minutes. The pellet was resuspended in 1 mL of fresh medium and transferred to a new flask containing 14 mL of fresh medium. Cells were maintained as in the case of Huh7 cells until the next passage.

All cells were regularly tested for mycoplasma contamination using the MycoAlert™ Mycoplasma Detection kit (Lonza, Basel, Switzerland) (Appendix 5.2.1).

2.4.2 Immunofluorescence microscopy

Huh7 cells were seeded in a 96-well plate at a density of 50% in 90 µL of medium per well, one day prior to transfection. Lipofectamine™ 3000 was used to transfect 100 ng of all TALEN plasmids [either pCMV TALEN (WT) or pCMV TALEN (Var)] according to the manufacturer's instructions (Thermo Scientific, CA, USA) (Appendix 5.2.2). In addition, 100 ng of pUC118 was transfected which served as a negative control and 100 ng of pCI-neo eGFP was transfected to assess transfection efficiency. These transfections were all carried out in triplicate and assessed for expression by immunofluorescence 48 hours after transfection.

Forty eight hours after transfection, the transfection efficiency was assessed by analysing GFP expression in Huh7 cells. Expression was monitored using a fluorescence microscope (Axiovert 100M, Zeiss, Germany) with the fluorescein isothiocyanate (FITC) filter. Following detection of GFP expression, medium was discarded from the wells and cells were washed with 100 µL of 1× phosphate buffered saline (PBS) (Thermo Scientific, CA, USA) (Appendix 5.2.3). The PBS was removed and cells were fixed in 100 µL of 4% paraformaldehyde (PFA) (Appendix 5.2.3) by incubating at room temperature for 15 minutes. The PFA was carefully removed and cells were washed twice with 100 µL of 1× PBS. The PBS was removed and cells were permeabilised in 100 µL of 0.1% Triton-X (Sigma-Aldrich, MO, USA) (Appendix 5.2.3) and incubated at room temperature for 10 minutes. Triton-X was removed and cells were washed twice in 100 µL of 1× PBS. The cells were blocked in 50 µL of 1% bovine serum albumin (BSA) (Roche Applied Science, Mannheim, Germany) (Appendix 5.2.3) for 1 hour in a humidity chamber.

Following the 1 hour incubation, BSA was removed and cells were incubated with 15 µL of mouse anti-HA primary antibody (diluted 1:200 in 1% BSA) for 1 hour in a humidity chamber. Cells were washed twice with 100 µL of 1× PBS and incubated with 15 µL of goat anti-mouse, Alexa flour 488 labelled secondary antibody (diluted 1:200 in 1% BSA) for 40 minutes in a humidity chamber. Cells were again washed twice in 100 µL 1× PBS, PBS was

removed and cells were incubated in 25 µL of 1×4,6-diamidine-2-phenylindole chloride (DAPI) (Appendix 5.2.3) at room temperature for 10 minutes. Cells were finally washed twice in 100 µL of 1× PBS and imaged by fluorescence microscopy under the FITC and DAPI filters.

2.4.3 HBsAg enzyme-linked immunosorbent assays (ELISA)

Huh7 cells were seeded in a 6-well plate at a cell density of 50% in 1750 µL of medium per well one day prior to transfection. Lipofectamine™ 3000 was used to co-transfect 300 ng of pCH-9/3091, 200 ng of pCI-neo eGFP and 1000 ng of each of the left and right TALEN plasmids [either pCMV TALEN (WT) or pCMV TALEN (Var)] or 2000 ng of pUC118 as a mock control. All transfections were performed according to the manufacturer's instructions, carried out in triplicate and assessed for HBsAg expression 48 hours after transfection.

Forty eight hours after transfection, the transfection efficiency was first assessed by analysing GFP expression using the fluorescence microscope (Appendix 5.2.4). Following detection of GFP expression, HBsAg expression was measured by an enzyme-linked immunosorbent assay (ELISA) using the Monolisa™ HBs Ag ULTRA kit (Bio-Rad, CA, USA). Briefly 100 µL of culture supernatant was added to a well of the provided microplate coated with monoclonal anti-HBsAg antibodies. Fifty microlitres of conjugate solution was added to the supernatant, mixed and incubated for 1.5 hours at 37 °C. After incubation the wells were washed five times with 1× washing solution using the ImmunoWash™ 1575 Microplate Washer (Bio-Rad, CA,USA). Thereafter 100 µL of enzyme development solution was added into each well. The microplate was incubated in the dark at room temperature for 30 minutes after which the reaction was stopped by adding 100 µL of stopping solution into each well. The optical density of each sample was read 4 minutes later at 490 nm and 655 nm using an iMARK™ Microplate reader (Bio-Rad, CA, USA). The OD reading at 655 nm was subtracted from the OD reading at 490 nm.

2.4.4 *In vitro* celI endonuclease assay

HepG2.2.15 cells were seeded in a 6-well plate at a cell density of 50% in 1750 µL of medium per well one day prior to transfection (Day 0). Lipofectamine™ 3000 was used to co-transfect 200 ng of pCI-neo eGFP and 1000 ng of the left and right TALEN plasmids [either pCMV TALEN (WT) or pCMV TALEN (Var)] or 2000 ng of pUC118 as a mock control (Day 1). All transfections were carried out in triplicate according to the manufacturer's instructions. All transfection efficiencies were assessed by analysing GFP expression using the fluorescence microscope (Appendix 5.2.5). Seventy two hours after transfection (Day 3) cells were washed and spent media was replaced. One hundred and twenty hours after transfection (Day 5) the cells were dissociated and 20% reseeded per well of a 6-well plate. The remaining 80% was stored in 1 mL of 1× PBS at -70 °C. This process (seeding, transfection and reseeding) was repeated twice (Figure 2.2). Cells from the final transfection were harvested and used to assess targeted cleavage.

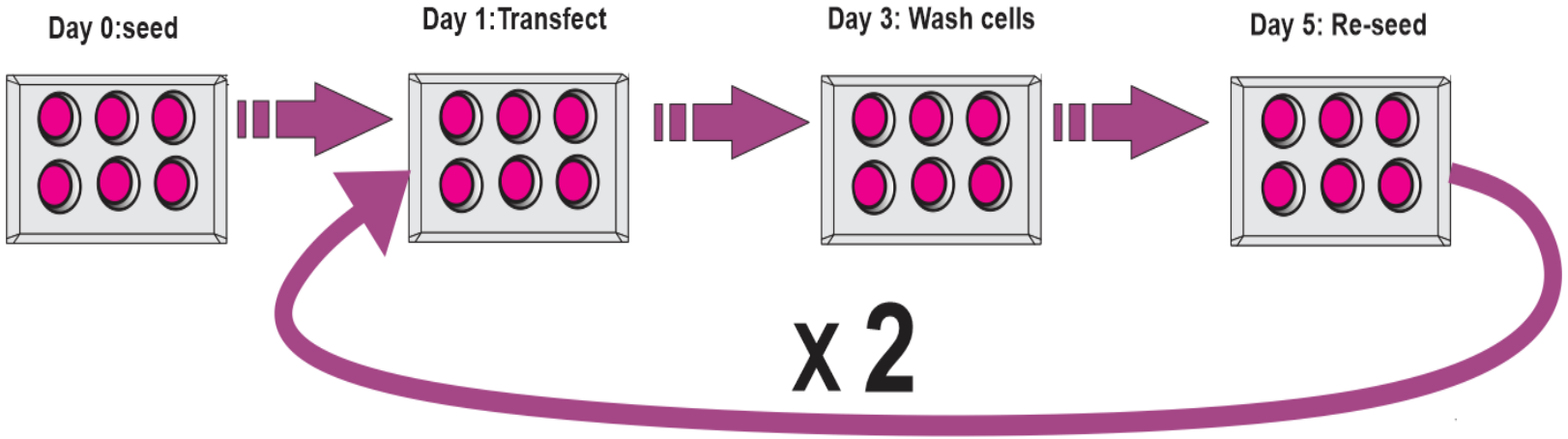

Figure 2.2: HepG2.2.15 transfections for the CelI assay.

Cells were seeded at a density of 50% on Day 0 and transfected with 200 ng pCI-neo eGFP and 1000 ng of the left and right TALEN plasmid [either pCMV TALEN (WT) or pCMV TALEN (Var)] or 2000 ng of pUC118 as a mock control on day 1. On Day 3 the wells were washed and 2000 µL of fresh medium was added. On Day 5 cells were re-seeded at a 1:5 ratio where the remaining cells were stored in 1 mL of 1% PBS at -70°C. This process was carried out 3 times in total.

Total DNA was extracted from HepG2.2.15 cells using the QIAamp DNA Mini Kit according to the manufacturer's Blood and Body Fluids Spin protocol (Qiagen, Hilden, Germany). Briefly, 20 µL of QIAGEN Protease was mixed with 200 µL of cell suspension followed by adding 200 µL of buffer AL and pulse vortexing for 15 seconds. This mixture was incubated at 56°C for 10 minutes after which 200 µL of 100% ethanol was added and the mixture pulse-vortexed for 15 seconds. The mixture was transferred to a QIAamp Spin Column and centrifuged at 6000×gfor 1 minute. The flow-through was discarded and 500 µL of buffer AW1 was added to the column and centrifuged as above. The flow-through was discarded and 500 µL of buffer AW2 was added to the column centrifuged at maximum speed in a benchtop centrifuge for 3 minutes. Additionally the flow-through was discarded and the columns were centrifuged for an extra minute to remove any residual wash buffer. The collection tube containing the flow-through was discarded and the column was transferred into a clean microcentrifuge tube. Total DNA was eluted by adding 30 µL of dH_2O to the column, incubating at room temperature for 1 minute and centrifuging at 6000× g for 1 minute.

The sequences spanning approximately 260 bp upstream and 260 bp downstream of the predicted target sites for the C and S TALENs were amplified by PCR. Wildtype and mutant *HBx* PCR amplicons mixed in a 1:1 ratio served as the positive control for the CelI assay. Sequences amplified from pUC118 treatment were used as a negative control. The amplicons (~520 bp) were amplified and subjected to heteroduplex formation. The PCR was set up as follows, 12.5 µL of 2× Ready Mix (KAPA HiFi HotStart Ready Mix PCR Kit), 10 pmol of each respective forward and reverse primers (Table 2.4), 5 µL of extracted DNA and 5.5 µL of dH_2O. The reaction was carried out with the Bio-Rad T100™ Thermal Cycler under the following conditions: initial denaturation at 95 °C for 15 seconds, annealing at 60 °C for 15 seconds, extension at 72 °C for 15 seconds, final elongation at 72 °C for 5 minutes and cooling to 4 °C. PCR products were resolved on a 1.5% agarose gel containing 0.3 µg/mL of ethidium bromide (Appendix 5.1.1) and imaged with a G:Box UV transilluminator (Syngene, Cambridge, UK). The PCR products were purified using the QIAquick® Gel Extraction Kit and eluted in 30 µL of dH_2O (Appendix 5.1.5). The purity and concentration of DNA was determined by spectrophotometry.

Table 2.4: Primer sequences used to amplify putative TALE binding and cleavage sites for *C* and *S* ORFs

Primer name	Primer sequence
Core forward	5'-GAACTAATGACTCTAGCTACCT-3'
Core reverse	5'-CCTACAAACTGTTCACATTT-3'
Surface forward	5'-CCTAGGACCCCTTTCTCGTGT-3'
Surface reverse	5'-ACTGAGCCAGGAGAAACGGG-3'

The CelI assay was set up as follows: 300 ng of PCR product, 2 µL of 10× NEB buffer 2 (New England Biolabs, NJ, USA) and dH_2O to a final volume of 12 µL. The reaction was carried out under the following conditions: initial denaturation at 95 °C followed by cooling to 35 °C at a ramp rate of -0.1 °C/s and holding at 35 °C for 2 minutes. At this point the samples were removed and incubated on ice for 5 minutes. One microlitre of CelI enzyme was added to the samples while 1 µL of dH_2O was added to the negative control (Appendix 5.2.7). Samples were returned the thermocycler and held at 4 °C for 10 minutes followed by heating to and incubating at 37 °C for 25 minutes. The samples were left to cool to 4 °C and remained at 4 °C for an additional 10 minutes. Cleaved products were resolved by agarose gel electrophoresis. Image J software was used to measure band intensities and targeted disruption was calculated as previously described (Guschin et al., 2010) (Appendix 5.2.8).

2.4.5 Cell viability assay

HEK293 cells were seeded in a 96-well plate at a cell density of 30% in 112.5 µL of medium per well 6 hours prior to transfection. Polyethylenimine (PEI) (0.1 mg/mL) was used to co-transfect 15 ng of pCH-9/3091, 15 ng of pCI-neo eGFP and 85 ng of the left and right TALEN plasmids [either pCMV TALEN (WT) or pCMV TALEN (Var)] or 170 ng of pUC118 as a mock control. Furthermore 50% dimethyl sulphoxide (DMSO) was used to transfect cells and served as a positive control. These transfections were all carried out in triplicate and assessed for cell viability 48 hours after transfection.

Forty eight hours after transfection, the transfection efficiency was assessed by analysing GFP expression using fluorescence microscopy (Appendix 5.2.9). Following detection of GFP, 20 µL of MTT (5 mg/mL dissolved in 1× PBS) (Sigma-Aldrich, MO, USA) was added into each well and incubated at 37 °C for 1 hour. After incubation culture medium was removed and 200 µL of DMSO was added and resuspended in each well. This was left to incubate for 5 minutes after which optical densities were measured at 570 nm and 655 nm using an iMARK™ Microplate reader (Bio-Rad, CA, USA). The OD reading at 655 nm was subtracted from the OD reading at 570 nm.

2.5 *In vivo* characterisation of heterodimeric TALENs

2.5.1 Hydrodynamic injection of NMRI mice with TALEN-expressing plasmids

TALEN-mediated silencing of viral replication was assessed in the hydrodynamic injection (HDI) mouse model of HBV replication. The injection creates hydrodynamic pressure generated by a rapid injection of a large volume of solution into the tail veins of mice which induces immediate congestion in the heart (Budker et al., 1996, Bonamassa et al., 2011). This causes the solution to accumulate in the inferior vena cava therefore creating intravascular pressure in the venous system. The solution then refluxes into the liver via the hepatic vein. The force carried by the pressurised solution enlarges the liver and permeabilises the plasma membrane to allow for delivery into the parenchyma hepatocytes. Injections were performed in the tail veins of 3-5 week old Naval Medical Research Institute (NMRI) mice, weighing between 20-30 g. All experiments conducted on NMRI mice were according to procedures approved by the University of the Witwatersrand Animal Ethics Screening Committee (Appendix 5.3.1). The mice were categorised into 5 groups, namely the mock group (n=7), the SWT group (n=7), the CWT group (n=5), the S Variant group (n=6) and the C Variant group (n=5). The injectates contained 30 µg of plasmid DNA and comprised 10% of the body weight of each mouse (Kovacsics and Raper, 2014). All plasmids were prepared using the Endo-Free Plasmid Maxi kit according to the manufacturer's instructions (Qiagen, Hilden, Germany) (Appendix 5.3.2).

Briefly, a solution of 5 µg of pCH-9/3091, 10 µg of each right and left TALEN plasmids [either pCMV TALEN (WT) or pCMV TALEN (Var)] or 20 µg of pUC118 as well as 5 µg of pCI-neo FLuc (luciferase reporter gene plasmid) were injected into mice. The pCI-neo FLuc plasmid was used to assess hepatic delivery. The mice were injected on day 0 and blood samples were collected on days 3 and 5 to measure HBV replication markers [(HBsAg and circulating viral particle equivalents (VPEs)] and to assess liver toxicity by measuring ALT. Immediately after collection the blood was allowed to clot at 4 °C for 1 hour prior to processing. The blood samples were subsequently centrifuged at 6000 ×g for 10 minutes to separate serum from whole blood. Furthermore, mice were euthanised on day 5 by CO_2 exposure and their livers were harvested to assess the effects of TALENs on HBV gene expression and site-directed targeted cleavage. Although the experiment is transient, the effects of TALEN cleavage will be permanent and therefore justify its potential as an effective therapy.

2.5.2 Bioluminescence imaging

To confirm efficient delivery of plasmids, bioluminescence imaging was performed on day 3 after HDI using an IVIS Kinetic In Vivo Optical Imaging System (Perkin Elmer Inc., MA, USA). Briefly, mice were intraperitoneally injected with 150 mg/kg of a 15 mg/mL D-luciferin solution (Perkin Elmer Inc., MA, USA) and placed in an induction chamber. Five percent isoflurane (anaesthetic) was pumped directly into the induction chamber and once the mice were unconscious they were immediately transferred to the imaging chamber with an anaesthetic mask delivering 2% isoflurane. Mice were imaged and returned to their cages.

2.5.3 ELISA

ELISAs were carried out on day 3 and 5 serum samples to determine HBsAg knockdown. The serum was carefully collected and diluted at a 1:4 ratio with saline and 100 µL used for the assay. The ELISA was carried out as described in Section 2.4.3.

2.5.4 Quantification of HBV VPEs

Real-time quantitative PCR (qPCR) was used to determine the amount of VPEs from serum of injected mice. The remaining serum from day 3 and 5 was carefully collected and diluted in a 1:8 ratio in saline. Total DNA was extracted using the QIAamp DNA Mini Kit as described in Section 2.4.4. Extracted DNA was used as the template for qPCR.

The AcroMetrix™ HBV Panel 1.2 mL (Thermo Scientific, CA, USA) was used to generate a standard curve. The qPCR was set up with the FastStart Essential DNA Green Master (Roche Applied Science, Mannheim, Germany) as follows: 10 µL of 2× Master mix, 10 pmol each of the HBV surface forward and reverse primers (Table 2.5), 5 µL of template DNA and 3 µL of nuclease-free water were mixed.

Table 2.5: Primer sequences used to amplify the HBV *surface* gene

Primer name	Primer sequence
HBV Surface forward	5'-TGCACCTGTATTCCCATC-3'
HBV Surface reverse	5'-CTGAAAGCCAAACAGTGG-3'

The qPCR reaction was carried out with the Bio-Rad CFX96™ Real Time System under the following cycling conditions: initial denaturation at 95 °C for 10 minutes followed by 40 cycles of denaturing at 95 °C for 20 seconds, annealing at 57 °C for 20 seconds and extension at 72 °C for 20 seconds with a single SYBR® Green signal acquisition at this step. For the

melting curve analysis DNA was denatured at 95 °C for 10 seconds followed by annealing at 65 °C for 5 minutes and then heating to 95 °C at a ramp rate of 0.1 °C/s with continuous SYBR® Green signal acquisition.

2.5.5 Assessing HBV gene expression

To assess HBV gene expression total RNA was extracted from 100 mg of mouse liver. The liver sections were homogenised in 1 mL of TRIzol® Reagent (Thermo Scientific, CA, USA) and incubated at room temperature for 5 minutes. The samples were centrifuged at10 000 ×g for 10 minutes at 4 °C to collect cellular debris, and the homogenates transferred to clean microcentrifuge tubes. Two hundred microlitres of chloroform was added to the homogenates followed by vigorous shaking for 15 seconds. This mixture was incubated at room temperature for 3 minutes and then centrifuged at 12 000 ×g for 15 minutes at 4 °C. At this point the mixture was separated into the organic phase (containing proteins), the interphase (containing DNA) and the upper aqueous phase (containing RNA). Approximately 500 µL of the aqueous phase was carefully transferred to clean microcentrifuge tubes. Thereafter 500 µL of isopropanol was added to the aqueous phase and gently mixed by inversion. This mixture was incubated at room temperature for 10 minutes and centrifuged at 12 000 ×g for 10 minutes at 4 °C. The resulting supernatant was removed and the pellet was washed in 1 mL of 75% ethanol followed by centrifugation at 7 500 ×g for 5 minutes at 4 °C. The pellet was resuspended in 200 µL of nuclease free water. The purity and concentration of RNA was determined by spectrophotometry.

The extracted RNA was reverse transcribed using the QuantiTect reverse transcription kit (Qiagen, Hilden, Germany). Briefly, the extracted RNA was initially treated to remove any genomic DNA (gDNA) contamination. The clearance of gDNA was set up as follows: 1 µg of RNA, 2 µL of 7× gDNA Wipeout buffer and RNase-free water up to 14 µL were mixed. This reaction was incubated at 42 °C for 8 minutes. The RNA was reverse transcribed to cDNA as follows: 14 µL treated RNA, 4 µL 5× QuantiTect reverse transcription buffer, 1 µL of QuantiTect reverse transcription primer mix and 1 µL of QuantiTect reverse transcription enzyme were mixed. The reaction was incubated at 42 °C for 30 minutes followed by heat inactivation at 95 °C for 3 minutes. The resulting cDNA was stored at -20 °C.

HBV *surface* mRNA and pgRNA were quantified relative to murine *glyceraldehyde-3-phosphate dehydrogenase* (m*GAPDH*) mRNA. Previous studies have shown that m*GAPDH* levels were not affected by transfections (Bloom et al., 2013, Chen et al., 2014). The qPCR

mixes were prepared and carried out as described in Section 2.5.4. Surface primers are indicated in Table 2.5 whereas core and mGAPDH primers are indicated in Table 2.6.

Table 2.6: Primer sequences used to amplify HBV and mGAPDH genes

Primer name	Primer sequence
HBV Core forward	5'-ACCACCAAATGCCCCTAT-3'
HBV Core reverse	5'-TTCTGCGAGGCGGCGA-3'
mGAPDH forward	5'-TTCACCACCATGGAGAAGG-3'
mGAPDH reverse	5'-GGCTGGACTGTGGTCATGA-3'

HBV gene expression was normalised to that of m*GAPDH* expression. Relative amounts were determined from Ct values.

2.5.6 Assessment of *in vivo* targeted cleavage

To assess targeted cleavage in murine samples, 25 mg of liver was dissected, homogenised and stored in 80 µL of 1× PBS. Total DNA was extracted with the QIAamp DNA Mini Kit (Tissue protocol). Briefly, 20 µL of QIAGEN Protease was added and resuspended in the lysate. This mixture was incubated at 56 °C for 4 hours until the liver was completely lysed. Four microlitres of RNase A (100 mg/mL) was added to the mixture and pulse vortexed for 15 seconds followed by incubating at room temperature for 2 minutes. Two hundred microlitres of AL buffer was added to the mixture, pulse vortexed for 15 seconds and incubated at 70 °C or 10 minutes. Two hundred microlitres of 100% ethanol was added to the mixture and pulse vortexed for 15 seconds. The mixture was transferred to a QIAamp Spin Column and centrifuged at 6000 ×g for 1 minute. The flow-through was discarded and 500 µL of buffer AW1 was added to the column and centrifuged as above. The flow-through was discarded and 500 µL of buffer AW2 was added to the column and centrifuged at maximum speed for 3 minutes. Once again the flow-through was discarded and the column was centrifuged at maximum speed for an extra minute to remove any residual wash buffer. Total DNA was eluted by adding 30 µL of dH_2O to the column, incubating at room temperature for 1 minute and centrifuging at 6000 ×g for 1 minute. The CelI assay was performed as described in Section 2.4.4. PCR products were resolved on a 1.5% agarose gel containing 0.3 µg/mL of ethidium bromide (Appendix 5.3.3). PCR products not treated with CelI served as an additional negative control (Appendix 5.3.4).

2.5.7 Assessing liver toxicity

Alanine aminotransferase (ALT) activity, which is indicative of liver damage, was measured at the National Health Laboratory Services (NHLS) at the Charlotte Maxeke Johannesburg Academic Hospital using an automated photometric analyser (Roche Diagnostics, Rotkrenz, Switzerland).

2.6 Data analysis

For the statistical analysis, the mean and standard error of the mean (SEM) were calculated and plotted for each data set. The statistical difference was determined by performing a Two-tailed Student's *t* test using GraphPad Prism 4.0 (GraphPad Software Inc., CA, USA). Only groups with $p < 0.05$ were considered to be significant.

Chapter 3

3 Results

3.1 Successful generation of obligate heterodimeric TALEN vectors

Two anti-HBV TALENs were re-engineered as obligate heterodimers to improve specificity of target cleavage and subsequently inhibition of viral replication. These heterodimeric TALEN sequences comprise DBDs, which have been specifically designed to target sequences within the *C* and *S* ORFs of HBV, and left or right variant *Fok*I nuclease domains for targeted cleavage (See Methods, Figure 2.1). The pUC118 plasmid that does not contain any TALE sequences was used as a negative control in all experiments. The obligate heterodimeric TALEN vectors were generated by replacing the wildtype *Fok*I nuclease domain-encoding sequences from the pCMV TALEN (WT) vectors with variant *Fok*I nuclease domain-encoding sequences from the pAC-AAVS1 plasmids, using standard molecular cloning techniques (Section 2.2) (Appendix 5.1.3).

This gave rise to pCMV CLTALEN (Var), pCMV CRTALEN (Var), pCMV SLTALEN (Var) and pCMV SRTALEN (Var) plasmids. Clones were screened to differentiate between pCMV TALEN (WT) and pCMV TALEN (Var) plasmids, to ensure that the correct DBDs were present in each TALEN and finally to discriminate between the left and the right obligate heterodimeric *Fok*I nuclease domain-encoding sequences.

To differentiate between WT and Variant TALENs, *Eco*RI and *Dra*I restriction enzymes were used. *Eco*RI cuts WT TALENs once and Variant TALENs twice whereas *Dra*I cuts WT TALENs thrice and Variant TALENs twice (Figure 3.1.1). In addition, *Bgl*I restriction digests were performed to confirm that Variant TALENs contain the same DBD patterns as the WT (Figure 3.1.2). A final restriction digest was performed with *Pdi*I. This enzyme was used to differentiate between the left and right *Fok*I Variant sequences as *Pdi*I cuts the left Variant twice and the right Variant thrice (Figure 3.1.3). In accordance with the plasmid maps, sequencing alignment data and agarose gels, all clones presented the correct banding patterns (Appendix 5.1.2-5.1.4) (Figures 3.1.1-3.1.3).

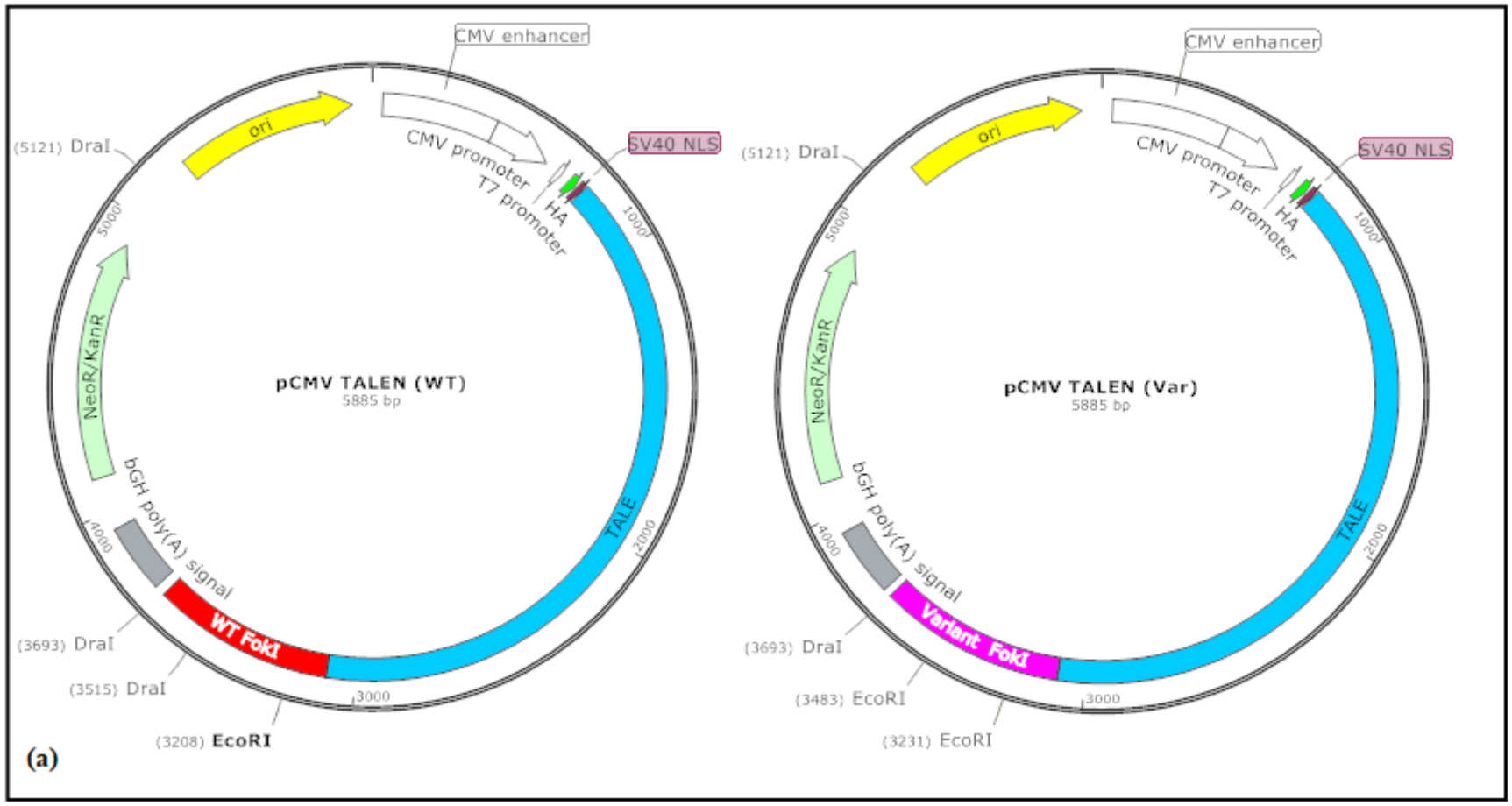
CMV enhancer
ori
CMV promoter
T7 promoter
HA
SV40 NLS
(5121) DraI
5000
1000
NeoR/KanR
pCMV TALEN (WT)
5885 bp
TALE
2000
bGH poly(A) signal
4000
WT FokI
(3693) DraI
(3515) DraI
3000
(3208) EcoRI
(a)
CMV enhancer
ori
CMV promoter
T7 promoter
HA
SV40 NLS
(5121) DraI
5000
1000
NeoR/KanR
pCMV TALEN (Var)
5885 bp
TALE
2000
bGH poly(A) signal
4000
Variant FokI
(3693) DraI
(3483) EcoRI
3000
(3231) EcoRI

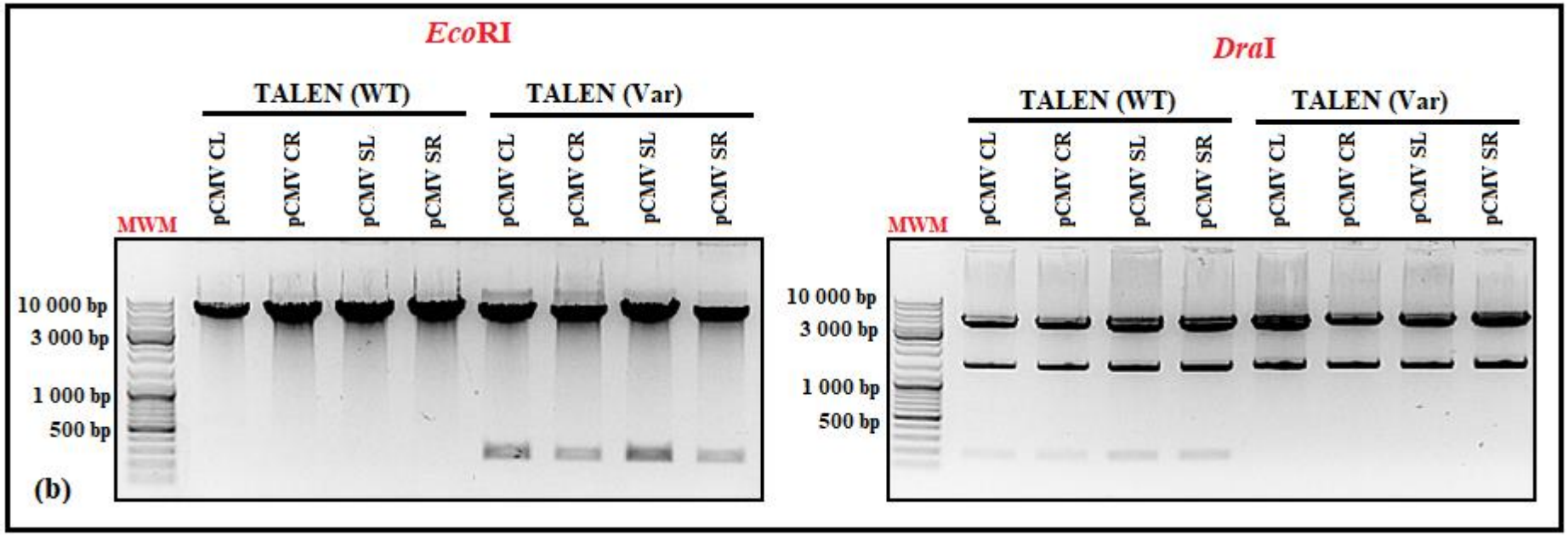

Figure 3.1.1: Verification of WT and Variant TALEN assembly.

The Variant TALENs were produced by removing the *Fok*I nuclease domain DNA sequence from existing pCMV TALEN plasmids and replacing it with either the left or right variant *Fok*I nuclease domain sequences from the pAC-AAVS1 plasmids. **(a)** The vector maps indicating the selected restriction digest enzymes are shown. **(b)** One percent agarose gel electrophoresis confirmed banding patterns for pCMV TALEN (WT) plasmids with *Eco*RI producing a 5885 bp band and *Dra*I producing 4279, 1428 as well as 178 bp bands. Banding patterns for pCMV TALEN (Var) plasmids were also correct with *Eco*RI producing 5633 and 252 bp bands while *Dra*I produced 4457 and 1428 bp bands. (MWM: molecular weight marker, O'GeneRuler 1 kb DNA Ladder, Thermo Scientific, CA, USA).

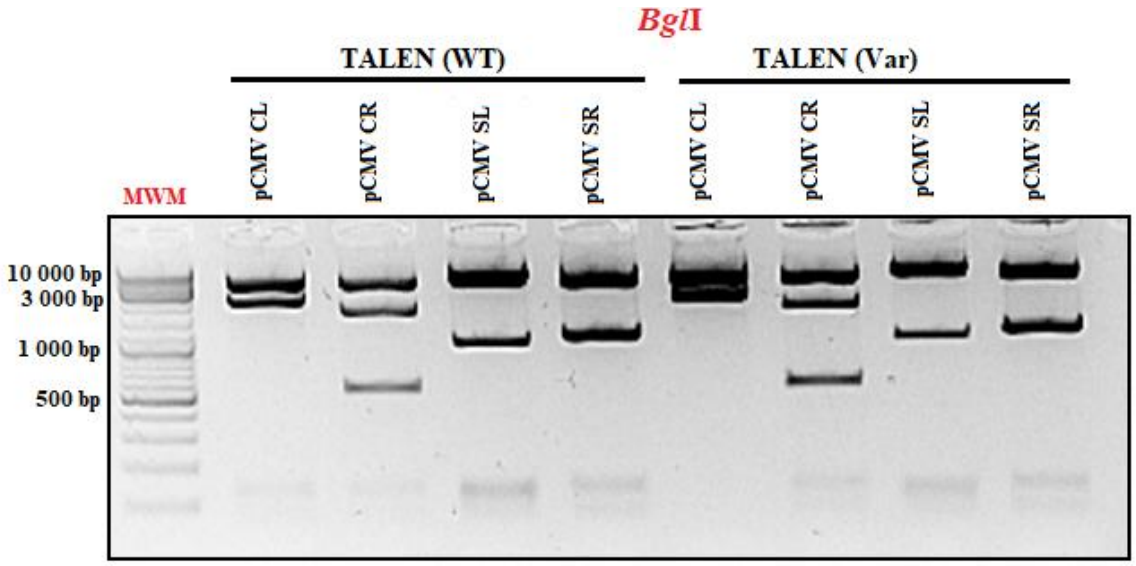

Figure 3.1.2: Verification of TALEN DNA binding domain (DBD)-encoding sequences.

The pCMV TALEN (WT) and pCMV TALEN (Var) contain the same DBDs. *Bgl*I produces distinct banding patterns of the DBDs for both (WT) and (Var) TALENs. One percent agarose gel electrophoresis confirmed that pCMV TALEN (Var) plasmids produced the same banding patterns as pCMV TALEN (WT) plasmids. (MWM: molecular weight marker, O'GeneRuler 1 kb DNA Ladder, Thermo Scientific, CA, USA).

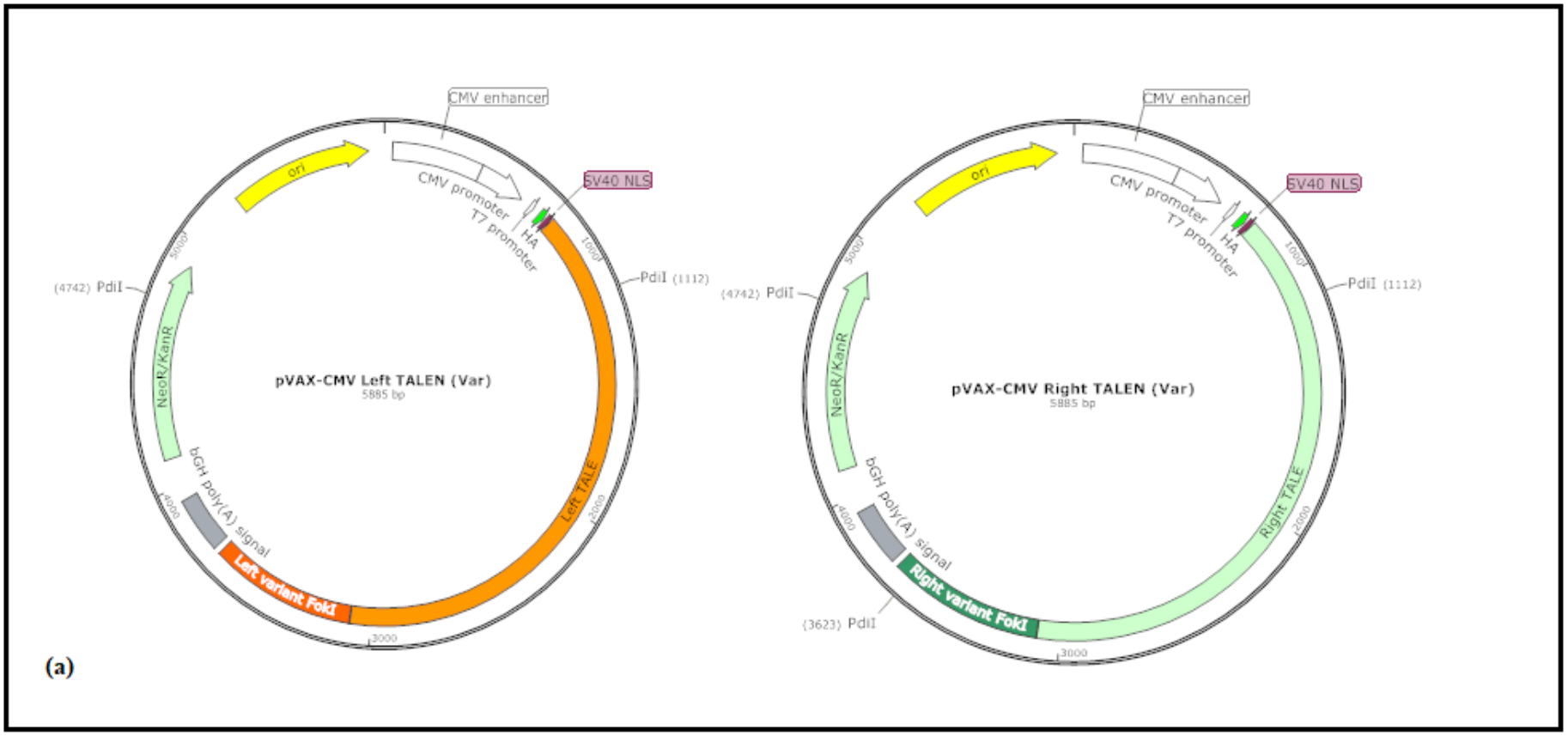
CMV enhancer
ori
CMV promoter
T7 promoter
HA
SV40 NLS
(4742) PdiI
PdiI (1112)
NeoR/KanR
pVAX-CMV Left TALEN (Var)
5885 bp
bGH poly(A) signal
Left variant FokI
Left TALE
5000
1000
2000
3000
4000
CMV enhancer
ori
CMV promoter
T7 promoter
HA
SV40 NLS
(4742) PdiI
PdiI (1112)
NeoR/KanR
pVAX-CMV Right TALEN (Var)
5885 bp
bGH poly(A) signal
Right variant FokI
Right TALE
(3623) PdiI
5000
1000
2000
3000
4000

(a)

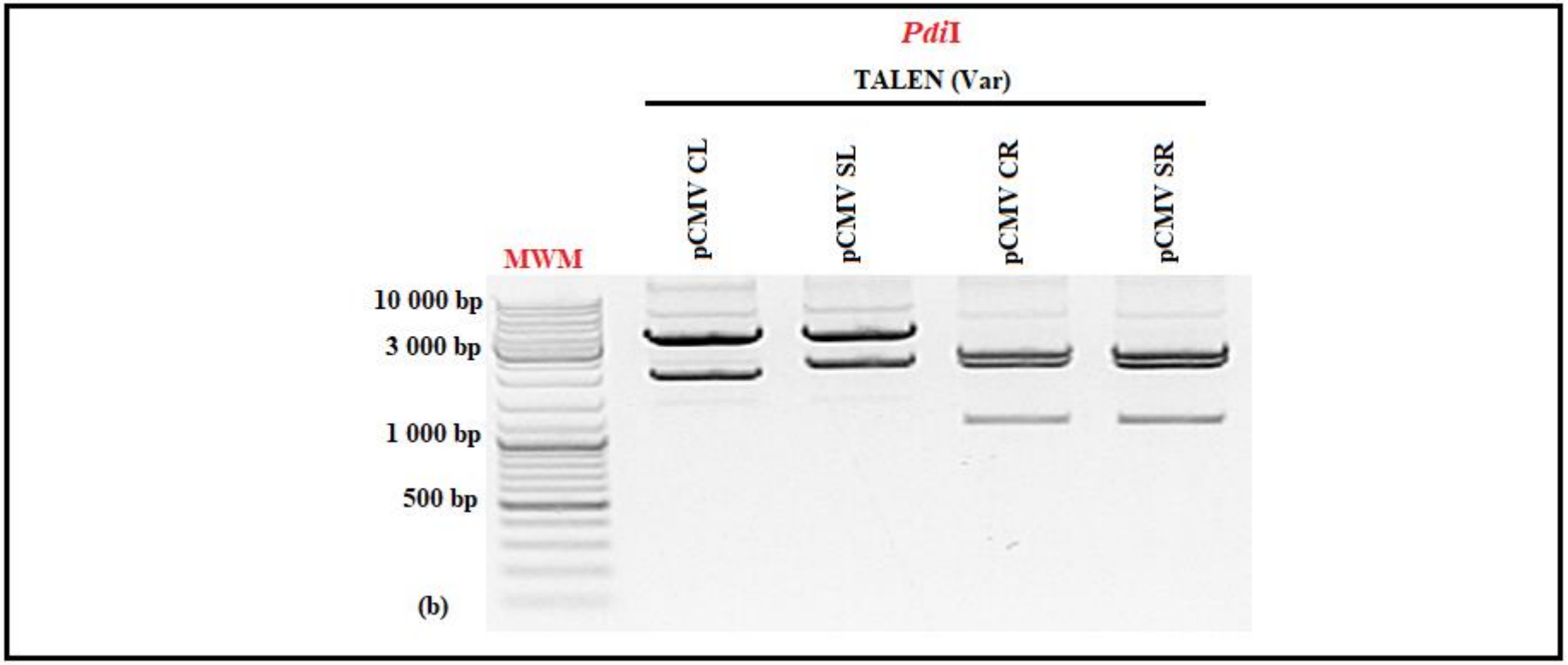

Figure 3.1.3: Verification of vectors carrying Variant nuclease domain sequences.

To distinguish between left and right nuclease domain sequences of the pCMV TALEN (Var) plasmids, *Pdi*I restriction digestion was performed. **(a)** Vector maps indicating the selected restriction digest enzyme are shown. **(b)** One percent agarose gel electrophoresis confirmed banding patterns for the left variant nucleases which produced 3630 and 2255 bp bands, whereas the right variant nucleases produced 2511, 2225 and 1119 bp bands. (MWM: molecular weight marker, O'GeneRuler 1 kb DNA Ladder, Thermo Scientific, CA, USA).

3.2 Obligate heterodimeric TALENs are efficiently expressed in liver-derived cells

The WT and the Variant TALENs contain an HA epitope that is useful for detecting *in vitro* and *in vivo* expression. To confirm TALEN expression in liver-derived cells, Huh7 cells were transiently transfected with left or right TALEN plasmids [either pCMV TALEN (WT) or pCMV TALEN (Var)] or with the pUC118 plasmid which does not contain an HA epitope and was used as a negative control. In a separate transfection cells were transfected with pCI-neo eGFP as a control to assess transfection efficiency. Immunofluorescence was assessed by staining transfected cells with anti-HA primary antibody followed by staining with fluorescently labelled secondary antibody.

GFP expression was detected in the control cells (Figure 3.2). This suggests that transfection of Huh7 cells with plasmids expressing TALEN monomers were also successful. Immunofluorescence staining for the TALEN monomers produced a blue signal from DAPI staining as well as a green signal resulting from detection of the HA epitope in the cytoplasm and nuclei of cells (Figure 3.2). Cells transfected with pUC118 only produced a blue signal from DAPI staining and did not produce green signal. These results demonstrate the expression of each TALEN monomer in liver-derived cells.

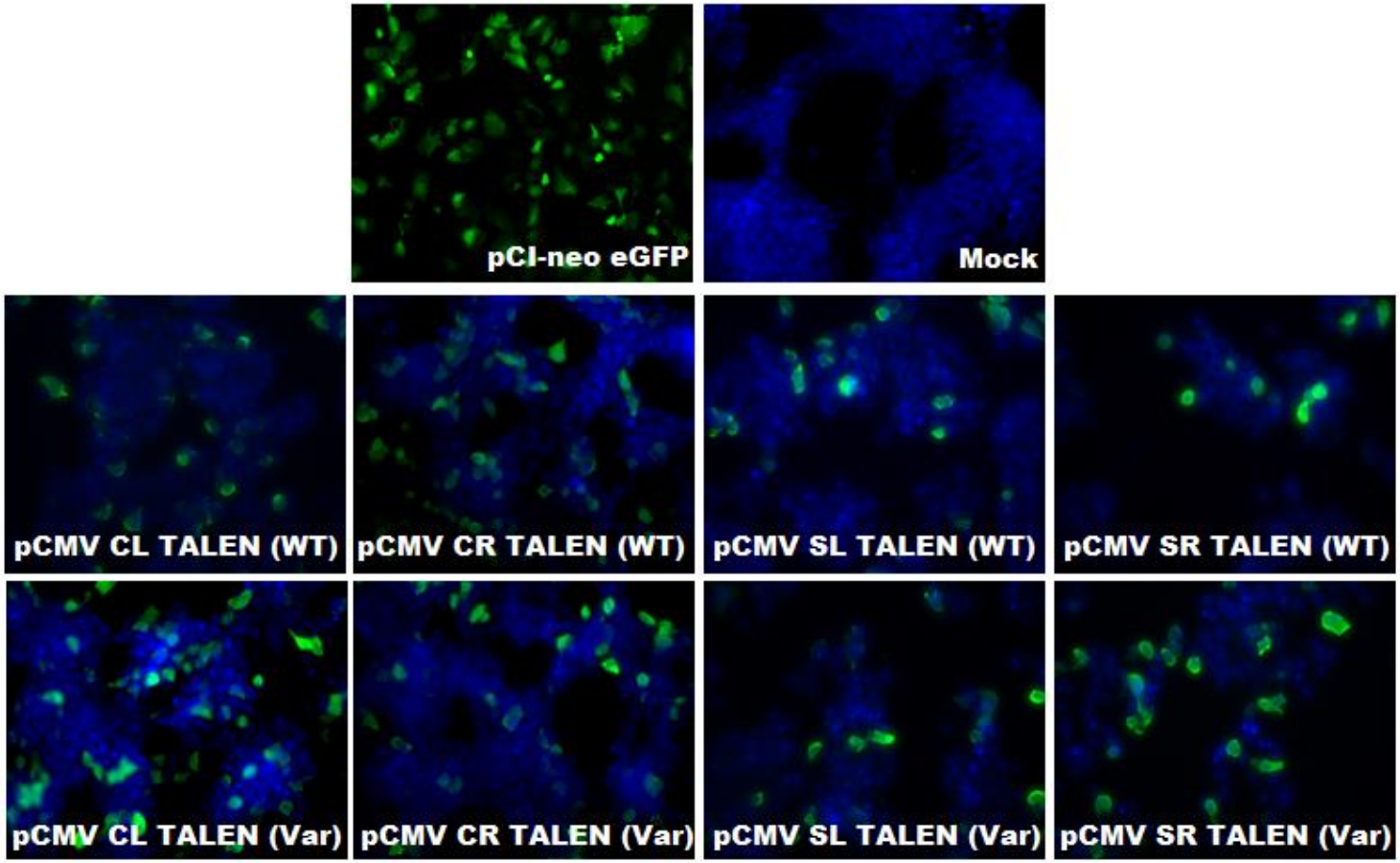

Figure 3.2: Immunofluorescence detection of TALEN monomers in Huh7 cells.

Huh7 cells were transiently transfected with left or right TALEN monomers to determine TALEN expression in cultured cells. Cells were transfected with GFP to determine transfection efficiency and also transfected with a mock plasmid (pUC118). An anti-HA primary antibody followed by fluorescently labelled secondary antibody was used to detect the HA epitope. Immunofluorescence was detected using microscopy. The nuclei were stained with DAPI and cells were imaged at 20× magnification.

3.3 Obligate heterodimeric TALENs mediate efficient inhibition of HBsAg expression in Huh7 cells

After confirming heterodimeric TALENs are expressed efficiently, antiviral efficacy was assessed. This was achieved by measuring the amount of secreted HBsAg which serves as a replication marker of HBV. Huh7 cells were transiently transfected with left and right TALEN plasmids [either pCMV TALEN (WT) or pCMV TALEN (Var)], pCI-neo eGFP for transfection efficiency and pCH-9/3091 replication competent plasmid. pCH-9/3091 mimics HBV replication *in vitro* and *in vivo*. Huh7 cells transfected with pUC118, pCI-neo eGFP and pCH-9/3091 served as a negative control. Transfections were performed in triplicate and 48 hours after transfection the secreted HBsAg levels from the cell culture medium was measured.

Equivalent GFP expression was detected in transiently transfected cells (Appendix 5.2.4). Huh7 cells that were transfected with CWT TALENs did not demonstrate significant HBsAg knockdown compared to mock treated cells with as little as 4% knockdown observed (Figure 3.3). However cells transfected with C Variant TALENs demonstrated a significant decrease in HBsAg levels with 52% knockdown observed. Huh7 cells that were transfected with SWT and S Variant TALENs also demonstrated a significant decrease in HBsAg levels compared to mock treated cells with as much 84% knockdown in SWT and 80% knockdown in S Variant TALEN-treated cells (Figure 3.3).

These results demonstrate that the S TALENs (both WT and Variant) which target the *S* ORF are more efficient than the C TALENs at knocking down HBsAg. Although TALEN-mediated HBsAg knockdown is only expected to occur through direct targeted disruption of the *S* ORF by its recognition of S TALENs, it was observed that C Variant TALENs significantly reduced HBsAg knockdown. This suggests that C Variant TALENs could be inhibiting viral protein expression through transcriptional interference.

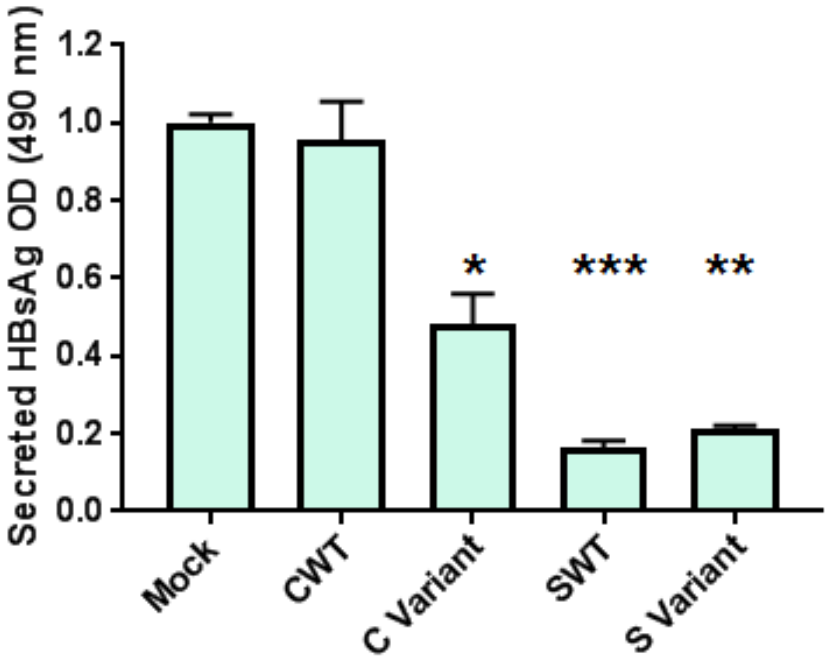

Figure 3.3: TALEN-mediated HBsAg knockdown in Huh7 cells.

To determine anti-HBV activity of the TALENs, secreted HBsAg levels from culture media was measured. Huh7 cells were transiently transfected with left and right TALEN plasmids [either pCMV TALEN (WT) or pCMV TALEN (Var)] and pCH-9/3091. Cells were also transfected with pUC118 and pCH-9/3091 as the mock treated cells. HBsAg was assessed 48 hours after transfection. Data obtained were averaged and the means were normalised to the mock. Error bars are indicative of the normalised SEM where n=3, (*: $p<0.05$; **: $p<0.01$; ***: $p<0.001$).

3.4*In vitro* TALEN-mediated targeted disruption

To confirm that TALENs caused site-directed targeted disruption, a CelI assay was performed on HBV DNA extracted from HepG2.2.15 cells. HepG2.2.15 cells contain an integrated HBV sequence and as a consequence transfection with the HBV replication-competent pCH-9/3091 plasmid was not necessary. HepG2.2.15 cells were triple-transfected with left and right TALEN plasmids [either pCMV TALEN (WT) or pCMV TALEN (Var)], pCI-neo eGFP was co-transfected to determine transfection efficiencies. HepG2.2.15 cells transfected with pUC118 and pCI-neo eGFP served as a negative control.

GFP expression was readily detected in transiently transfected cells over the three weeks of the assay (Appendix 5.2.5). This suggests successful transfection of TALEN plasmids in the HepG2.2.15 cells. Total DNA was extracted from cells and the TALEN target sequences were amplified by PCR to produce ~520 bp amplicons (Appendix 5.2.6). These amplicons were then subjected to CelI treatment. CelI is a mismatch-sensitive enzyme that will detect and cleave heteroduplexes (Figure 3.4.1). As an internal negative control for the CelI assay amplicons were subjected to the same treatment but without the CelI enzyme (Appendix 5.2.7). Wildtype and mutant *HBx* PCR amplicons mixed in a 1:1 ratio served as the positive control.

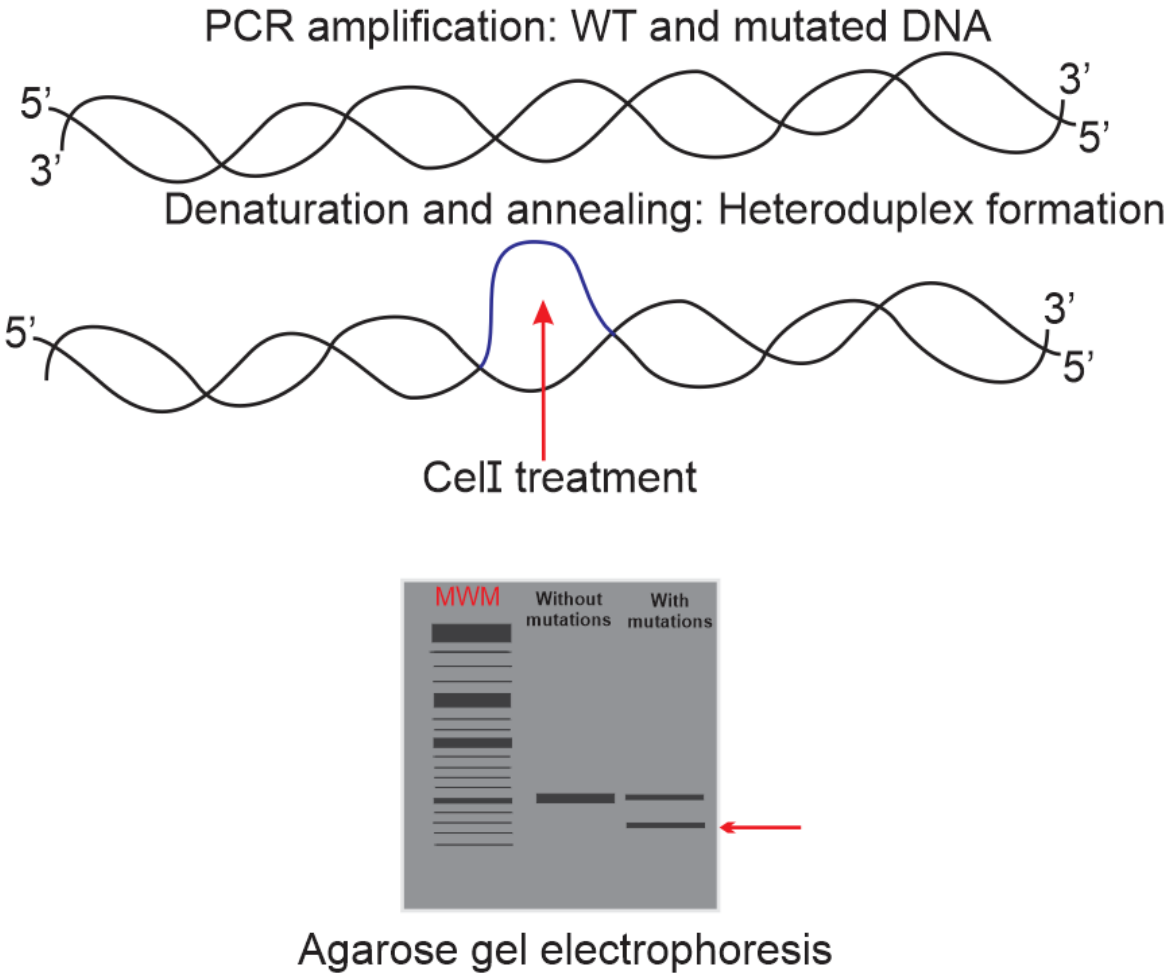

Figure 3.4.1: Gel electrophoresis after CelI treatment.

The sequences spanning the predicted target sites for the C and S TALENs were amplified by PCR. Heteroduplexes were formed during denaturation and subsequent annealing of DNA. The CelI enzyme, which recognises mismatched DNA was then used to cleave the heteroduplexes. The cleaved products were subsequently subjected to agarose gel electrophoresis. DNA sequences that were unaffected by TALEN cleavage should run as one band.

Targeted disruption was not observed in the mock but was observed in the positive control (Figure 3.4.2). The positive control was generated by annealing a wildtype *HBx* amplicon with a mutant *HBx* amplicon (4 bp mismatch). This will always yield heteroduplexes that will be cleaved after CelI treatment. The CWT and C Variant TALENs generated 6.3% and 5.6% targeted disruption respectively whereas the SWT and S Variant TALENs generated 10% and 8% targeted disruption respectively (Figure 3.4.2)

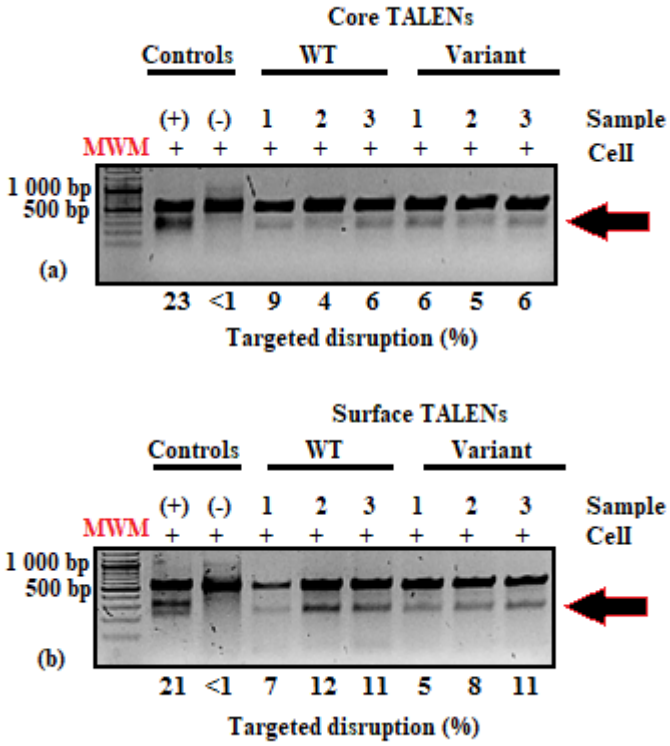

Figure 3.4.2: TALEN-mediated site-directed targeted mutagenesis in HepG2.2.15 cells.

To determine the degree of targeted disruption mediated by the TALENs *in vitro,* viral DNA was interrogated for indels. HepG2.2.15 cells were transiently transfected thrice with left and right TALEN plasmids [either pCMV TALEN (WT) or pCMV TALEN (Var)] or pUC118 (mock). Site-directed targeted cleavage was assessed 12 days after the first transfection by the CelI assay. The sequences incorporating the TALE binding site for both WT and Variant TALENs were amplified to allow for heteroduplex formation. The resulting amplicons were subjected to CelI cleavage. **(a)** Arrow depicts CWT and C Variant mediated targeted disruption, **(b)** Arrow depicts SWT and S Variant mediated targeted disruption. (MWM: molecular weight marker, O'GeneRuler 1 kb DNA Ladder (Thermo Scientific, CA, USA), Positive (+) Control: HBx heteroduplex, negative (-) Control; pUC118).

3.5 Assessing potential TALEN-mediated cellular toxicity

To ascertain if nuclease expression caused any toxic effects, an MTT assay was carried out on cells transiently transfected with TALEN vectors. MTT is a tetrazolium dye that is reduced to formazan which is an insoluble purple product. Mitochondrial NAD(P)H-dependent cellular oxidoreductase enzymes are responsible for this reduction which only occurs in viable cells. The amount of formazan produced is therefore an indication of cell viability. HEK293 cells are loosely adherent and sensitive therefore serving as a widely used model in determining cellular toxicity. HEK293 cells were transiently transfected with left and right TALEN plasmids [either pCMV TALEN (WT) or pCMV TALEN (Var)], pCH-9/3091 and pCI-neo eGFP. Cells were also transfected with pUC118, pCH-9/3091 and pCI-neo eGFP as a negative control. Additionally cells were treated with DMSO (50%) as a positive control for cell death. Finally, to rule out possible transfection reagent toxicity, untransfected cells were used. These cells were not transfected with plasmid DNA, however they received treatment with the same amount of transfection reagents normally used to deliver the TALENs. Transfections were performed in triplicate and the MTT assay was carried out 48 hours after transfection.

Equivalent GFP expression was detected in transiently transfected cells (Appendix 5.2.9). There was no significant difference observed between TALEN-treated cells compared to the mock and untreated controls (Figure 3.5). This demonstrates that cellular activity of the TALEN-transfected cells was comparable with that of the negative controls. These results suggest that expression of TALENs do not cause toxicity and more importantly the anti-HBV effects mediated by TALENs are not caused by cellular toxicity but rather by TALEN-mediated cleavage.

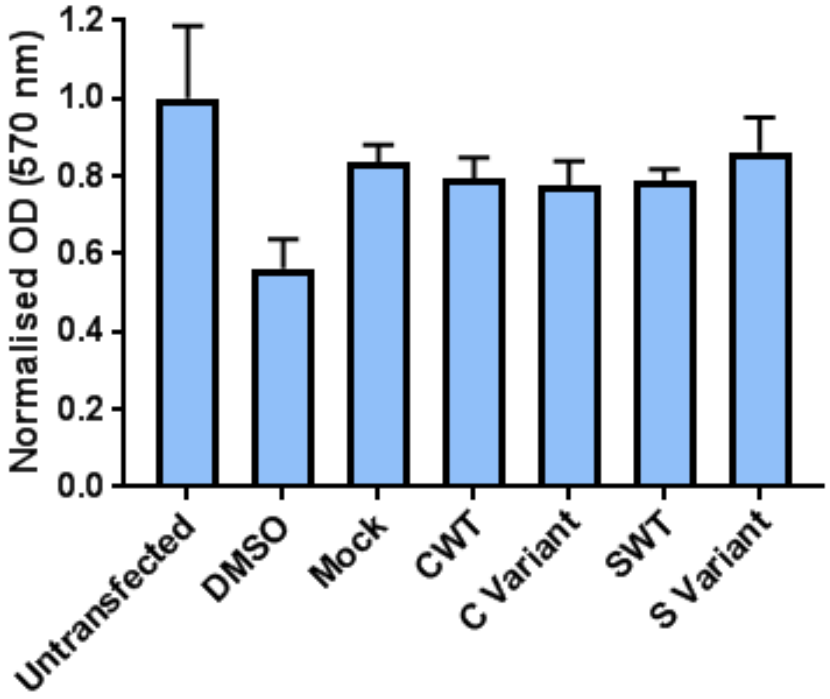

Figure 3.5: Absence of TALEN-associated cellular toxicity.

To determine TALEN-associated toxicity an MTT assay was performed. HEK293 cells were transiently transfected with pCH-9/3091 as well as left and right TALEN plasmids [either pCMV TALEN (WT) or pCMV TALEN (Var)]. Mock treated cells were transfected with pUC118 and pCH-9/3091 only whereas cells treated with DMSO (50%) served as the positive control. Untransfected cells did not contain any plasmid DNA, however these cells were treated with transfection reagents normally used to deliver the TALENs. MTT reduction was assessed 48 hours after transfection. Data obtained from this assay were averaged and normalised to untransfected controls. Error bars are indicative of the normalised SEM where n=3.

3.6TALEN-mediated silencing of viral gene expression *in vivo*

3.6.1 Hydrodynamic injections of TALEN-expressing plasmids in NMRI mice

Following the knockdown of HBsAg expression and targeted disruption of cccDNA observed *in vitro*, the silencing effects of TALENs against viral replication was assessed *in vivo*. To test this effect, HDI was performed in 3-5 week old NMRI mice. The injection solution contained left and right TALEN plasmids [either pCMV TALEN (WT) or pCMV TALEN (Var)], pCH-9/3091 and pCI-neo FLuc (which is a luciferase gene reporter plasmid, to determine hepatic delivery efficiency). The mock treated mice were injected with a solution containing pUC118, pCH-9/3091 and pCI-neo FLuc. The experiment was carried out over a 5 day period (Figure 3.6.1). Briefly, mice were injected on day 0 and blood samples were collected on days 3 and 5 to assess for anti-HBV effects. Mice were sacrificed on day 5 and their livers were harvested to assess TALEN-mediated cleavage and HBV gene suppression as well as to assess potential liver induced toxicity.

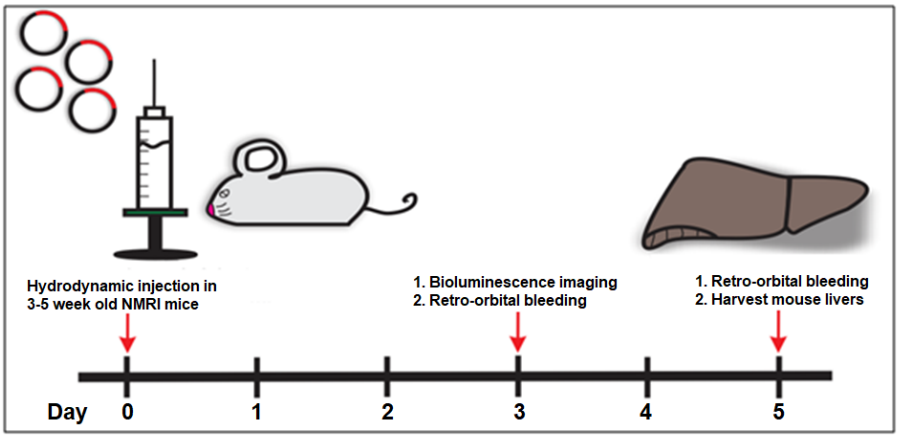

Figure 3.6.1: Timeline representing the experimental procedure of TALEN-treated mice.

The experiment took place over 5 days. Mice were injected into their tail veins with left and right TALEN plasmids [either pCMV TALEN (WT) or pCMV TALEN (Var)], pCH-9/3091 and pCI-neo FLuc. Mock treated mice were injected with pUC118, pCH-9/3091 and pCI-neo FLuc. Bioluminescence imagining was performed on day 3, in addition blood samples were collected by retro-orbital bleeding, for assessing surface protein and circulating viral particle equivalents as well as assessing liver toxicity by measuring ALT. Blood samples were also collected on day 5 by retro-orbital bleeding. The mice were then euthanised by CO_2 asphyxiation. Livers were harvested to test for targeted cleavage and HBV gene expression.

3.6.2 Bioluminescence imaging

To confirm efficient hepatic delivery in mice, bioluminescence imaging was performed 3 days after injection. Bioluminescence detected Firefly luciferase expression and images infer that TALEN plasmids were efficiently delivered to mice livers (Figure 3.6.2).

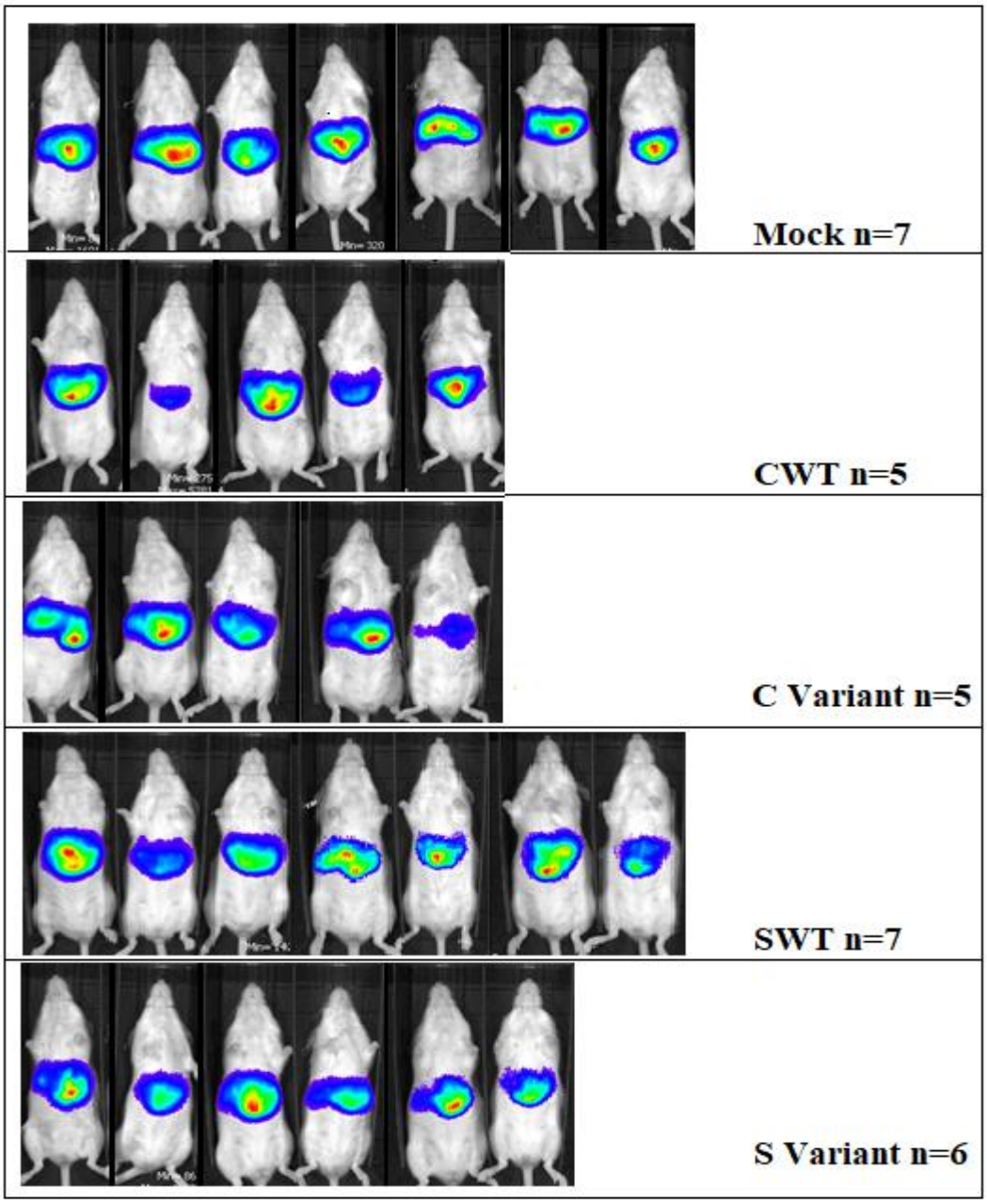

Figure 3.6.2: Bioluminescence imaging of NMRI mice.

Mice were injected with left and right TALEN plasmids [either pCMV TALEN (WT) or pCMV TALEN (Var)] and pCH-9/3091, or pUC118 and pCH-9/3091 as mock treated mice. Additionally mice were injected with pCI-neo FLuc. Live imaging of Firefly luciferase expression was performed on mice on day 3 post injection.

3.6.3 Obligate heterodimeric TALENs mediate efficient inhibition of HBsAg expression *in vivo*

After efficient hepatic delivery was observed, TALEN-mediated inhibition of HBsAg secretion was assessed. Compared to mock treated mice, the CWT and C Variant TALENs significantly reduced HBsAg by 46% and 56% on day 3, as well as 67% and 65% on day 5 respectively (Figure 3.6.3). The SWT and S Variant TALENs significantly reduced HBsAg by 98% and 96% on day 3 and by 97% and 93% on day 5 respectively (Figure 3.6.3).

These results suggest that the S TALENs were more efficient at inhibiting surface protein expression than the C TALENs. However the C TALEN effects seem to have improved over time with greater knockdown efficiencies on day 5. Collectively, both S and C TALENs demonstrate considerable inhibitory effects on protein expression.

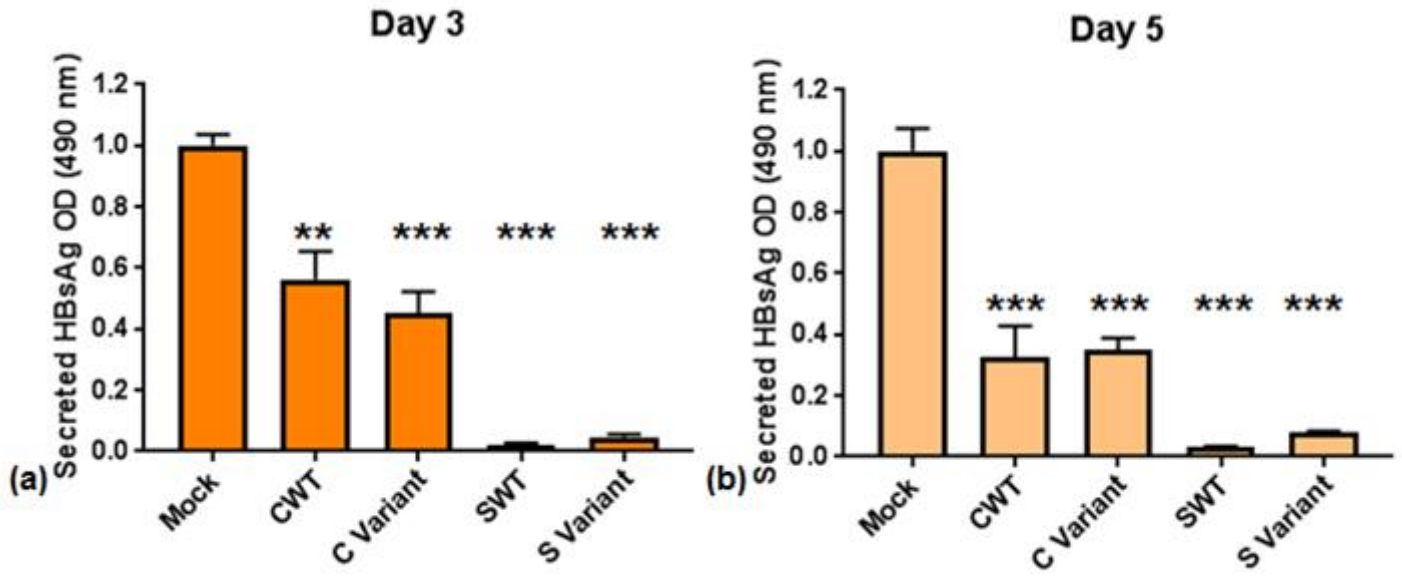

Figure 3.6.3: TALEN-mediated HBsAg knockdown in NMRI mice.

The HDI method was used to deliver left and right TALEN plasmids [either pCMV TALEN (WT) or pCMV TALEN (Var)] and pCH-9/3091 or pUC118 and pCH-9/3091 as mock treated mice. To determine the anti-HBV effects of TALEN-treated mice, blood samples were collected on days 3 (a) and 5 (b) post-injection. HBsAg levels in mouse serum were measured by ELISA. Data obtained from this assay were averaged and normalised to pUC118. Error bars are indicative of the normalised SEM where n=7 (Mock and SWT treated mice), n=6 (S Variant treated mice) and n=5 (CWT and C Variant treated mice), (**: $p<0.01$; ***: $p<0.001$).

3.6.4 TALEN-mediated inhibition of HBV replication *in vivo*

To determine whether TALENs had a direct effect on HBV virion secretion, circulating VPEs were measured from serum samples of mice. Serum was separated from whole blood samples and collected on days 3 and 5. DNA was extracted and the rcDNA was quantified by real-time qPCR to determine the amount of circulating VPEs present in blood serum samples.

Compared to the mock treated mice, the number of circulating VPEs in the CWT and C Variant TALEN-treated mice demonstrated a significant decrease ($p<0.05$) on day 3 (Figure 3.6.4). By day 5 however, CWT-mediated silencing was not significantly different whereas C Variant treated mice demonstrated an even further decrease of circulating VPEs. Compared to the mock treated mice, the number of circulating VPEs in the SWT and S Variant TALEN-treated mice also demonstrated a significant decrease ($p<0.05$) on day 3 (Figure 3.6.4). By day 5 the SWT treated mice demonstrated an even further decrease in circulating VPEs whereas S Variant mediated silencing was no longer significantly different. These results suggest that the C TALENs, particularly the C Variant TALENs, are efficient at reducing HBV replication. Taken together, the Variant TALENs demonstrate comparable anti-HBV effects as the WT TALENs.

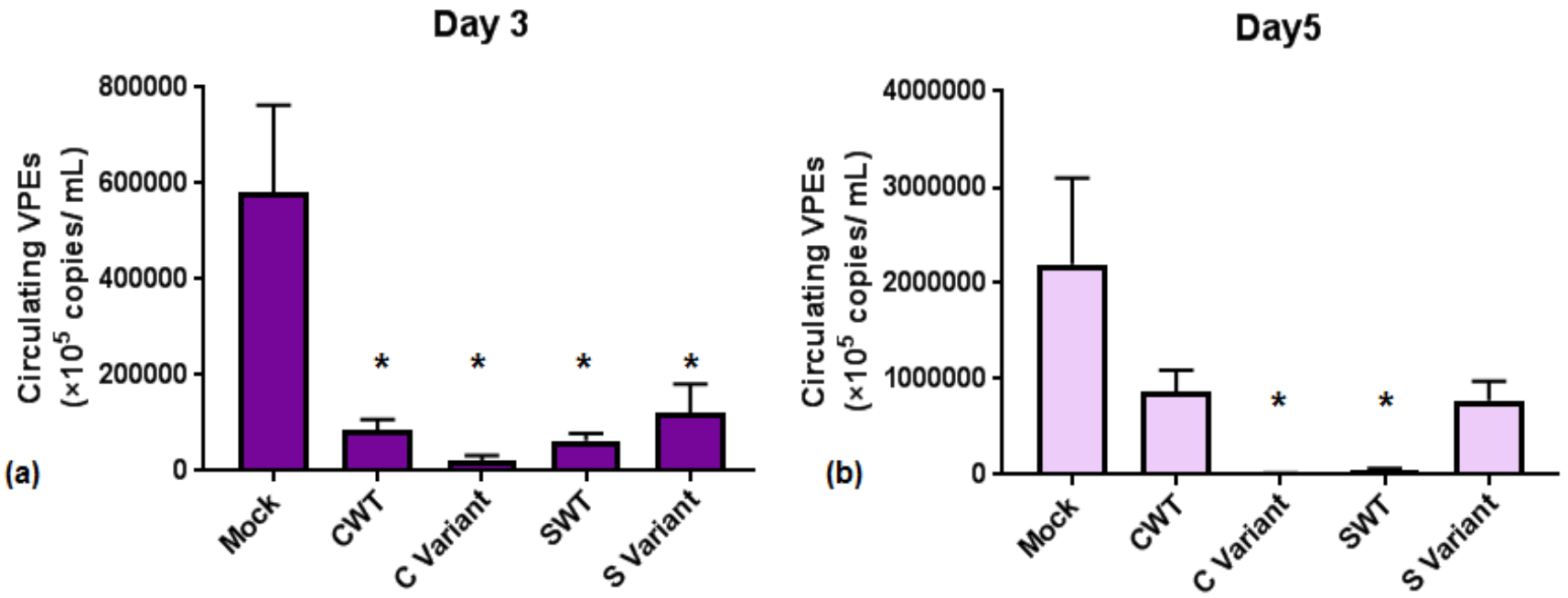

Figure 3.6.4: TALEN-mediated viral replication inhibition.

DNA was extracted from serum samples on day 3 **(a)** and 5 **(b)** post-injection. rcDNA was quantified using real-time qPCR to measure circulating VPEs in serum samples. Data obtained from this assay were averaged and normalised to pUC118. Error bars are indicative of the normalised SEM where n=7 (Mock and SWT treated mice), n=6 (S Variant treated mice) and n=5 (CWT and C Variant treated mice), (*: $p<0.05$).

3.6.5 *In vivo* TALEN-mediated repression of HBV *core* and *surface* transcripts

Following anti-HBV effects on surface protein production and viral replication inhibition, the anti-HBV effects of TALENs on transcription were assessed. pgRNA plays an important role in HBV gene expression. It serves as a template for reverse transcription leading to the formation of partially double-stranded rcDNA [reviewed in (Seeger and Mason, 2000)]. The rcDNA is also the precursor for cccDNA. Furthermore the presence of hepatic pgRNA is indicative of viral persistence and active gene expression (Bai et al., 2013). To measure HBV gene expression in TALEN-treated mice, RNA was extracted from the murine liver samples and converted to cDNA. The pgRNA and HBV *surface* mRNA levels were measured by qPCR and relativised to m*GAPDH*.

Compared to mock treated mice, all TALENs demonstrated a significant reduction in pgRNA levels where CWT- and C Variant-treated mice demonstrated an 89% and 79% decrease respectively (Figure 3.6.5). SWT- and S Variant-treated mice demonstrated an 89% and 88% decrease respectively (Figure 3.6.5). Only the S TALEN-treated mice demonstrated a significant reduction in *surface* mRNA levels (Figure 3.6.5). The BCP drives expression of pgRNA whereas pre-S1 and pre-S2 promoters drive expression of the two *surface* mRNAs. Taken together these results demonstrate that the Variant TALENs are as effective as the WT TALENs in suppressing transcription from the BCP however the S TALENs are only effective in suppressing transcription from the pre-S1 and pre-S2 promoters, particularly the S Variant TALEN.

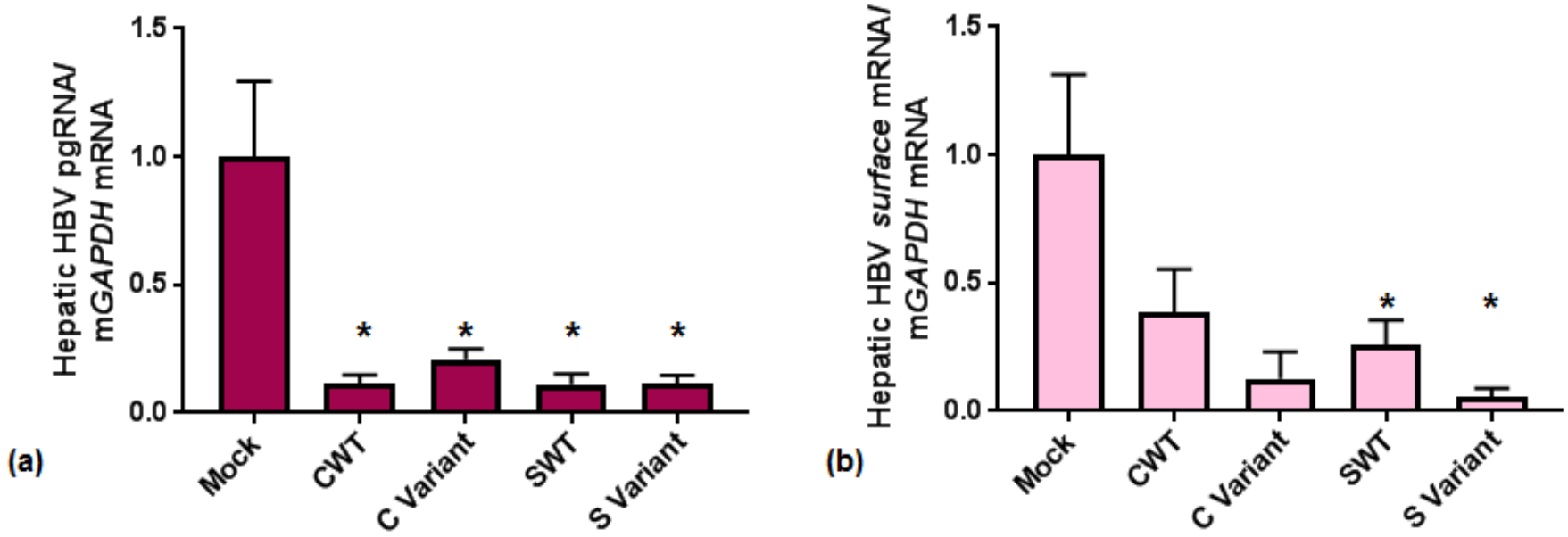

Figure 3.6.5: *In vivo* TALEN-mediated knockdown of HBV mRNA.

To measure HBV gene expression in TALEN-treated mice, HBV mRNA levels were measured from murine liver samples on day 5 post HDI. **(a)** pgRNA and **(b)** *surface* mRNA levels were measured by qPCR and relativised to murine *GAPDH* mRNA levels. Means were calculated and normalised to pUC118. Error bars are indicative of the normalised SEM where n=7 (Mock and SWT treated mice), n=6 (S Variant treated mice) and n=5 (CWT and C Variant treated mice), (*: $p<0.05$).

3.6.6 *In vivo* TALEN-mediated targeted disruption

To confirm that TALENs caused targeted disruption, a CelI assay was performed on HBV DNA extracted from liver samples of mice (as described in section 3.1.2). In addition to the mock control, an HBx heteroduplex sequence was used as a positive control. PCR products are illustrated in the Appendix (5.3.3 and 5.3.4).

Targeted disruption was not observed in the mock controls but was observed in the HBx heteroduplex sequence (Figure 3.6.6). The CWT and C Variant amplicons generated 11.6% and 13% targeted disruption respectively whereas the SWT and S Variant amplicons generated 14.6% and 15.2% targeted disruption respectively (Figure 3.6.6). These results suggest that the TALENs are capable of causing targeted disruption within HBV-encoded DNA, resulting in the inhibition of surface proteins observed in prior experiments.

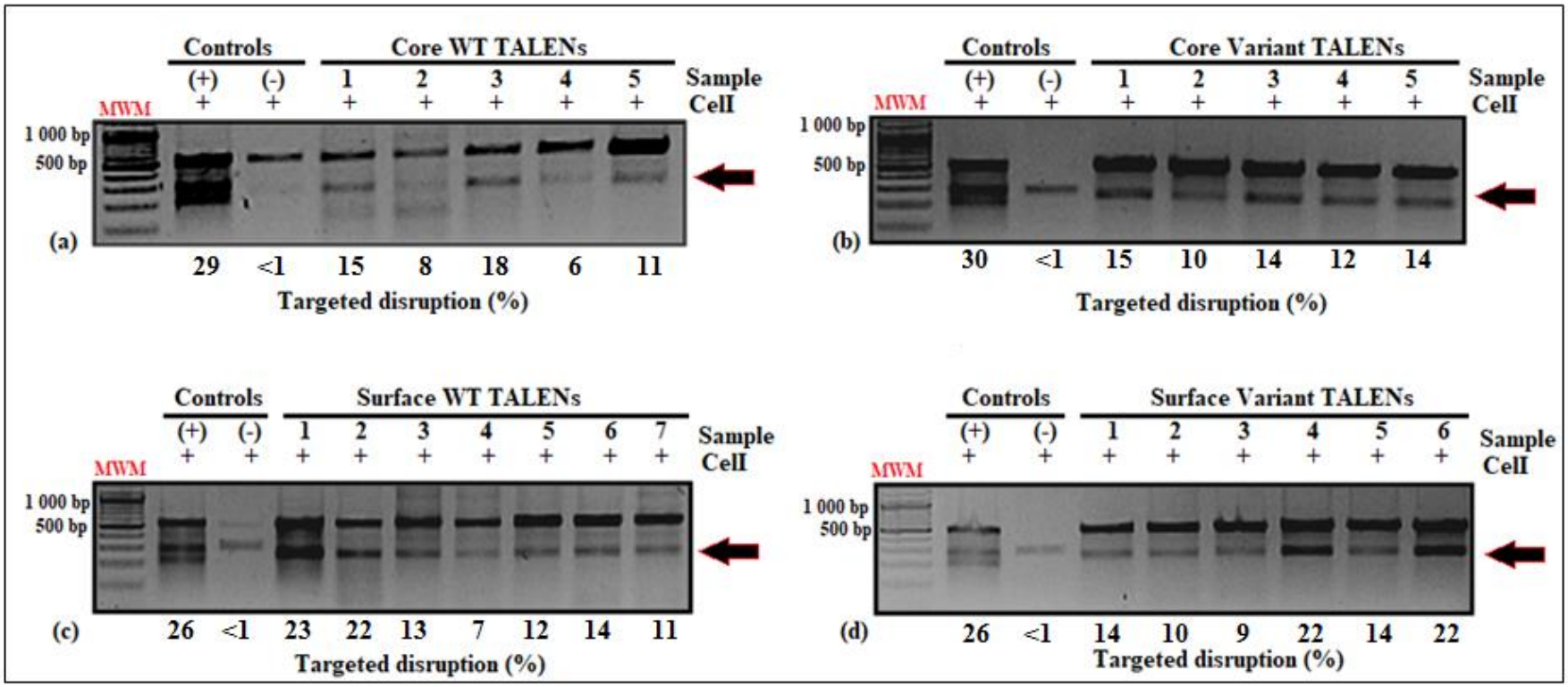

Figure 3.6.6: TALEN-mediated targeted disruption of HBV-encoding DNA in murine liver samples.

To determine the levels of targeted disruption mediated by the TALENs *in vivo,* total DNA was extracted from murine liver and target sites amplified by PCR to allow for heteroduplex formation. The resulting amplicons were subjected to CelI cleavage assays. Arrows depict **(a)** CWT targeted disruption, **(b)** C Variant targeted disruption, **(c)** SWT targeted disruption and **(d)** S Variant targeted disruption.(MWM: molecular weight marker, O'GeneRuler 1 kb DNA Ladder (Thermo Scientific, CA, USA), Positive (+) Control: HBx heteroduplex, negative(-) Control; pUC118).

3.6.7 *In vivo* liver toxicity analysis

The administration of TALENs *in vivo* could potentially be cytotoxic as a result of DSBs at unintended sites (Bloom et al., 2013). To ensure that TALEN-mediated effects in all *in vivo* experiments were non-toxic, ALT levels, which are indicative of liver damage, were measured (Figure 3.6.7). ALT levels were comparable between mock and TALEN-treated mice. Importantly ALT levels did not exceed the threshold of 100 IU/L demonstrating that there was no significant TALEN-associated toxicity.

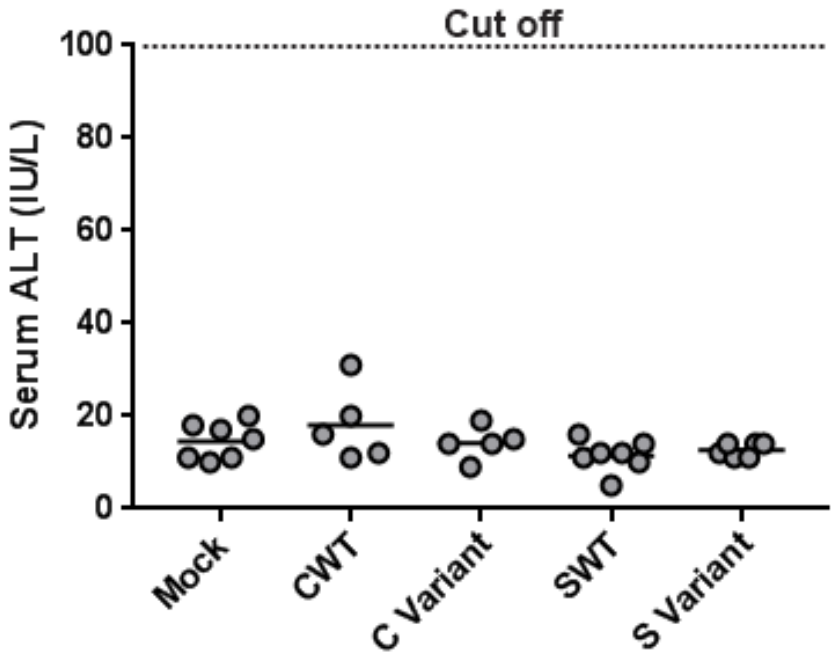

Figure 3.6.7: Absence of hepatic toxicity in TALEN-treated NMRI mice.

To determine *in vivo* TALEN-associated toxicity, ALT levels were measured in serum of mock and TALEN-treated mice at day 5 after injection. No significant hepatotoxicity was observed. Data obtained from individual samples are represented where n=7 (Mock and SWT treated mice), n=6 (S Variant treated mice) and n=5 (CWT and C Variant treated mice).

Overall the results obtained from this study indicate that obligate heterodimeric TALENs exhibit anti-HBV effects on replication, surface protein production and gene expression of HBV. The CelI assay correlates with the TALEN-mediated effects as these TALENs are capable of inducing targeted disruption with no significant cellular toxicity observed in either *in vitro* or *in vivo* settings. Taken together these results demonstrate the first successful use of obligate heterodimeric TALENs against HBV.

Chapter 4

4. Discussion

HBV infection rates remain high, particularly in hyperendemic regions such as sub-Saharan Africa and Asia (Luo et al., 2012). Chronic HBV infection occurs as a result of the persistence of cccDNA (Werle–Lapostolle et al., 2004). In South Africa alone, 2.5 million people are chronically infected (Spearman and Sonderup, 2014). cccDNA serves as a template for viral RNA transcription which is subsequently translated to viral protein. While current treatment effectively inhibits the reverse transcription of pregenomic RNA, it is largely ineffective in eradicating cccDNA (Werle–Lapostolle et al., 2004). In addition, cccDNA remains episomal and can reside in the nucleus to continuously produce viral RNA. (Rehermann et al., 1996). A therapeutic approach targeting cccDNA directly is therefore greatly needed to combat chronic infection.

4.1 Wildtype TALENs are prone to off-target effects

TALENs have emerged as an effective tool in targeting cccDNA. The development of several cloning strategies allowed for efficient assembly of custom TALE arrays (Cermak et al., 2011), giving rise to a widely used gene editing tool. In comparison to ZFNs, which function in a similar fashion, TALENs exhibit improved specificity and adaptability towards targeted cleavage. Previous studies have demonstrated significant viral replication inhibition and successful disabling of cccDNA with the use of TALENs (Bloom et al., 2013). However the wildtype *Fok*I nuclease domain used in the design of these TALENs may be prone to off-target effects (Mussolino et al., 2014, Pattanayak et al., 2014). Off-target effects are highly undesirable in a therapeutic context hence this study highlights the importance of the use of obligate heterodimeric TALENs.

4.2 Successful generation of obligate heterodimeric TALENs

This study is the first to demonstrate the use of obligate heterodimeric TALENs targeted against HBV cccDNA. These TALENs have been modified to comprise obligate heterodimeric *Fok*I nuclease domain variants. The variant nuclease domains were designed to be more specific to site-directed cleavage thus preventing off-target effects. Obligate heterodimeric TALENs serve as a novel candidate therapeutic approach against the virus, targeting cccDNA and subsequently inhibiting HBV replication.

4.2.1 Obligate heterodimeric TALENs inhibit HBV replication

The obligate heterodimeric TALENs were designed to target the *C* and *S* ORFs. As a result of the remarkably compact viral genome, S and C TALENs also target the overlapping *P* ORF (Bloom et al., 2013). This study demonstrated that the S Variant TALEN reduced secreted HBsAg levels by 80% which was comparable to the SWT TALEN which knocked down HBsAg by 84% *in vitro*. Interestingly the C Variant TALEN also reduced HBsAg by 52%. Furthermore both C and S TALENs from WT and Variants were shown to significantly reduce secreted HBsAg levels on days 3 and 5 *in vivo*. The effects on HBsAg knockdown from the C TALENs were more apparent in the *in vivo* samples.

The circulating VPEs were significantly reduced by all TALENs on day 3 and only significantly reduced by the C Variant and SWT TALENs on day 5; however CWT and S Variant TALEN treated mice still demonstrated reductions of greater than 50% by day 5 *in vivo*. The core protein plays an important role in assembling into its capsid-like structure, surrounding the genome. The effect of the C TALENs leads to mutations in the *C* ORF. This results in mutated RNA which subsequently leads to mutations in the core protein. The core protein is still produced but it is mutated so extensively that it is non-functional. Consequently it cannot encapsidate pgRNA which in turn prevents assembly thus inhibiting new virion formation. This coincides with the decrease observed in surface protein knockdown. The S TALENs demonstrated considerable knockdown of surface proteins as well as circulating VPEs. This suggests that the S TALENs are cleaving at their binding sites and causing mutations in the DNA which in turn causes in mutations in the protein, resulting in non-functional protein. This means that virion assembly does not proceed correctly therefore inactivating viral replication.

In a study by Bloom et al HBV gene expression was not affected by the WT TALENs as these TALENs were shown to induce mutations at targeting sites resulting in truncated protein production (Bloom et al., 2013). Unexpectedly the data from this study contradicts the findings of Bloom et al as both WT and Variant TALENs displayed considerable knockdown of intrahepatic viral RNA levels demonstrating that these TALENs exhibit transcriptional interference. As previously mentioned, the *C* ORF encompasses the BCP promoter and the *S* ORF encompasses the pre-S1 and pre-S2 promoters. It is possible that the TALENs transcriptionally interfere with these promoters therefore exhibiting indirect transcriptional inhibition of HBV gene expression. Indeed a similar occurrence was observed by Bloom and colleagues whereby TALENs targeted against the *P* ORF significantly reduced HBsAg and

this was likely caused by transcriptional interference rather than direct cleavage (Bloom et al., 2013).

4.2.2 Obligate heterodimeric TALENs mediate targeted cleavage of HBV DNA

To determine whether the anti-HBV effects that were observed in treated samples were as a result of TALEN binding and cleavage of cognate target sites, targeted cleavage efficiency was assessed using the CelI mismatch sensitive enzyme. In this study HepG2.2.15 cells were used for *in vitro* targeted cleavage testing and NMRI mice were used for *in vivo* targeted cleavage testing. In the HepG2.2.15 cells the CWT and C Variant TALENs demonstrated 6.3% and 5.7% targeted disruption respectively whereas the SWT and S Variant TALENs demonstrated 10% and 8% targeted disruption respectively. In murine hepatocytes, all TALENs demonstrated higher cleavage efficiencies compared to the *in vitro* results. The obligate heterodimeric TALENs demonstrated higher targeted cleavage compared to the WT TALENs *in vivo*.

The inconsistent targeted cleavage data observed between *in vitro* and *in vivo* samples from the same TALEN can be explained by a number of factors. In HepG2.2.15 cells, transfection efficiencies could affect TALEN efficacy, because these cells are difficult to transfect and even after three transfections only 65-70% of the cells expressed TALENs. pCH-9/3091 HBV replication competent plasmids are introduced into murine hepatocytes by the HDI method. However NMRI mice are not predisposed to HBV infection therefore cccDNA pools are not established. Despite the absence of active infection, viral replication still takes place and results in the secretion of new virions as well as circulating VPEs (Yang et al., 2002). HepG2.2.15 cells unlike murine hepatocytes are capable of establishing cccDNA and produce up to 10 more cccDNA copies per cell compared to normal chronically infected hepatocytes (Rabe et al., 2006). HepG2.2.15 cells retain substantial cccDNA pools, therefore TALEN efficacy will be underestimated in these cells.

Compared to the investigation by Bloom et al, this study demonstrated far less targeted cleavage efficiencies (Bloom et al., 2013). This could be explained by use of CelI as opposed to T7 endonuclease 1 (T7E1) to measure targeted mutation. CelI may not be as sensitive in detecting targeted cleavage (Vouillot et al., 2015).Furthermore, in this study total DNA was extracted from HepG2.2.15 cells. To improve estimation of targeted cleavage efficiency, the CelI assay should be conducted on cccDNA-enriched DNA extractions. In order to enrich for cccDNA, a Hirt extraction of treated cells followed by plasmid safe ATP-dependent DNase treatment (PSADT) needs to be performed. The Hirt extraction procedure extracts low

molecular weight DNA such as plasmids and will therefore include both cccDNA and rcDNA (Bloom et al., 2013).

Genomic DNA contamination is typically negligible in Hirt extractions as demonstrated by amplification of genomic sequences (e.g. alpha-1 antitrypsin) (Bloom et al., 2013). PSADT degrades linear and circular single-stranded DNA such as rcDNA while leaving cccDNA intact. Hirt extraction followed by PSADT therefore enriches for cccDNA and analysis of this preparation indicates an effect on cccDNA. However a major disadvantage of PSADT is that it also degrades nicked cccDNA and so the TALEN-mediated effects on cccDNA could be underestimated.

4.2.3 Obligate heterodimeric TALENs do not illicit cytotoxic effects

One of the biggest challenges facing gene therapy is unwanted cytotoxic effects upon the introduction of exogenous DNA. Unlike the most widely used ZFNs, TALEN design is more specific due to single nucleotide recognition as opposed to triple nucleotide recognition (Elrod-Erickson et al., 1996, Yan et al., 2013). Granted that TALENs were designed for improved target site recognition they have also shown diminished cytotoxicity in previous studies (Bloom et al., 2013, Chen et al., 2014). In this study the MTT assay demonstrated that HEK293 cells were not negatively affected after TALEN treatment, moreover, cells remained viable and TALENs were not associated with cytotoxicity. The MTT assay does however have a major limitation in that tetrazolium reduction represents cellular metabolism and not viable cell numbers [reviewed in (Berridge et al., 2005)]. Cellular metabolism rates can differ between viable cells. However to further test for potential liver cytotoxicity, ALT activity which is a biomarker for liver health was measured. ALT levels remain one of the most widely used indicators of liver damage and are often used by several investigators when assessing liver health (Anderson et al., 2000, Chiu et al., 2017, Mahady et al., 2017). TALEN treated samples did not present significantly raised ALT levels. Taken together these data confirms that the obligate heterodimeric TALENs are not cytotoxic, suggesting that off-target effects are minimal.

4.3 Obligate heterodimeric TALENs represents a safe and efficient tool for disabling HBV replication

Obligate heterodimeric TALENs have shown comparable effects against HBV replication to that of the WT TALENs. This is promising as one of the potential drawbacks associated with heterodimeric *Fok*I nuclease domains is that in the process of preventing off-targeted cleavage they reduce hybridisation energy between L and R monomers (Szczepek et al., 2007). The reduction in hybridisation energy essentially means that cleavage efficiencies will also be reduced to ensure safer toxicity profiles. Interestingly, it has been observed that obligate heterodimeric TALENs display comparable or higher cleavage efficiencies against HBV replication with no evidence of cellular toxicity.

4.4 Current challenges hindering successful HBV therapy

An important aspect to consider for gene therapy is tissue specificity. Because HBV affects hepatocytes it is important for the TALENs to target the liver only. Replacement of the ubiquitous CMV promoter with a liver-specific promoter would thus be preferable. Two such promoters include the modified murine transthyretin (mTTR) and phosphoenolpyruvate carboxykinase (PEPCK) transcriptional regulatory elements. mTTR promoters have been used to reduce HBV replication through expression of artificial primary microRNAs in cassettes delivered with helper-dependent adenoviruses (Mowa et al., 2014). The PEPCK promoter has demonstrated long-term liver-specific transgene activity (Mian et al., 2004, Brunetti-Pierri et al., 2007).

One of the challenges of gene therapy is identifying good animal models. The HBV transgenic mice, initially developed by Chisari et al comprised the HBV *envelope*, *core*, *precore* or *X* sequences (Chisari et al., 1985, Milich et al., 1990, Kim et al., 1991). This mouse model was further developed by Guidotti et al to comprise 1.3×greaterthan-genome length HBV DNA integrated into the host genome (Guidotti et al., 1994). This model allows for constant HBV replication which leads to a continuous secretion of new virions. However these mice do not naturally recapitulate HBV infection and cccDNA pools are still not established, nevertheless this model will still be useful for determining TALEN-mediated targeted disruption of integrated HBV sequences. To circumvent the lack of naturally occurring HBV infection in mice, researchers ablated the entire mouse liver and transplanted human hepatocytes into mice. This resulted in chimaeric mice which are susceptible to HBV infection and more importantly a cccDNA pool is established (Meuleman et al., 2005, Meuleman and Leroux-Roels, 2008).

The need for a safe yet effective delivery vehicle is crucial to ensure long-lasting TALEN-mediated therapeutic effects. The delivery of naked DNA into animal models are associated with several undesirable drawbacks such as degradation by intra- and extracellular enzymes as well as difficulties in passing through the plasma membrane by large, negatively charged therapeutic nucleic acid sequences (Schreier, 1994). Both viral and non-viral vectors have been developed for the delivery of therapeutic genes (Nayerossadat et al., 2012). Viral vectors have been exploited for their natural replication and tropism characteristics. In recent years a number of viral vectors have been developed for use of gene therapy.

These include lentiviruses (Connolly, 2002), adenoviruses (SM Wold and Toth, 2013) and AAVs (Daya and Berns, 2008, Maepa et al., 2017). Several non-viral delivery mechanisms have also been established. These include particle bombardment, electroporation and chemical carriers which are lipid- and polymer-based (Lee and Lee, 2012, Ramamoorth and Narvekar, 2015). Each delivery vector exhibits both advantages and disadvantages so there is no "one-measure-fits-all" resolution to gene therapy delivery.

To date there has not been any data published on the use of mTTR or PEPCK promoters for TALEN-mediated targeting of HBV. It would therefore be beneficial to explore use of liver-specific promoters coupled with a delivery system to ensure long-term obligate heterodimeric TALEN-mediated expression. Another consideration would be to convert TALEN-encoding sequences to mRNA. There are several advantages associated with the use of TALEN mRNA as a therapy. Some of which are i) there is no risk of genome integration upon entering the cell, ii) mRNA is easily scalable as transcription can take place *in vitro* and iii) since mRNA functions in the cytoplasm, it will have immediate effect in the cell upon endocytosis whereas DNA needs to access the nucleus (Youn and Chung, 2015).

4.5 Conclusion

Taken together this study demonstrates that obligate heterodimeric TALENs are capable of mediating anti-HBV effects by targeting cccDNA and silencing HBV replication. Both C and S Variant TALENs were capable of significantly reducing HBsAg expression *in vitro* and *in vivo*. Furthermore these TALENs were shown to reduce circulating VPEs by more than 64% and pgRNA as well as *surface* mRNA levels by more than 78%. The effects of C TALENs against HBsAg, VPEs and HBV *surface* mRNA reductions demonstrate that these TALENs have an indirect, yet effective response against HBV surface protein production. Finally targeted cleavage was observed both *in vitro* and *in vivo* without any cytotoxic effects. The obligate heterodimeric TALENs have been proven to significantly reduce HBV replication showing promise as a curative approach against the virus.

4.6 Future studies

The obligate heterodimeric TALENs demonstrated comparable results with the WT TALENs throughout all experiments. Assessing off-target effects by bioinformatic analysis using Predicted Report of Genome-wide Nuclease Off-target Sites (PROGNOS) software and selective Next-generation sequencing (NGS) should therefore be considered to ultimately determine the cleavage specificity of obligate heterodimeric TALENs. Long-term objectives include converting TALEN-encoding sequences to mRNA. mRNA is safer for incorporation into non-viral vectors, therefore the obligate heterodimeric TALEN DNA will serve as a template for *in vitro* transcription to mRNA and will be encapsulated by modified liposomes. The obligate heterodimeric TALEN mRNA, together with the lipoplex delivery system will facilitate long-term therapy against HBV chronic infection.

Chapter 5

5. Appendix

5.1 Generation of anti-HBV obligate heterodimeric TALENs

5.1.1 Agarose gel electrophoresis protocol

Material required

- 50× Tris Acetate EDTA (TAE) Buffer
- Agarose
- TAE (50×) was made by adding 242 g of Tris base, 57.1 mL of glacial acetic acid and 100 mL of 500 mM EDTA to 700 mL of dH_2O. pH was adjusted to 8 and the solution adjusted to a volume of 1 L.
- Ethidium bromide (10 mg/mL)

Procedure:

A 1% agarose gel was made by weighing out 1 g of agar into 100 mL of 1× TAE buffer in a flask. For 1.5% and 2% agarose gels, agar was weighed out to 1.5 g and 2 g respectively. This mixture was heated in a microwave for 5 minutes and allowed to cool at room temperature for 5 minutes after which 3 µL of ethidium bromide was added to the flask and slowly stirred. The liquid gel was then poured into a casting tray and the appropriate gel combs were inserted into the gel. The gel was left to solidify at room temperature for 20 minutes. After loading the samples the gel was set to run at 120 V for 30 minutes or until DNA was sufficiently resolved.

For the CelI experiment a 2% agarose gel was run at 80 V for 8 minutes and then 120 V for 5 minutes. Cleavage products can become faint after prolonged electrophoresis at high voltage.

5.1.2 pCMV TALEN (WT) and pAC AAVS1 plasmid maps

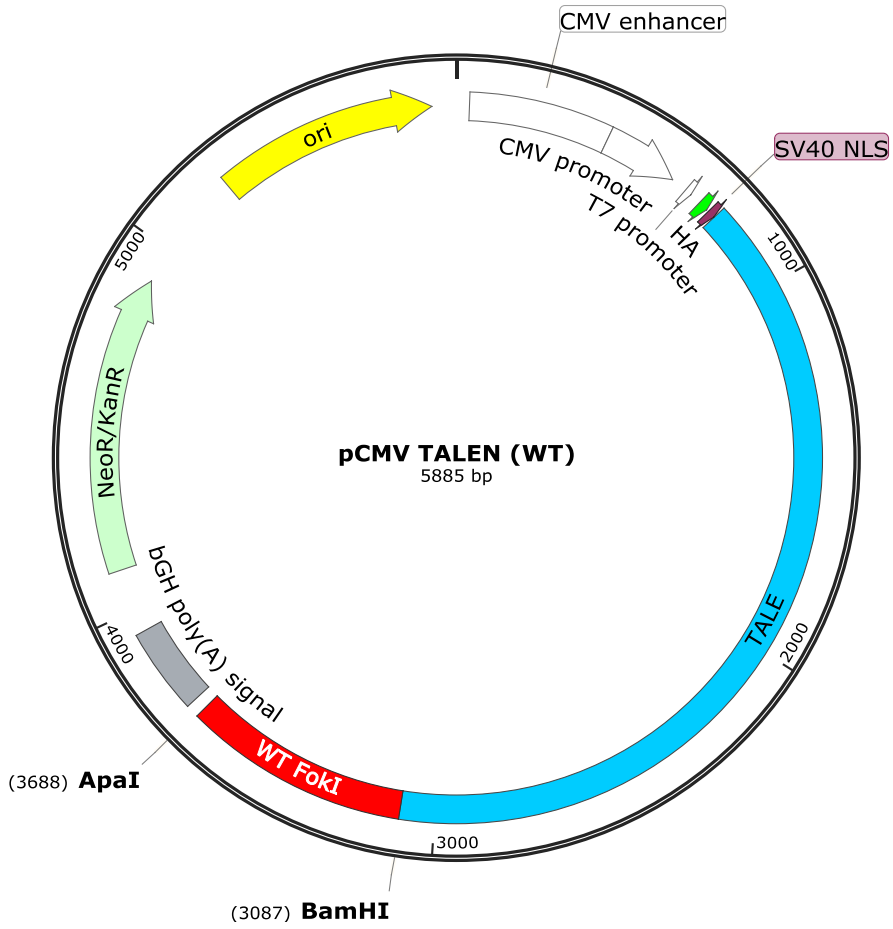

Figure 5.1: pCMV TALEN (WT) plasmid map.

This vector sequence encodes a CMV promoter which drives the expression of WT TALEN monomers (TALE plus WT *Fok*I nuclease domain), a HA epitope serving as a protein tag to detect TALEN expression as well as a nuclear localisation signal (NLS), signalling transport to the nucleus once translated. This plasmid confers resistance to neomycin and kanamycin (NeoR/KanR). Restriction enzymes used in the cloning strategy are indicated on the map. The map was generated using SnapGene® (available at snapgene.com).

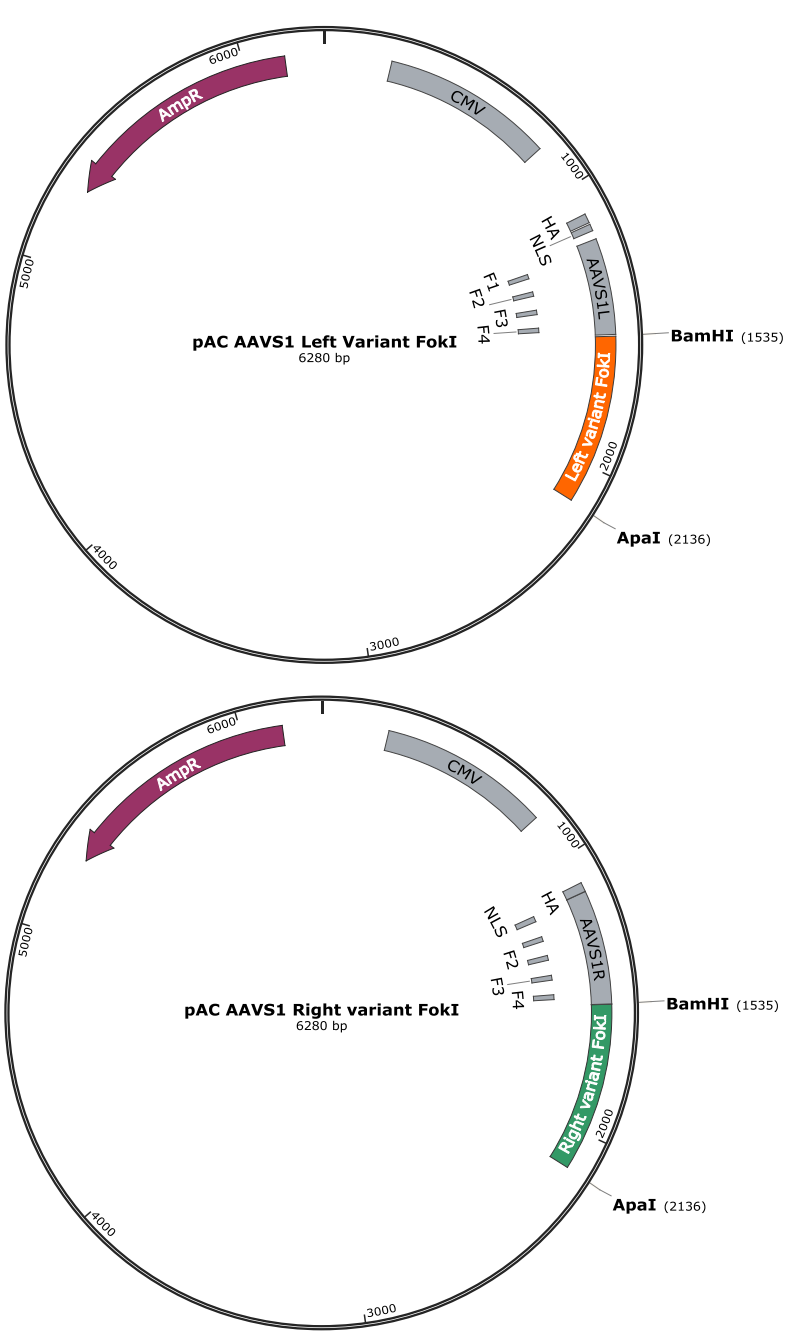

Figure 5.2: pAC AAVS1 left and right TALEN Variant.

The left (top vector) and right variant (bottom vector) *Fok*I nuclease domain-encoding sequences are driven by a CMV promoter. The plasmid confers resistance to ampicillin (AmpR). Restriction enzymes used in the cloning strategy are indicated on the map. The map was generated using SnapGene® (available at snapgene.com).

5.1.3 Gel electrophoresis images of TALE and nuclease generation

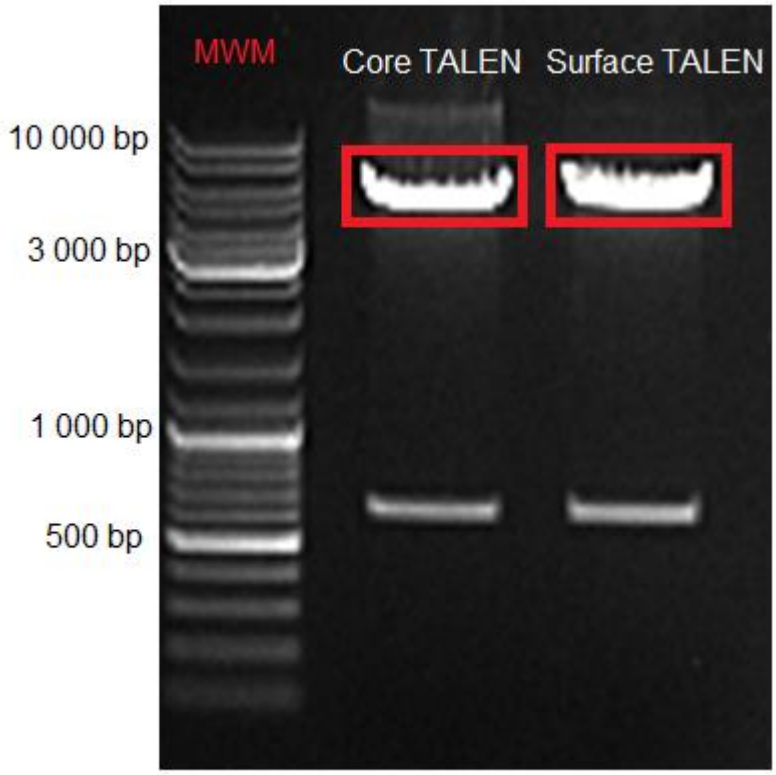

Figure 5.3: One percent agarose gel electrophoresis of C and SWT TALENs.

*Apa*I and *Bam*HI restriction digestion generated two bands, 5 284 bp and 601 bp in size. The top bands (indicated in red) were excised and purified. (MWM: molecular weight marker, O'GeneRuler 1 kb DNA Ladder, Thermo Scientific, CA, USA).

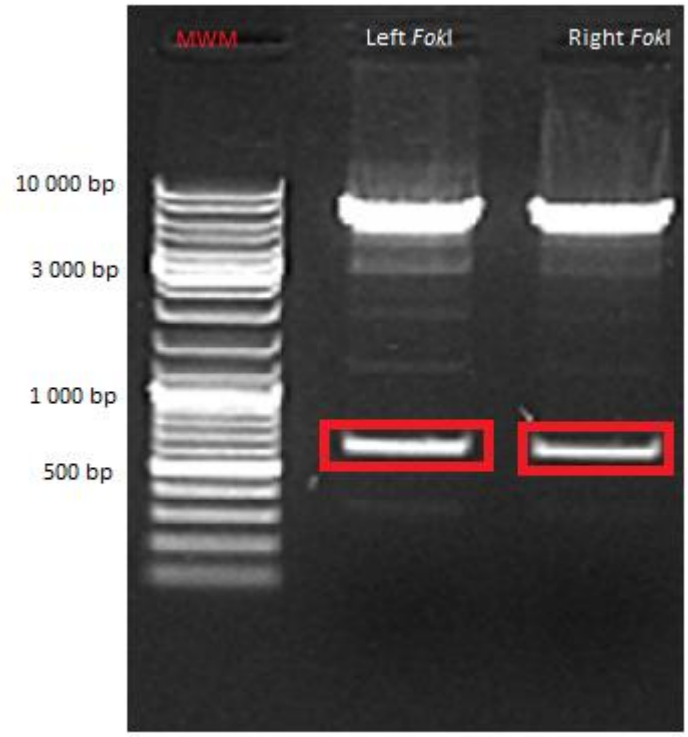

Figure 5.4: One percent agarose gel electrophoresis of plasmids encoding heterodimeric *Fok*I nuclease.

*Apa*I and *Bam*HI restriction digestion generated two bands, 5 679 bp and 601 bp in size. The bottom bands (indicated in red) were excised and purified. (MWM: molecular weight marker, O'GeneRuler 1 kb DNA Ladder, Thermo Scientific, CA, USA).

5.1.4 Left and right *Fok*I multiple protein sequence alignment

Reference sequence (*Fok*I Left Variant domain sequence)
GSQLVKSELEEKKSELRHKLKYVPHEYIELIEIARNSTQDRILEMKVMEFFMKVYGYRGK
CL WT
GSQLVKSELEEKKSELRHKLKYVPHEYIELIEIARNSTQDRILEMKVMEFFMKVYGYRGK
SL WT
GSQLVKSELEEKKSELRHKLKYVPHEYIELIEIARNSTQDRILEMKVMEFFMKVYGYRGK
CL Variant
GSQLVKSELEEKKSELRHKLKYVPHEYIELIEIARNSTQDRILEMKVMEFFMKVYGYRGK
SL Variant
GSQLVKSELEEKKSELRHKLKYVPHEYIELIEIARNSTQDRILEMKVMEFFMKVYGYRGK

Reference sequence (*Fok*I Left Variant domain sequence)
HLGGSRKPDGAIYTVGSPIDYGVIVDTKAYSGGYNLPIGQADEMERYVEENQTRNKHANP
CL WT
HLGGSRKPDGAIYTVGSPIDYGVIVDTKAYSGGYNLPIGQADEMQRYVEENQTRNKHINP
SL WT
HLGGSRKPDGAIYTVGSPIDYGVIVDTKAYSGGYNLPIGQADEMQRYVEENQTRNKHINP
CL Variant
HLGGSRKPDGAIYTVGSPIDYGVIVDTKAYSGGYNLPIGQADEMERYVEENQTRNKHANP
SL Variant
HLGGSRKPDGAIYTVGSPIDYGVIVDTKAYSGGYNLPIGQADEMERYVEENQTRNKHANP

Reference sequence (*Fok*I Left Variant domain sequence)
NEWWKVYPSSVTEFKFLFVSGHFKGNYKAQLTRLNHITNCNGAVLSVEELLIGGEMIKAG
CL WT
NEWWKVYPSSVTEFKFLFVSGHFKGNYKAQLTRLNHITNCNGAVLSVEELLIGGEMIKAG
SL WT
NEWWKVYPSSVTEFKFLFVSGHFKGNYKAQLTRLNHITNCNGAVLSVEELLIGGEMIKAG
CL Variant
NEWWKVYPSSVTEFKFLFVSGHFKGNYKAQLTRLNHITNCNGAVLSVEELLIGGEMIKAG
SL Variant
NEWWKVYPSSVTEFKFLFVSGHFKGNYKAQLTRLNHITNCNGAVLSVEELLIGGEMIKAG

Reference sequence (*Fok*I Left Variant domain sequence)
TLTLEEVRRKFNNGEINF*GP
CL WT
TLTLEEVRRKFNNGEINF*GP
SL WT
TLTLEEVRRKFNNGEINF*G
CL Variant
TLTLEEVRRKFNNGEINF*GP
SL Variant
TLTLEEVRRKFNNGEINF*GP

Figure 5.5: Heterodimeric left *Fok*I multiple sequence alignment.

Displayed are the aligned *Fok*I amino acid sequences from the pCMV CL/SL TALEN (WT), pCMV CL/SL TALEN (Var) plasmids compared with the reference sequence (*Fok*I Left Variant domain sequence). The mutations Q486E and I499A are indicated in purple and the WT sequences are indicated in blue.

Reference sequence (*Fok*I Right Variant domain sequence)
GSQLVKSELEEKKSELRHKLKYVPHEYIELIEIARNSTQDRILEMKVMEFFMKVYGYRGK
CR WT
GSQLVKSELEEKKSELRHKLKYVPHEYIELIEIARNSTQDRILEMKVMEFFMKVYGYRGK
SR WT
GSQLVKSELEEKKSELRHKLKYVPHEYIELIEIARNSTQDRILEMKVMEFFMKVYGYRGK
CR Variant
GSQLVKSELEEKKSELRHKLKYVPHEYIELIEIARNSTQDRILEMKVMEFFMKVYGYRGK
SR Variant
GSQLVKSELEEKKSELRHKLKYVPHEYIELIEIARNSTQDRILEMKVMEFFMKVYGYRGK

Reference sequence (*Fok*I Right Variant domain sequence)
HLGGSRKPDGAIYTVGSPIDYGVIVDTKAYSGGYNLPIGQADEMQRYVKENQTRNKHINP
CR WT
HLGGSRKPDGAIYTVGSPIDYGVIVDTKAYSGGYNLPIGQADEMQRYVEENQTRNKHINP
SR WT
HLGGSRKPDGAIYTVGSPIDYGVIVDTKAYSGGYNLPIGQADEMQRYVEENQTRNKHINP
CR Variant
HLGGSRKPDGAIYTVGSPIDYGVIVDTKAYSGGYNLPIGQADEMQRYVKENQTRNKHINP
SR Variant
HLGGSRKPDGAIYTVGSPIDYGVIVDTKAYSGGYNLPIGQADEMQRYVKENQTRNKHINP

Reference sequence (*Fok*I Right Variant domain sequence)
NEWWKVYPSSVTEFKFLFVSGHFKGNYKAQLTRLNHVTNCNGAVLSVEELLIGGEMIKAG
CR WT
NEWWKVYPSSVTEFKFLFVSGHFKGNYKAQLTRLNHITNCNGAVLSVEELLIGGEMIKAG
SR WT
NEWWKVYPSSVTEFKFLFVSGHFKGNYKAQLTRLNHITNCNGAVLSVEELLIGGEMIKAG
CR Variant
NEWWKVYPSSVTEFKFLFVSGHFKGNYKAQLTRLNHVTNCNGAVLSVEELLIGGEMIKAG
SR Variant
NEWWKVYPSSVTEFKFLFVSGHFKGNYKAQLTRLNHVTNCNGAVLSVEELLIGGEMIKAG

Reference sequence (*Fok*I Right Variant domain sequence
TLTLEEVRRKFNNGEINF*GP
CR WT
TLTLEEVRRKFNNGEINF*GP
SR WT
TLTLEEVRRKFNNGEINF*GP
CR Variant
TLTLEEVRRKFNNGEINF*GP
SR Variant
TLTLEEVRRKFNNGEINF*GP

Figure 5.6: Heterodimeric right *Fok*I multiple sequence alignment.

Displayed are the aligned *Fok*I amino acid sequences from the pCMV CR/SR TALEN (WT), pCMV CR/SR TALEN (Var) plasmids compared with the reference sequence (*Fok*I Right Variant domain sequence). The mutations E490K and I538V are indicated in purple and the WT sequences are indicated in blue.

5.1.5 Gel extraction protocol

Material required

- QIAquick® Gel Extraction Kit (Qiagen, Hilden, Germany)
- G:BOX UV transilluminator (Syngene, Cambridge, UK).

Procedure

All centrifugation steps were carried out at room temperature at maximum speed in a benchtop centrifuge. DNA bands were excised from the gel using a clean sharp blade. The excised gel pieces were weighed and 3 volumes of buffer QG was added to 1 volume of gel. This was incubated at 50 °C until the gel pieces were completely dissolved. One gel volume of isopropanol was added to the dissolved gel, vortexed and then transferred to QIAquick Spin Columns. This was centrifuged for 1 minute and the flow-through was discarded. Seven hundred and fifty microlitres of wash buffer PE was added to the columns and centrifuged for 1 minute. The flow-through was discarded and the column was centrifuged for an additional minute to remove any excess wash buffer. The column was transferred to a clean microcentrifuge tube and the DNA was eluted by adding 35 µL of dH_2O to the column (allowing it to stand at room temperature for 5 minutes to increase DNA yield) followed by centrifugation and stored at -2 °C

In the case of PCR clean-ups, 300 µL of buffer QG was added to the PCR products followed by adding 150 µL of isopropanol. This mixture was transferred to the QIAquick Spin Columns. The remaining procedure was then followed as above.

5.1.6 Ligation molar ratios

Table 5.1: Ligation of *Fok*I insert: TALE backbone

Insert	**Vector backbone**	**Molar ratio (Insert: backbone)**
Left variant *Fok*I	Left Core TALE	3:1
Right variant *Fok*I	Right Core TALE	9:1
Left variant *Fok*I	Left Surface TALE	9:1
Right variant *Fok*I	Right Surface TALE	3:1

5.1.7 Preparation and transformation of $CaCl_2$competentbacterial cells

Material required

- *Escherichia coli* cells
- Luria Bertani medium

Ten grams of tryptone, 5 g of yeast extract and 5 g of NaCl was added together in 1 L of dH_2O. This solution was autoclaved at 121 °C and 1 kg/cm^2 for 20 minutes. Luria Bertani medium was cooled and stored at room temperature.

- Ampicillin (100 mg/mL)

1000×stock (100 mg/mL) = 1 g/10 mL

∴1 g in 5mL of dH_2O and 5 mL of 100% ethanol and stored at -20 °C

- Transformation buffer

Transformation buffer was made by adding 1.4702 g of $CaCl_2.H_2O$ (100 mM), 0.3024 g of PIPES (10 mM) and 15 mL of glycerol together in 80 mL of dH_2O. The pH of this solution was adjusted to 7 and dH_2O was added up to 100 mL. This solution was autoclaved at 121 °C and 1 kg/cm^2 for 20 minutes. Transformation buffer was stored at -20 °C.

Procedure:

Twenty microlitres of *E. coli* were added into 10 mL of Luria Bertani medium and grown overnight at 37 °C in a shaking incubator. As a negative control to ensure that *E. coli* was not contaminated, 20 µL of *E. coli* was added into 10 mL of Luria Bertani medium containing ampicillin to a concentration of 100 µg/mL. Following overnight incubation, 10 mL of the bacterial culture was transferred to 150 mL of Luria Bertani medium and this was incubated at 37 °C for 4 hours in a shaking incubator. The bacterial culture was divided into three 50 mL tubes and centrifuged for 25 minutes at 2000 ×g at 4 °C. The supernatant was discarded and the pellet was resuspended in 1 mL of transformation buffer. The resuspensions were pooled together in one tube and made up to 35 mL with transformation buffer. This was incubated on ice for 30 minutes and then centrifuged for 10 minutes at 1000 ×g at 4 °C. The supernatant was discarded and the pellet was resuspended in 2 mL of transformation buffer. Smaller volumes of this solution were aliquoted and stored at -80 °C.

Transformation

Material required

- Chemically competent *E.* cells
- Luria Bertani medium containing agar (Oxoid Ltd, Hampshire, England)
- 1000× Ampicillin
- 1000× Kanamycin

1000× stock (40 mg/mL) = 0.4 g/10 mL

∴0.4 g in 10 mL of dH_2O, filter sterilised and stored at -20 °C

- Agar plates

One and a half grams of agar (Oxoid Ltd, Hampshire, England) was added to 500 mL of Luria Bertani medium solution. This solution was autoclaved at 121 °C and 1 kg/cm^2 for 20 minutes. Agar solution was left to cool for 30-45 minutes and either ampicillin or kanamycin was added to a final concentration of 100 µg/mL or 40 µg/mL, respectively. The agar solution was poured into petri dishes and left to solidify at room temperature for an hour. Plates were stored at 4 °C.

Procedure

Plasmid DNA not exceeding 10 µL was added to 100 µL of competent *E. coli* and incubated on ice for 30 minutes followed by heat shock activation at 42 °C for 2 minutes. *E. coli* were then left to recover on ice for 5 minutes prior to plating on agar plates containing Luria Bertani medium supplemented with 100 µg/mL ampicillin or 40 µg/mL kanamycin. The plates were sealed and left incubating at 37 °C overnight.

5.1.8 Small scale plasmid preparation

Material required

- EconoSpin™ All-in-One Mini Spin Columns, (Epoch Life Sciences, TX, USA).
- MX1 buffer (6.06 g Tris-HCl, 3.72g EDTA, RNaseA (100 µg/mL), pH 8.01 in 1 L)
- MX2 buffer (8 g NaOH, 10 g SDS in 1 L)
- MX3 buffer (294.5 g potassium acetate, pH 4.2 in 1 L)
- WS buffer (1.2 g Tris-HCl, 80% ethanol, pH 7.56 in 1 L)
- Bacterial culture

Procedure

Pellets were harvested from 10 mL bacterial culture by centrifuging at 10 000 ×g for 1 minute. The supernatant was discarded and 250 µL MX1 Buffer was added to the pellet and mixed by pulse-vortexing. The resuspension was transferred to a microcentrifuge tube. Two hundred and fifty microlitres of MX2 Buffer was then added to the resuspension and gently mixed by inverting the tube 5 times. This was incubated at room temperature for 5 minutes after which 350 µL of MX3 Buffer was added and gently mixed by inversion. The solution was centrifuged at 14 000 ×g for 10 minutes. The supernatant was then carefully transferred to EconoSpin™ All-in-One Mini Spin Column and centrifuged at 2000 ×g for 1 minute. The flow-through was discarded and 500 µL WS Buffer was added to the columns followed by centrifugation at 14 000 ×g for 1 minute. This step was repeated and the flow-through was discarded. An additional 1 minute spin at 14 000 ×g was repeated to remove residual buffer. The flow-through was discarded and the column was transferred to a new microcentrifuge tube. The DNA was eluted by adding 100 µL of dH_2O to the column and centrifuged at maximum speed in a benchtop centrifuge for 1 minute. DNA was stored at -20 °C.

5.1.9 Large scale plasmid preparation

Material required

- QIAGEN Plasmid Maxi Kit (Qiagen, Hilden, Germany)
- Bacterial culture

Procedure

For bulk plasmid preparation, plasmids were transformed as described in 5.1.7. One colony was selected and added to 200 mL of Luria Bertani medium containing either ampicillin or kanamycin and grown overnight at 37 °C in a shaking incubator. Pellets were harvested from 200 mL bacterial culture by centrifuging at 6000 ×g for 15 minutes at 4 °C. The supernatant was discarded and the pellet was resuspended in 10 mL of buffer P1. Ten millilitres of buffer P2 was then added to the resuspensions mixed by inversion and incubation at room temperature for 5 minutes. Ten millilitres of buffer P3 was added and mixed by inversion and centrifuged at 20 000 ×g for 30 minutes at 4 °C. During centrifugation, 10 mL of buffer QBT was added to a QIAGEN-tip 500 to equilibrate it. After centrifugation the supernatant was filtered through a cloth sieve and carefully applied to the QIAGEN-tip. The supernatant was allowed to enter the resin of the QIAGEN-tip by gravity flow. Once the supernatant completely passed through the QIAGEN-tip it was washed twice with 30 mL of buffer QC. The QIAGEN-tip was transferred to a 50 mL tube and the DNA eluted with 15 mL of QN buffer. DNA was precipitated by adding 10.5 mL of isopropanol and centrifuging at 15 000 ×g for 40 minutes at 4 °C. The supernatant was discarded and the pellet was washed in 5 mL of 70% ethanol and centrifuged at 15 000 ×g for 20 minutes at 4 °C. The supernatant was carefully discarded and the pellet air dried for 10 minutes. The pellet was then dissolved in 100 µL of dH_2O. The purity and concentration of DNA was determined by spectrophotometry.

5.2 *In vitro* experiments

5.2.1 Mycoplasma detection

Material required

- MycoAlert™ Mycoplasma Detection kit (Lonza, Basel, Switzerland)
- Cell culture

Procedure

Two millilitres of cell culture supernatant was added to a microcentrifuge tube and centrifuged at 200 ×g for 3 minutes. One hundred microlitres of the supernatant was transferred to a clean tube. One hundred microlitres of MycoAlert™ reagent was added to the supernatant and incubated at room temperature for 5 minutes. The luminescence was then measured with the Veritas™ Microplate Luminometer (Promega, WI, USA) (reading A). One hundred microlitres of MycoAlert™ substrate was added to the supernatant and this was incubated at room temperature for 10 minutes. The luminescence was again measured (reading B). The ratio of reading B/reading A was calculated with a value < 0.9 indicating no mycoplasma contamination, 0.9-1.2 being borderline and a value >1.2 being positive for mycoplasma contamination.

5.2.2 Transfection mixes

Lipofectamine® 3000

Cells were transfected 24 hours after seeding. A maximum of 2500 ng of DNA was required for the DNA-Lipid complex of a 6-well plate. Lipofectamine® 3000 and Opti-MEM (Gibco®, BRL, UK) were required to make the DNA-Lipid complex according to the volumes indicated in Table 5.2. This was incubated at room temperature for 15 minutes. Following the incubation, 250 µL of the transfection mix was added to each well. A maximum of 100 ng of DNA was required for the DNA-Lipid complex of a 96-well plate. This was incubated at room temperature for 15 minutes. Following the incubation, 10 µL of the transfection mix was added to each well.

Polyethylenimine

Cells were transfected 6 hours after seeding. For the DNA-PEI complex of a 96-well plate, 3.125 µL of NaCl and dH_2O up to 6.25 µL was added to 250 ng of DNA. For the PEI dilution in a 96-well plate, 3.125 µL of PEI (10×), 5 µL of NaCl and 2.5 µL of dH_2O was mixed and added to the DNA-PEI complex. This was incubated at room temperature for 20 minutes. Following the incubation, 12.75 µL of the transfection mix was added to each well.

Table 5.2: Lipofectamine® 3000 Transfection mix

	DNA-Lipid complex per well			**Lipofectamine® 3000 dilution Volume per well**			
Culture vessel	DNA (ng)	P3000 (µL)	Opti-MEM (µL)	Lipofectamine® 3000 (µL)	Opti-MEM (µL)	Volume (Media) (µL)	Volume (Transfection mix) (µL)
6-well	2500	5	125	7.5	125	1750	250
96-well	100	0.2	5	0.3	5	90	10

5.2.3 Immunocytochemistry

PBS was made by dissolving 1 PBS tablet (Thermo Scientific, CA, USA) in 500 mL of dH_2O. This solution was autoclaved at 121℃ and 1 kg/cm^2 for 20 minutes, cooled and stored at room temperature.

Four percent paraformaldehyde (PFA) was made by adding 4 g of PFA into 80 mL of 1× PBS. This solution was incubated at 60 ℃ and 1 M NaOH was added drop-wise until solution was clear. The solution was cooled for 30 minutes at room temperature and the pH was adjusted to 6.9 and the volume adjusted to 100 mL with 1× PBS. This was filter sterilised and stored at -20 ℃.

Triton X (0.1 %) (Sigma-Aldrich, MO, USA) was made by adding 10 µL of Triton X to 10 mL of 1× PBS.

BSA (1%) (Roche Applied Science, Mannheim, Germany) was made by adding 0.1 g of BSA to 10 mL of 1× PBS.

DAPI was made by dissolving 1 mg of DAPI into 1 mL of dH_2O. This was filter sterilised and 1× DAPI was made by diluting 1:1000 in 1× PBS

5.2.4 Immunofluorescence images from Huh7 cells

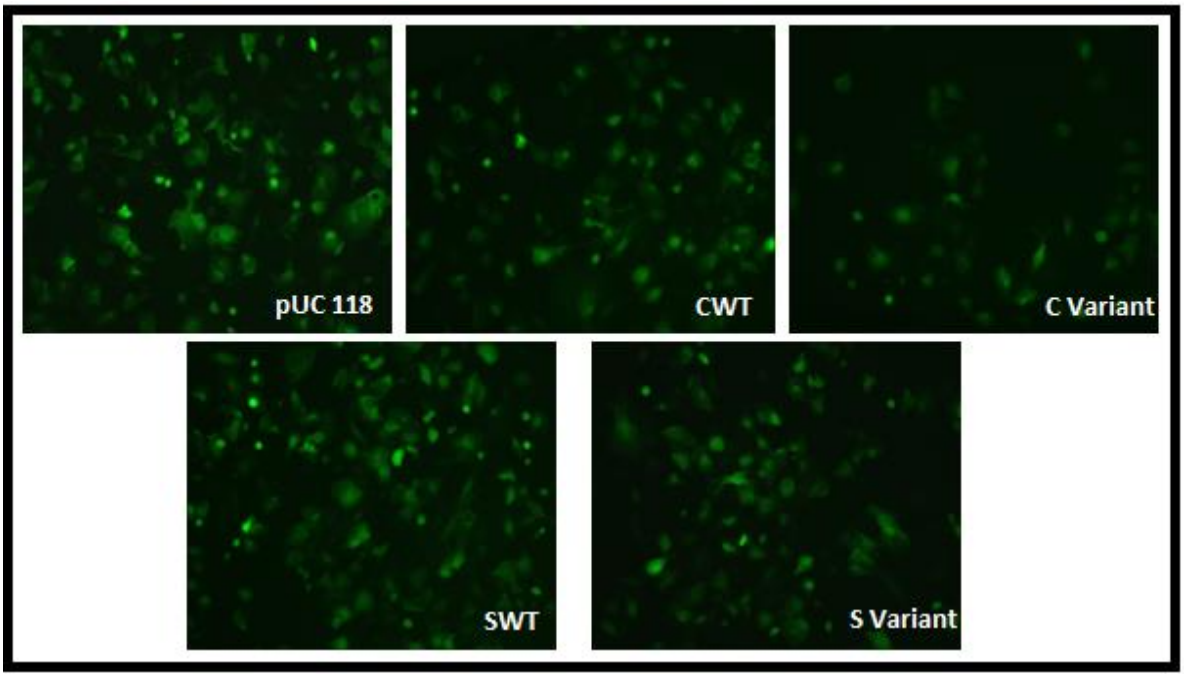

Figure 5.7: GFP visualisation in transiently transfected Huh7 cells from the enzyme-linked immunosorbent assay.

Fluorescence microscopy was used to assess transfection efficiency for the ELISA. Huh7 cells were co-transfected with300 ng of pCH-9/3091, 200 ng of pCI-neo eGFP and 1000 ng of the left and right TALEN plasmids [either pCMV TALEN (WT) or pCMV TALEN (Var)] or 2000 ng of pUC118. Cells were imaged 48 hours after transfection. Representative images of pUC118, CWT, C Variant, SWT and S Variant are shown.

5.2.5 Immunofluorescence images from HepG2.2.15 cells

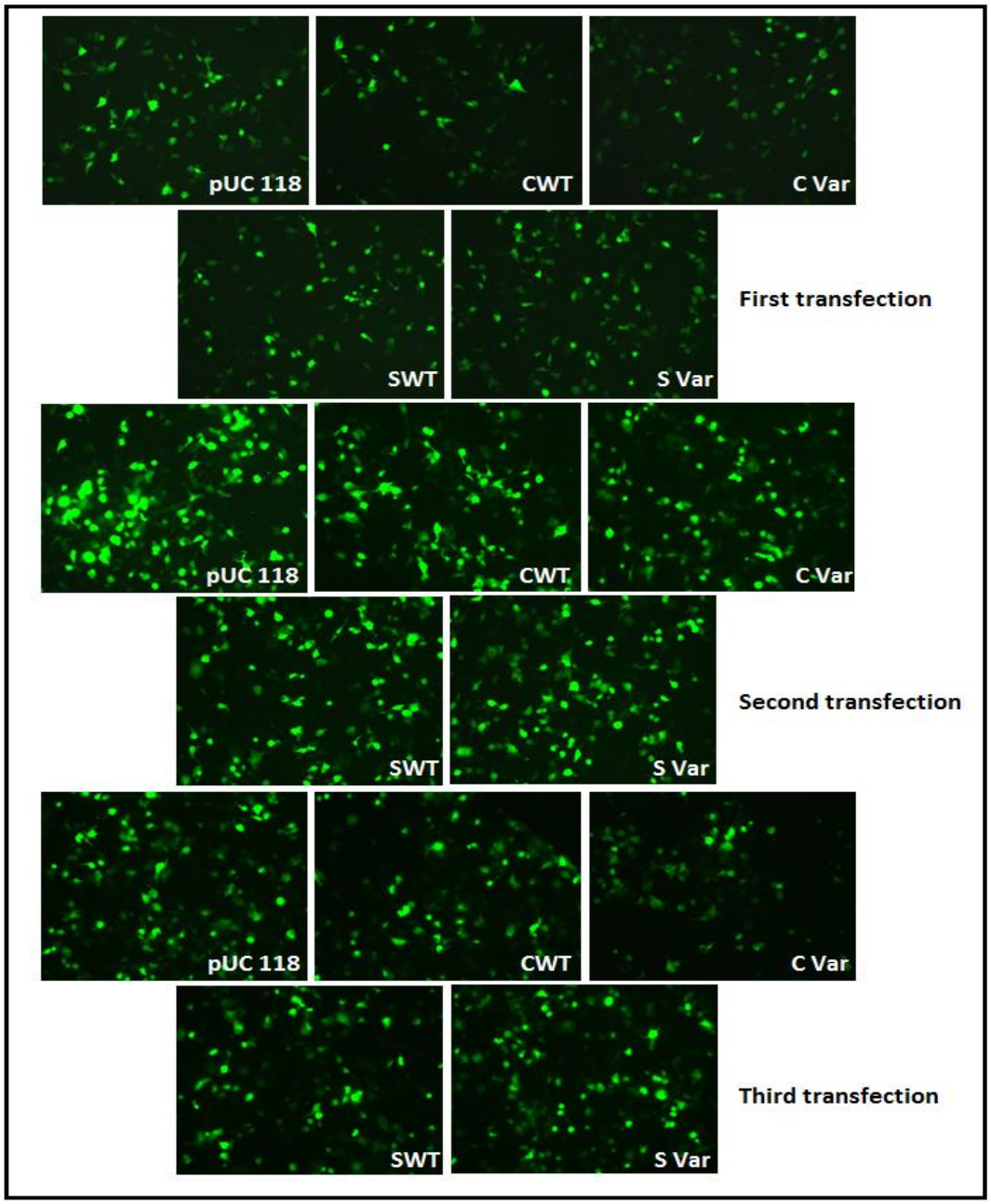

Figure 5.8: Transient co-transfections in HepG2.2.15 cells.

Fluorescence microscopy was used to assess transfection efficiency for the celI assay. HepG2.2.15 cells were co-transfected with 200 ng of pCI-neo eGFP and 1000 ng of the left and right TALEN plasmids [either pCMV TALEN (WT) or pCMV TALEN (Var)] or 2000 ng of pUC118.Cells were imaged 48 hours after transfection. Images are from the first, second and third transfections. Representative images of pUC118, CWT, C Variant, SWT and S Variant from each transfection are shown.

5.2.6 PCR carried out on samples from HepG2.2.15 cells

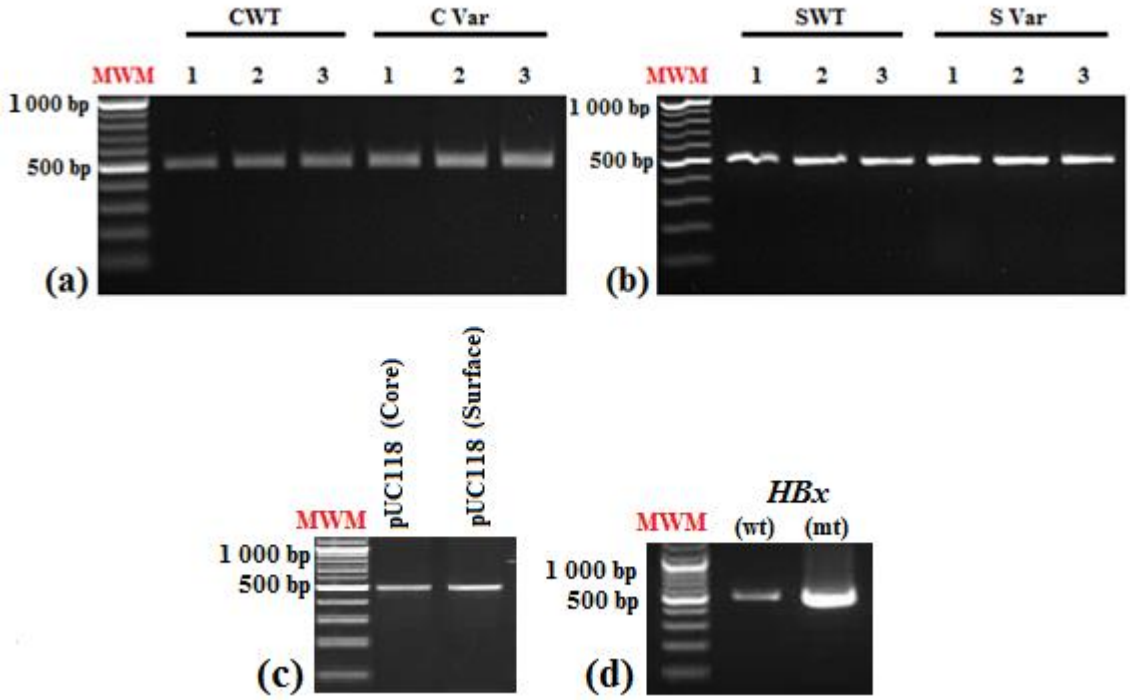

Figure 5.9: Agarose gel electrophoresis of PCR products obtained from treated HepG2.2.15 cells.

HepG2.2.15 cells were transfected with pCMV C TALENs (WT), pCMV C TALENs (Var), pCMV S TALENs (WT), and pCMV S TALENs (Var) plasmids as well as pUC118 as a negative control. Total DNA was extracted from treated cells. The sequences spanning predicted target sites for the C **(a)** and S **(b)** TALENs were amplified by PCR. Three PCR products per TALEN treatment represents the triplicate transfection. Only the C target was amplified from DNA of cells treated with the C TALENs whereas only the S target was amplified from DNA of cells treated with the S TALENs. **(c)** The C (core) and S (Surface) target was amplified from DNA of cells treated with pUC118.**(d)**Wildtype (wt) and mutant (mt) *HBx* PCR amplicons mixed in a 1:1 ratio served as the positive control. This generated amplicons of 500 bp. (MWM: molecular weight marker, O'GeneRuler 1 kb DNA Ladder, Thermo Scientific, CA, USA).

5.2.7 CelI assay carried out on PCR products from HepG2.2.15 cells

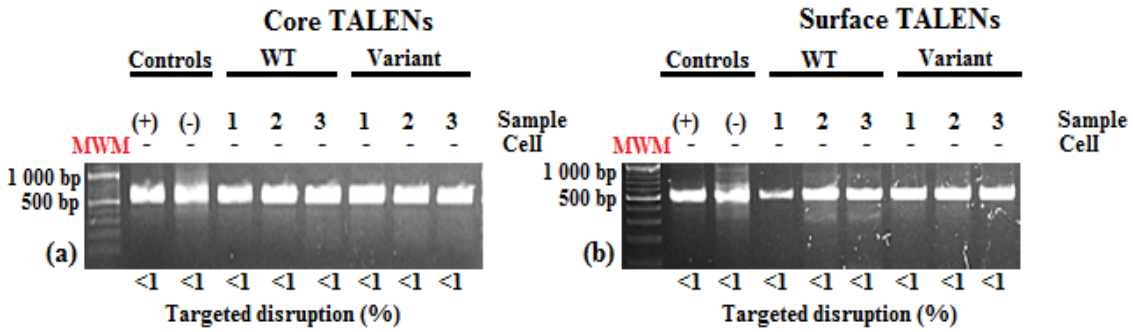

Figure 5.10: TALEN-induced site-directed targeted mutagenesis in HepG2.2.15 cells.

One microlitre of dH_2O was added to each PCR product for the CWT and C Var controls **(a)** as well as for the SWT and S Var controls **(b)**. Wildtype and mutant *HBx* PCR amplicons mixed in a 1:1 ratio served as the positive control (+) whereas PCR amplicons from pUC118-treated cells was used as a negative control (-). (MWM: molecular weight marker, O'GeneRuler 1 kb DNA Ladder, Thermo Scientific, CA, USA).

5.2.8 CelI targeted disruption calculation

Image J (Freely available from http://imagej.net/Welcome) was used to measure band intensities from targeted disruption. This was achieved by measuring intensities of a defined area (fraction).

The following equation was used to calculate targeted disruption:

$$100 \times (1 - \left(1 - \frac{fraction\ cleaved}{fraction\ cleaved + fraction\ uncleaved}\right)^{0.5})$$

5.2.9 Immunofluorescence images from HEK293 cells

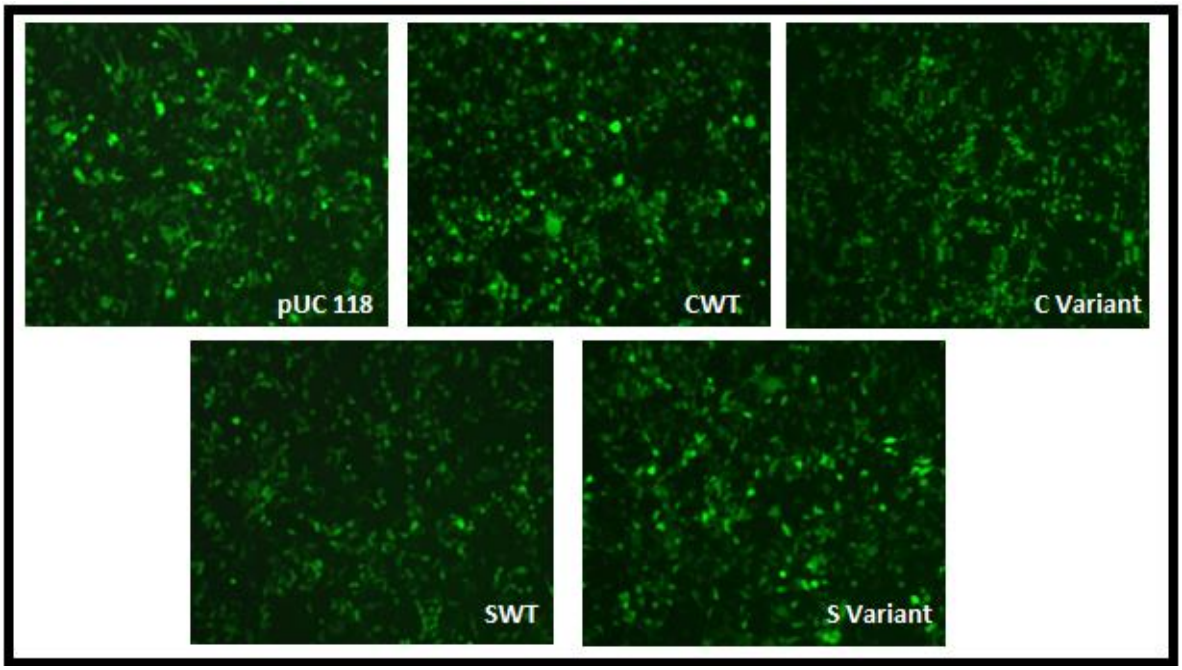

Figure 5.11: GFP efficiency in transiently transfected HEK293 cells from the cell viability assay.

Fluorescence microscopy was used to assess transfection efficiency for the cell viability assay. HEK293 cells were co-transfected with 15 ng of pCH-9/3091, 15 ng of pCI-neo eGFP and 85 ng of the left and right TALEN plasmids [either pCMV TALEN (WT) or pCMV TALEN (Var)] or 170 ng of pUC118. Cells were imaged 48 hours post transfection. Representative images of pUC118, CWT, C Variant, SWT and S Variant transfected cells are shown.

Chapter 5-Appendix

5.3 *In vivo* experiments

5.3.1 Ethics certificate

STRICTLY CONFIDENTIAL

ANIMAL ETHICS SCREENING COMMITTEE (AESC)

CLEARANCE CERTIFICATE NO. 2016/11/45/B

***APPLICANT:** Ms P Singh

SCHOOL: Molecular Medicine and Haematology
DEPARTMENT:
LOCATION:

PROJECT TITLE: Inactivation of hepatitus virus (HBV) using heterodimeric transcription activator-like effector nucleases (TALENs) delivered by hydrodynamic injection to mice livers

Number and Species

60 3-5 week old NMRI Mice

Approval was given for the use of animals for the project described above at an AESC meeting held on 2016/11/29. This approval remains valid until 2019/01/30.
Unreported changes to the application may invalidate the clearance given by the AESC

The use of these animals is subject to AESC guidelines for the use and care of animals, is limited to the procedures described in the application form and is subject to any additional conditions listed below:

None

Signed: _____ (Chairperson, AESC) Date: 31/01/2017

I am satisfied that the persons listed in this application are competent to perform the procedures therein, in terms of Section 23 (1) (c) of the Veterinary and Para-Veterinary Professions Act (19 of 1982)

Signed: _____ (Registered Veterinarian) Date: 31.01.17

cc: Supervisor: Professor P Arbuthnot
Director: CAS

Works 2000/lain0015/AESCCert.wps

*****The applicant, Miss P. Singh, applied for the ethics clearance certificate for a total of 60 mice; this included the mice I required. I was a co-applicant with Miss Singh. My name does appear under **Section A, 2.a** of the application (See next page).

Chapter 5-Appendix

SECTION A
(Undergraduate students may not complete this section)

1. Please classify this application (mark with one X only).

CLASSIFICATION	X	COURSES/TOPIC CODE	
Research (including some BSc Honours degrees and higher degrees [MSc and PhD degrees])	X	Postgraduate Research	
Postgraduate teaching (including some BSc Honours degrees and higher degrees)			
Undergraduate teaching			

2. Please give details of your current status in the box below:

2a. Applicant

Name:	Prashika Singh	Qualifications:	BHSc (Honours)
Univ. Dept:	Molecular Medicine and Haematology	Tel No: e-mail address	0117172467 prashika.singh.ps@gmail.com
Staff No:		Student No:[1]	671465

Name:	Tiffany Smith	Qualifications:	BHSc (Honours)
Univ. Dept:	Molecular Medicine and Haematology	Tel No: e-mail address	0117172465 tiffsmith7777@gmail.com
Staff No:		Student No:[1]	682336

[1] Please enter student number if you are currently registered for a higher degree at the University

2b. Co-workers
Please list in the table below the names, qualifications and duties of co-workers whether at Wits or not, directly or indirectly involved in this experiment. The names of persons responsible for performing the surgery and administering the anaesthetic should be clearly indicated if applicable.

Name	Qualification	Specific Duties	Tel No.	Registration[1]
Patrick Arbuthnot	MBBCh, PhD	Intravenous injection, bleeding, sample collection and analysis and supervision of experiments, handling of scheduled drugs.	0117172365	HPCSA
Abdullah Ely	PhD	Intravenous injection, bleeding, sample collection and analysis and supervision of experiments	0117172561	SAVC
Betty Maepa	PhD	Bleeding, sample collection and analysis	0117172266	

[1] Please indicate if any researchers or co-workers for this protocol are registered with the Health Professions

5.3.2 Endotoxin-free large scale plasmid preparation

Material required

- Endo-Free Plasmid Maxi kit (Qiagen, Hilden, Germany)
- Bacterial culture

Procedure

Bulk endotoxin plasmid preparation was carried out similarly to the procedure described in 5.10.7. Transformation and colony selection were performed as described in 5.10.3 and 5.10.7. Pellets were harvested from 200 mL bacterial culture by centrifuging at 6000 ×g for 30 minutes at 4 °C. The supernatant was discarded and the pellet was resuspended in 10 mL of buffer P1. Ten millilitres of buffer P2 was then added to the resuspensions and vigorously inverted followed by a five minute incubation at room temperature. Ten millilitres of buffer P3 was added and mixed by vigorous inversion. This lysate was poured into the barrel of the QIAfilter Cartridge and incubated at room temperature for 10 minutes. After the incubation, 2.5 mL of buffer ER was added to the lysate. The lysate was then filtered into a clean 50 mL tube and left to incubate on ice for 30 minutes. During this incubation, 10 mL of buffer QBT was added to a QIAGEN-tip 500 column to equilibrate it. The supernatant was then left to enter the resin of the column by gravity flow. Once the supernatant completely passed through the column, 30 mL of endo-free buffer QC was added to the column, and allowed to drain by gravity flow. The wash step was repeated a second time. The DNA was eluted into a clean 50 mL tube with 15 mL of QN buffer. DNA was precipitated by adding 10.5 mL of isopropanol to the eluted DNA, mixed and centrifuged at 15 000 ×g for 40 minutes at 4 °C. The supernatant was discarded, the pellet was washed in 5 mL of Endo-free 70% ethanol and centrifuged at 15 000 ×g for 20 minutes at 4 °C. The supernatant was carefully discarded and the pellet was air dried for 10 minutes. The pellet was then dissolved in 100 µL of Endo-free buffer TE. The purity and concentration of DNA was determined by spectrophotometry. The DNA was stored at -20 °C

5.3.3 PCR carried out on samples from murine hepatocytes

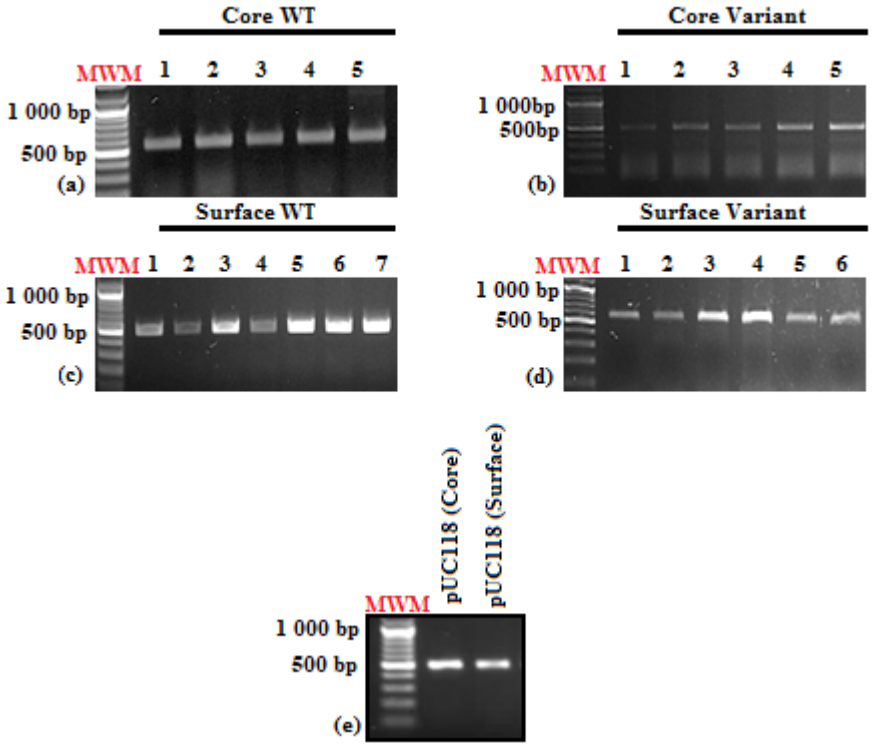

Figure 5.12: Agarose gel electrophoresis of PCR products obtained from NMRI mice.

NMRI mice were injected with pCMV C TALENs (WT), pCMV C TALENs (Var), pCMV S TALENs (WT), and pCMV S TALENs (Var) plasmids as well as pUC118 as a negative control. Total DNA was extracted from murine hepatocytes. The sequences spanning predicted target sites for the C WT **(a),** C Var **(b)**, S WT **(c)** and S Var **(d)** TALENs were amplified by PCR. Each PCR product was from a different murine sample. Only the C target was amplified from DNA of cells treated with the C TALENs whereas only the S target was amplified from DNA of cells treated with the S TALENs. **(e)**The C (Core) and S (Surface) target was amplified from murine hepatocytes treated with pUC118. This generated amplicons of 500 bp. (MWM: molecular weight marker, O'GeneRuler 1 kb DNA Ladder, Thermo Scientific, CA, USA).

5.3.4 CelI assay carried out on PCR products from murine hepatocytes

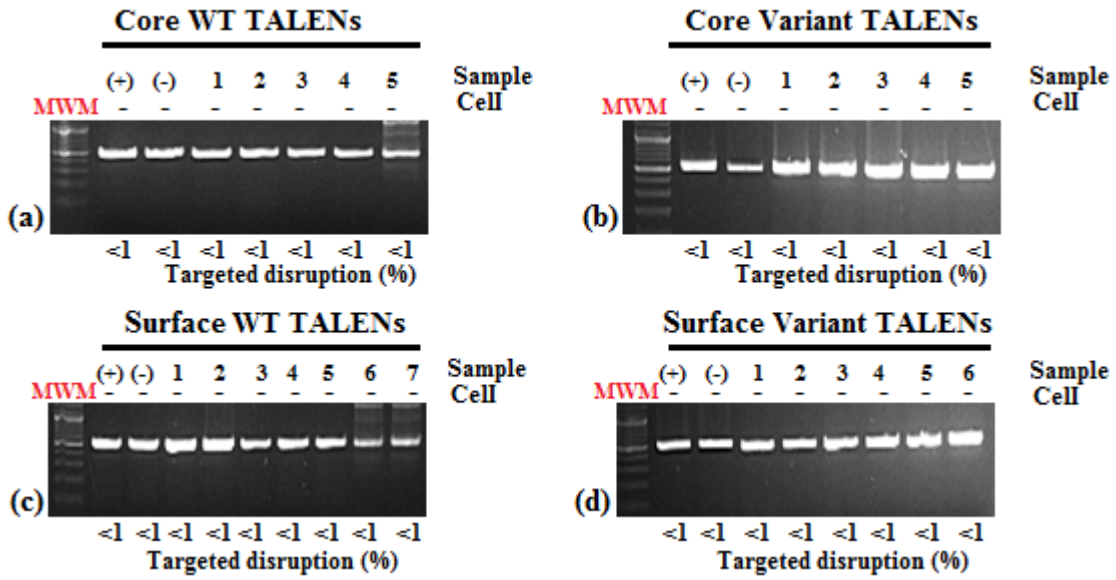

Figure 5.13: TALEN-induced site-directed targeted mutagenesis in murine hepatocytes.

One microlitre of dH_2O was added to each PCR product for the C WT **(a)**, C Var **(b)**, SWT **(c)** and S Var **(d)** controls. Wildtype and mutant *HBx* PCR amplicons mixed in a 1:1 ratio served as the positive control (+) whereas PCR amplicons from pUC118-treated mice was used as a negative control (-). (MWM: molecular weight marker, O'GeneRuler 1 kb DNA Ladder, Thermo Scientific, CA, USA).

6. References

ALEXOPOULOU, A. & KARAYIANNIS, P. 2014. HBeAg negative variants and their role in the natural history of chronic hepatitis B virus infection. *World Journal of Gastroenterology: WJG,* 20**,** 7644.

ALLWEISS, L. & DANDRI, M. 2017. The role of cccDNA in HBV maintenance. *Viruses,* 9**,** 156.

AMER, M. H. 2014. Gene therapy for cancer: present status and future perspective. *Molecular and cellular therapies,* 2**,** 27.

ANDERSON, F. H., ZENG, L., ROCK, N. R. & YOSHIDA, E. M. 2000. An assessment of the clinical utility of serum ALT and AST in chronic hepatitis C. *Hepatology Research,* 18**,** 63-71.

ANDY, S. Y., CHEUNG, R. C. & KEEFFE, E. B. 2006. Hepatitis B vaccines. *Infectious Disease Clinics,* 20**,** 27-45.

BAI, F., YANO, Y., FUKUMOTO, T., TAKEBE, A., TANAKA, M., KURAMITSU, K., ANGGOROWATI, N., RINONCE, H. T., WIDASARI, D. I. & SAITO, M. 2013. Quantification of pregenomic RNA and covalently closed circular DNA in hepatitis B virus-related hepatocellular carcinoma. *International journal of hepatology,* 2013.

BARRANGOU, R., FREMAUX, C., DEVEAU, H., RICHARDS, M., BOYAVAL, P., MOINEAU, S., ROMERO, D. A. & HORVATH, P. 2007. CRISPR provides acquired resistance against viruses in prokaryotes. *Science,* 315**,** 1709-1712.

BAVAND, M., FEITELSON, M. & LAUB, O. 1989. The hepatitis B virus-associated reverse transcriptase is encoded by the viral pol gene. *Journal of virology,* 63**,** 1019-1021.

BECK, J. & NASSAL, M. 2007. Hepatitis B virus replication. *World journal of gastroenterology: WJG,* 13**,** 48.

BERNAL, W., AUZINGER, G., DHAWAN, A. & WENDON, J. 2010. Acute liver failure. *The Lancet,* 376**,** 190-201.

BERRIDGE, M. V., HERST, P. M. & TAN, A. S. 2005. Tetrazolium dyes as tools in cell biology: new insights into their cellular reduction. *Biotechnology annual review,* 11**,** 127-152.

BEUMER, K., BHATTACHARYYA, G., BIBIKOVA, M., TRAUTMAN, J. K. & CARROLL, D. 2006. Efficient gene targeting in Drosophila with zinc-finger nucleases. *Genetics,* 172**,** 2391-2403.

BLOOM, K., ELY, A., MUSSOLINO, C., CATHOMEN, T. & ARBUTHNOT, P. 2013. Inactivation of hepatitis B virus replication in cultured cells and in vivo with engineered transcription activator-like effector nucleases. *Molecular Therapy,* 21**,** 1889-1897.

BOCH, J. & BONAS, U. 2010. Xanthomonas AvrBs3 family-type III effectors: discovery and function. *Annual review of phytopathology,* 48.

BOCH, J., SCHOLZE, H., SCHORNACK, S., LANDGRAF, A., HAHN, S., KAY, S., LAHAYE, T., NICKSTADT, A. & BONAS, U. 2009. Breaking the code of DNA binding specificity of TAL-type III effectors. *Science,* 326**,** 1509-1512.

BONAMASSA, B., HAI, L. & LIU, D. 2011. Hydrodynamic gene delivery and its applications in pharmaceutical research. *Pharmaceutical research,* 28**,** 694-701.

BOOHER, N. J. & BOGDANOVE, A. J. 2014. Tools for TAL effector design and target prediction. *Methods,* 69**,** 121-127.

BRUNETTI-PIERRI, N., STAPLETON, G. E., PALMER, D. J., ZUO, Y., MANE, V. P., FINEGOLD, M. J., BEAUDET, A. L., LELAND, M. M., MULLINS, C. E. & NG, P.

2007. Pseudo-hydrodynamic delivery of helper-dependent adenoviral vectors into non-human primates for liver-directed gene therapy. *Molecular Therapy,* 15**,** 732-740.

BUDKER, V., ZHANG, G., KNECHTLE, S. & WOLFF, J. 1996. Naked DNA delivered intraportally expresses efficiently in hepatocytes. *Gene therapy,* 3**,** 593-598.

CAI, D., MILLS, C., YU, W., YAN, R., ALDRICH, C. E., SAPUTELLI, J. R., MASON, W. S., XU, X., GUO, J.-T. & BLOCK, T. M. 2012. Identification of disubstituted sulfonamide compounds as specific inhibitors of hepatitis B virus covalently closed circular DNA formation. *Antimicrobial agents and chemotherapy,* 56**,** 4277-4288.

CERMAK, T., DOYLE, E. L., CHRISTIAN, M., WANG, L., ZHANG, Y., SCHMIDT, C., BALLER, J. A., SOMIA, N. V., BOGDANOVE, A. J. & VOYTAS, D. F. 2011. Efficient design and assembly of custom TALEN and other TAL effector-based constructs for DNA targeting. *Nucleic acids research***,** gkr218.

CHANG, J., GUO, F., ZHAO, X. & GUO, J.-T. 2014. Therapeutic strategies for a functional cure of chronic hepatitis B virus infection. *Acta Pharmaceutica Sinica B,* 4**,** 248-257.

CHEN, J., ZHANG, W., LIN, J., WANG, F., WU, M., CHEN, C., ZHENG, Y., PENG, X., LI, J. & YUAN, Z. 2014. An efficient antiviral strategy for targeting hepatitis B virus genome using transcription activator-like effector nucleases. *Molecular Therapy,* 22**,** 303-311.

CHISARI, F., PINKERT, C., MILICH, D., FILIPPI, P., MCLACHLAN, A., PALMITER, R. & BRINSTER, R. 1985. A transgenic mouse model of the chronic hepatitis B surface antigen carrier state. *Science,* 230**,** 1157-1160.

CHIU, Y.-M., LAI, M.-S. & CHAN, K. A. 2017. Assessing risk of liver enzyme elevation in patients with immune-mediated diseases and different hepatitis B virus serostatus receiving anti-TNF agents: a nested case-control study. *Arthritis research & therapy,* 19**,** 214.

CHRISTIAN, M., CERMAK, T., DOYLE, E. L., SCHMIDT, C., ZHANG, F., HUMMEL, A., BOGDANOVE, A. J. & VOYTAS, D. F. 2010. Targeting DNA double-strand breaks with TAL effector nucleases. *Genetics,* 186**,** 757-761.

CHURIN, Y., RODERFELD, M. & ROEB, E. 2015. Hepatitis B virus large surface protein: function and fame. *Hepatobiliary surgery and nutrition,* 4**,** 1.

CLARK, D. N. & HU, J. 2015. Unveiling the roles of HBV polymerase for new antiviral strategies. *Future virology,* 10**,** 283-295.

CONG, L., ZHOU, R., KUO, Y.-C., CUNNIFF, M. & ZHANG, F. 2012. Comprehensive interrogation of natural TALE DNA-binding modules and transcriptional repressor domains. *Nature communications,* 3**,** 968.

CONNOLLY, J. 2002. Lentiviruses in gene therapy clinical research. *Gene therapy,* 9**,** 1730.

CRADICK, T. J., KECK, K., BRADSHAW, S., JAMIESON, A. C. & MCCAFFREY, A. P. 2010. Zinc-finger nucleases as a novel therapeutic strategy for targeting hepatitis B virus DNAs. *Molecular Therapy,* 18**,** 947-954.

CROAGH, C. M., DESMOND, P. V. & BELL, S. J. 2015. Genotypes and viral variants in chronic hepatitis B: A review of epidemiology and clinical relevance. *World journal of hepatology,* 7**,** 289.

D-S, C., HSU, N. & SUNG, J. 1988. A mass vaccination program in Taiwan against hepatitis B. virus infection in infants of hepatitis B surface antigen-carrier mothers. *International Journal of Gynecology & Obstetrics,* 26**,** 332-332.

DANDRI, M. & LOCARNINI, S. 2012. New insight in the pathobiology of hepatitis B virus infection. *Gut,* 61**,** i6-i17.

DANDRI, M. & PETERSEN, J. 2016. Mechanism of hepatitis B virus persistence in hepatocytes and Its carcinogenic potential. *Clinical Infectious Diseases,* 62**,** S281-S288.

DANE, D., CAMERON, C. & BRIGGS, M. 1970. Virus-like particles in serum of patients with Australia-antigen-associated hepatitis. *The lancet,* 295**,** 695-698.

References

DATTA, S., CHATTERJEE, S., VEER, V. & CHAKRAVARTY, R. 2012. Molecular biology of the hepatitis B virus for clinicians. *Journal of clinical and experimental hepatology,* 2**,** 353-365.

DAYA, S. & BERNS, K. I. 2008. Gene therapy using adeno-associated virus vectors. *Clinical microbiology reviews,* 21**,** 583-593.

DE CLERCQ, E., FÉRIR, G., KAPTEIN, S. & NEYTS, J. 2010. Antiviral treatment of chronic hepatitis B virus (HBV) infections. *Viruses,* 2**,** 1279-1305.

DECORSIÈRE, A., MUELLER, H., VAN BREUGEL, P. C., ABDUL, F., GEROSSIER, L., BERAN, R. K., LIVINGSTON, C. M., NIU, C., FLETCHER, S. P. & HANTZ, O. 2016. Hepatitis B virus X protein identifies the Smc5/6 complex as a host restriction factor. *Nature,* 531**,** 386.

DENG, D., YAN, C., WU, J., PAN, X. & YAN, N. 2014. Revisiting the TALE repeat. *Protein & cell,* 5**,** 297-306.

DOITSH, G. & SHAUL, Y. 2004. Enhancer I predominance in hepatitis B virus gene expression. *Molecular and cellular biology,* 24**,** 1799-1808.

DORIA, M., KLEIN, N., LUCITO, R. & SCHNEIDER, R. 1995. The hepatitis B virus HBx protein is a dual specificity cytoplasmic activator of Ras and nuclear activator of transcription factors. *The EMBO journal,* 14**,** 4747.

DOZIER, J. K. & DISTEFANO, M. D. 2015. Site-specific PEGylation of therapeutic proteins. *International journal of molecular sciences,* 16**,** 25831-25864.

ELROD-ERICKSON, M., ROULD, M. A., NEKLUDOVA, L. & PABO, C. O. 1996. Zif268 protein–DNA complex refined at 1.6 Å: a model system for understanding zinc finger–DNA interactions. *Structure,* 4**,** 1171-1180.

ELY, A. & ARBUTHNOT, P. 2010. Silencing hepatitis B virus replication with antiviral pri-miR shuttles generated from liver-specific Pol II promoter. Nova Publishers, New York, NY, USA.

ELY, A., MOYO, B. & ARBUTHNOT, P. 2016. Progress with developing use of gene editing to cure chronic infection with hepatitis B virus. *Molecular Therapy,* 24**,** 671-677.

FORBI, J. C., BEN-AYED, Y., XIA, G.-L., VAUGHAN, G., DROBENIUC, J., SWITZER, W. M. & KHUDYAKOV, Y. E. 2013. Disparate distribution of hepatitis B virus genotypes in four sub-Saharan African countries. *Journal of Clinical Virology,* 58**,** 59-66.

FU, Y., FODEN, J. A., KHAYTER, C., MAEDER, M. L., REYON, D., JOUNG, J. K. & SANDER, J. D. 2013. High-frequency off-target mutagenesis induced by CRISPR-Cas nucleases in human cells. *Nature biotechnology,* 31**,** 822-826.

FUNG, J., LAI, C.-L., SETO, W.-K. & YUEN, M.-F. 2011. Nucleoside/nucleotide analogues in the treatment of chronic hepatitis B. *Journal of antimicrobial chemotherapy***,** dkr388.

GAJ, T., GERSBACH, C. A. & BARBAS, C. F. 2013. ZFN, TALEN, and CRISPR/Cas-based methods for genome engineering. *Trends in biotechnology,* 31**,** 397-405.

GALLINA, A., BONELLI, F., ZENTILIN, L., RINDI, G., MUTTINI, M. & MILANESI, G. 1989. A recombinant hepatitis B core antigen polypeptide with the protamine-like domain deleted self-assembles into capsid particles but fails to bind nucleic acids. *Journal of virology,* 63**,** 4645-4652.

GAVILANES, F., GONZALEZ-ROS, J. M. & PETERSON, D. L. 1982. Structure of hepatitis B surface antigen. Characterization of the lipid components and their association with the viral proteins. *Journal of biological chemistry,* 257**,** 7770-7777.

GLEBE, D. & URBAN, S. 2007. Viral and cellular determinants involved in hepadnaviral entry. *World journal of gastroenterology: WJG,* 13**,** 22.

GRAU, J., BOCH, J. & POSCH, S. 2013. TALENoffer: genome-wide TALEN off-target prediction. *Bioinformatics,* 29**,** 2931-2932.

References

GUIDOTTI, L. G., MARTINEZ, V., LOH, Y.-T., ROGLER, C. E. & CHISARI, F. V. 1994. Hepatitis B virus nucleocapsid particles do not cross the hepatocyte nuclear membrane in transgenic mice. *Journal of virology,* 68**,** 5469-5475.

GUIDOTTI, L. G., MATZKE, B., SCHALLER, H. & CHISARI, F. V. 1995. High-level hepatitis B virus replication in transgenic mice. *Journal of virology,* 69**,** 6158-6169.

GUO, X., CHEN, P., HOU, X., XU, W., WANG, D., WANG, T.-Y., ZHANG, L., ZHENG, G., GAO, Z.-L. & HE, C.-Y. 2016. The recombined cccDNA produced using minicircle technology mimicked HBV genome in structure and function closely. *Scientific reports,* 6**,** 25552.

GUSCHIN, D. Y., WAITE, A. J., KATIBAH, G. E., MILLER, J. C., HOLMES, M. C. & REBAR, E. J. 2010. A rapid and general assay for monitoring endogenous gene modification. *Engineered Zinc Finger Proteins: Methods and Protocols***,** 247-256.

HABIG, J. W. & LOEB, D. D. 2006. Sequence identity of the direct repeats, DR1 and DR2, contributes to the discrimination between primer translocation and in situ priming during replication of the duck hepatitis B virus. *Journal of molecular biology,* 364**,** 32-43.

HAMADALNIL, Y. M. & BAKHEIT, S. 2017. Hepatitis B Virus_Surface Gene Mutations and their Clinical Implications. *Sudan Journal of Medical Sciences (SJMS),* 12**,** 101-113.

HATTON, T., ZHOU, S. & STANDRING, D. 1992. RNA-and DNA-binding activities in hepatitis B virus capsid protein: a model for their roles in viral replication. *Journal of virology,* 66**,** 5232-5241.

HOCKEMEYER, D., SOLDNER, F., BEARD, C., GAO, Q., MITALIPOVA, M., DEKELVER, R. C., KATIBAH, G. E., AMORA, R., BOYDSTON, E. A. & ZEITLER, B. 2009. Efficient targeting of expressed and silent genes in human ESCs and iPSCs using zinc-finger nucleases. *Nature biotechnology,* 27**,** 851-857.

HRUSKA, J. F., CLAYTON, D., RUBENSTEIN, J. & ROBINSON, W. 1977. Structure of hepatitis B Dane particle DNA before and after the Dane particle DNA polymerase reaction. *Journal of virology,* 21**,** 666-672.

HU, J. & BOYER, M. 2006. Hepatitis B virus reverse transcriptase and ε RNA sequences required for specific interaction in vitro. *Journal of virology,* 80**,** 2141-2150.

HUS, C., RAD, N.-T. F.-T., HACKBARTH, J. S., LEE, S., MENG, X. W., VROMAN, B. T., KAUFMANN, S. H. & KARNITZ, L. M. 2004. S-peptide epitope tagging for protein purification, expression monitoring, and localization in mammalian cells. *Biotechniques,* 37**,** 835-839.

JANKELE, R. & SVOBODA, P. 2014. TAL effectors: tools for DNA targeting. *Briefings in functional genomics,* 13**,** 409-419.

JEAN-JEAN, O., LEVRERO, M., HANS, W., PERRICAUDET, M. & ROSSIGNOL, J.-M. 1989. Expression mechanism of the hepatitis B virus (HBV) C gene and biosynthesis of HBe antigen. *Virology,* 170**,** 99-106.

JINEK, M., CHYLINSKI, K., FONFARA, I., HAUER, M., DOUDNA, J. A. & CHARPENTIER, E. 2012. A programmable dual-RNA–guided DNA endonuclease in adaptive bacterial immunity. *science***,** 1225829.

JORDHEIM, L. P., DURANTEL, D., ZOULIM, F. & DUMONTET, C. 2013. Advances in the development of nucleoside and nucleotide analogues for cancer and viral diseases. *Nature reviews Drug discovery,* 12**,** 447-464.

JUTAVIJITTUM, P., YOUSUKH, A., JIVIRIYAWAT, Y., KUNACHIWA, W. & TORIYAMA, K. 2008. Genotypes of hepatitis B virus among children in Chiang Mai, Thailand. *Southeast Asian Journal of Tropical Medicine and Public Health,* 39**,** 394.

KANG, L., PAN, J., WU, J., HU, J., SUN, Q. & TANG, J. 2015. Anti-HBV drugs: progress, unmet needs, and new hope. *Viruses,* 7**,** 4960-4977.

References

KANN, M., SCHMITZ, A. & RABE, B. 2007. Intracellular transport of hepatitis B virus. *World journal of gastroenterology: WJG,* 13**,** 39.

KAPPUS, M. R. & STERLING, R. K. 2013. Extrahepatic manifestations of acute hepatitis B virus infection. *Gastroenterology & hepatology,* 9**,** 123.

KARAYIANNIS, P. 2012. Direct acting antivirals for the treatment of chronic viral hepatitis. *Scientifica,* 2012.

KELLY, D. 2006. Viral hepatitis B and C in children. *Journal of the Royal Society of Medicine,* 99**,** 353-357.

KENNEDY, E. M., BASSIT, L. C., MUELLER, H., KORNEPATI, A. V., BOGERD, H. P., NIE, T., CHATTERJEE, P., JAVANBAKHT, H., SCHINAZI, R. F. & CULLEN, B. R. 2015. Suppression of hepatitis B virus DNA accumulation in chronically infected cells using a bacterial CRISPR/Cas RNA-guided DNA endonuclease. *Virology,* 476**,** 196-205.

KIESSLICH, D., CRISPIM, M. A., SANTOS, C., DE LIMA FERREIRA, F., FRAIJI, N. A., KOMNINAKIS, S. V. & DIAZ, R. S. 2009. Influence of hepatitis B virus (HBV) genotype on the clinical course of disease in patients coinfected with HBV and hepatitis delta virus. *The Journal of infectious diseases***,** 1608-1611.

KIM, C.-M., KOIKE, K., SAITO, I., MIYAMURA, T. & JAY, G. 1991. HBx gene of hepatitis B virus induces liver cancer in transgenic mice. *Nature,* 351**,** 317.

KIM, H. & KIM, J.-S. 2014. A guide to genome engineering with programmable nucleases. *Nature Reviews Genetics,* 15**,** 321-334.

KIM, Y.-G., CHA, J. & CHANDRASEGARAN, S. 1996. Hybrid restriction enzymes: zinc finger fusions to Fok I cleavage domain. *Proceedings of the National Academy of Sciences,* 93**,** 1156-1160.

KLUG, A. 2010. The discovery of zinc fingers and their development for practical applications in gene regulation and genome manipulation. *Quarterly reviews of biophysics,* 43**,** 1-21.

KOVACSICS, D. & RAPER, J. 2014. Transient expression of proteins by hydrodynamic gene delivery in mice. *Journal of visualized experiments: JoVE*.

KRAMVIS, A. & KEW, M. C. 2007. Epidemiology of hepatitis B virus in Africa, its genotypes and clinical associations of genotypes. *Hepatology research*, 37.

KURBANOV, F., TANAKA, Y. & MIZOKAMI, M. 2010. Geographical and genetic diversity of the human hepatitis B virus. *Hepatology Research,* 40**,** 14-30.

LAMONTAGNE, R. J., BAGGA, S. & BOUCHARD, M. J. 2016. Hepatitis B virus molecular biology and pathogenesis. *Hepatoma research,* 2**,** 163.

LANGE, A., MILLS, R. E., LANGE, C. J., STEWART, M., DEVINE, S. E. & CORBETT, A. H. 2007. Classical nuclear localization signals: definition, function, and interaction with importin α. *Journal of Biological Chemistry,* 282**,** 5101-5105.

LEE, C. M., CRADICK, T. J., FINE, E. J. & BAO, G. 2016a. Nuclease target site selection for maximizing on-target activity and minimizing off-target effects in genome editing. *Molecular Therapy,* 24**,** 475-487.

LEE, J.-H. & LEE, M.-J. 2012. Liposome-Mediated Cancer Gene Therapy: Clinical Trials and their Lessons to Stem Cell Therapy. *Bulletin of the Korean Chemical Society,* 33**,** 433-442.

LEE, J., CHUNG, J. H., KIM, H. M., KIM, D. W. & KIM, H. 2016b. Designed nucleases for targeted genome editing. *Plant biotechnology journal,* 14**,** 448-462.

LEPÈRE-DOUARD, C., TROTARD, M., LE SEYEC, J. & GRIPON, P. 2009. The first transmembrane domain of the hepatitis B virus large envelope protein is crucial for infectivity. *Journal of virology,* 83**,** 11819-11829.

LEVRERO, M., POLLICINO, T., PETERSEN, J., BELLONI, L., RAIMONDO, G. & DANDRI, M. 2009. Control of cccDNA function in hepatitis B virus infection. *Journal of hepatology,* 51**,** 581-592.

References

LIANG, T. J. 2009. Hepatitis B: the virus and disease. *Hepatology,* 49.

LIAO, S.-S., LI, R.-C., LI, H., YANG, J.-Y., ZENG, X.-J., GONG, J., WANG, S.-S., LI, Y.-P. & ZHANG, K.-L. 1999. Long-term efficacy of plasma-derived hepatitis B vaccine: a 15-year follow-up study among Chinese children. *Vaccine,* 17**,** 2661-2666.

LIAW, Y.-F., BRUNETTO, M. R. & HADZIYANNIS, S. 2010. The natural history of chronic HBV infection and geographical differences. *Antiviral therapy,* 15**,** 25.

LIEBER, M. R. 2010. The mechanism of double-strand DNA break repair by the nonhomologous DNA end-joining pathway. *Annual review of biochemistry,* 79**,** 181-211.

LIN, S.-R., YANG, H.-C., KUO, Y.-T., LIU, C.-J., YANG, T.-Y., SUNG, K.-C., LIN, Y.-Y., WANG, H.-Y., WANG, C.-C. & SHEN, Y.-C. 2014. The CRISPR/Cas9 system facilitates clearance of the intrahepatic HBV templates in vivo. *Molecular Therapy-Nucleic Acids,* 3.

LIU, B., WEN, X., HUANG, C. & WEI, Y. 2013. Unraveling the complexity of hepatitis B virus: from molecular understanding to therapeutic strategy in 50 years. *The international journal of biochemistry & cell biology,* 45**,** 1987-1996.

LUO, Z., LI, L. & RUAN, B. 2012. Impact of the implementation of a vaccination strategy on hepatitis B virus infections in China over a 20-year period. *International Journal of Infectious Diseases,* 16**,** e82-e88.

MAEPA, M. B., ELY, A., GRAYSON, W. & ARBUTHNOT, P. 2017. Sustained Inhibition of HBV Replication In Vivo after Systemic Injection of AAVs Encoding Artificial Antiviral Primary MicroRNAs. *Molecular Therapy-Nucleic Acids,* 7**,** 190-199.

MAHADY, S. E., GALE, J., MACASKILL, P., CRAIG, J. C. & GEORGE, J. 2017. Prevalence of elevated alanine transaminase in Australia and its relationship to metabolic risk factors: A cross-sectional study of 9,447 people. *Journal of gastroenterology and hepatology,* 32**,** 169-176.

MAHER, S. G., SHEIKH, F., SCARZELLO, A. J., ROMERO-WEAVER, A. L., BAKER, D. P., DONNELLY, R. P. & GAMERO, A. M. 2008. IFN-α and IFN-λ differ in their antiproliferative effects and duration of JAK/STAT signaling activity. *Cancer biology & therapy,* 7**,** 1109-1115.

MAO, Z., BOZZELLA, M., SELUANOV, A. & GORBUNOVA, V. 2008. Comparison of nonhomologous end joining and homologous recombination in human cells. *DNA repair,* 7**,** 1765-1771.

MARION, P. L. & ROBINSON, W. S. 1983. Hepadna viruses: hepatitis B and related viruses. *Current topics in microbiology and immunology.* Springer.

MCMAHON, B. J. 2009. The influence of hepatitis B virus genotype and subgenotype on the natural history of chronic hepatitis B. *Hepatology international,* 3**,** 334-342.

MCMAHON, B. J., ALWARD, W. L., HALL, D. B., HEYWARD, W. L., BENDER, T. R., FRANCIS, D. P. & MAYNARD, J. E. 1985. Acute hepatitis B virus infection: relation of age to the clinical expression of disease and subsequent development of the carrier state. *Journal of infectious diseases,* 151**,** 599-603.

MEIRELES, L. C., MARINHO, R. T. & VAN DAMME, P. 2015. Three decades of hepatitis B control with vaccination. *World journal of hepatology,* 7**,** 2127.

MENDY, M., WELZEL, T., LESI, O., HAINAUT, P., HALL, A., KUNIHOLM, M., MCCONKEY, S., GOEDERT, J., KAYE, S. & ROWLAND-JONES, S. 2010. Hepatitis B viral load and risk for liver cirrhosis and hepatocellular carcinoma in The Gambia, West Africa. *Journal of viral hepatitis,* 17**,** 115-122.

MERKERT, S. & MARTIN, U. 2016. Targeted genome engineering using designer nucleases: State of the art and practical guidance for application in human pluripotent stem cells. *Stem cell research,* 16**,** 377-386.

References

MEULEMAN, P. & LEROUX-ROELS, G. 2008. The human liver-uPA-SCID mouse: a model for the evaluation of antiviral compounds against HBV and HCV. *Antiviral research,* 80**,** 231-238.

MEULEMAN, P., LIBBRECHT, L., DE VOS, R., DE HEMPTINNE, B., GEVAERT, K., VANDEKERCKHOVE, J., ROSKAMS, T. & LEROUX-ROELS, G. 2005. Morphological and biochemical characterization of a human liver in a uPA-SCID mouse chimera. *Hepatology,* 41**,** 847-856.

MHAMDI, M., FUNK, A., HOHENBERG, H., WILL, H. & SIRMA, H. 2007. Assembly and budding of a hepatitis B virus is mediated by a novel type of intracellular vesicles. *Hepatology,* 46**,** 95-106.

MIAN, A., MCCORMACK, W. M., MANE, V., KLEPPE, S., NG, P., FINEGOLD, M., O'BRIEN, W. E., RODGERS, J. R., BEAUDET, A. L. & LEE, B. 2004. Long-term correction of ornithine transcarbamylase deficiency by WPRE-mediated overexpression using a helper-dependent adenovirus. *Molecular Therapy,* 10**,** 492-499.

MILICH, D. R., JONES, J. E., HUGHES, J. L., PRICE, J., RANEY, A. K. & MCLACHLAN, A. 1990. Is a function of the secreted hepatitis B e antigen to induce immunologic tolerance in utero? *Proceedings of the National Academy of Sciences,* 87**,** 6599-6603.

MILLER, J., MCLACHLAN, A. & KLUG, A. 1985. Repetitive zinc-binding domains in the protein transcription factor IIIA from Xenopus oocytes. *The EMBO journal,* 4**,** 1609-1614.

MILLER, J. C., HOLMES, M. C., WANG, J., GUSCHIN, D. Y., LEE, Y.-L., RUPNIEWSKI, I., BEAUSEJOUR, C. M., WAITE, A. J., WANG, N. S. & KIM, K. A. 2007. An improved zinc-finger nuclease architecture for highly specific genome editing. *Nature biotechnology,* 25**,** 778-785.

MILLER, J. C., ZHANG, L., XIA, D. F., CAMPO, J. J., ANKOUDINOVA, I. V., GUSCHIN, D. Y., BABIARZ, J. E., MENG, X., HINKLEY, S. J. & LAM, S. C. 2015. Improved specificity of TALE-based genome editing using an expanded RVD repertoire. *Nature methods,* 12**,** 465-471.

MOHANRAJU, P., MAKAROVA, K. S., ZETSCHE, B., ZHANG, F., KOONIN, E. V. & VAN DER OOST, J. 2016. Diverse evolutionary roots and mechanistic variations of the CRISPR-Cas systems. *Science,* 353**,** aad5147.

MOORE, R., CHANDRAHAS, A. & BLERIS, L. 2014. Transcription activator-like effectors: a toolkit for synthetic biology. *ACS synthetic biology,* 3**,** 708-716.

MORBITZER, R., ELSAESSER, J., HAUSNER, J. & LAHAYE, T. 2011. Assembly of custom TALE-type DNA binding domains by modular cloning. *Nucleic acids research,* 39**,** 5790-5799.

MOSCOU, M. J. & BOGDANOVE, A. J. 2009. A simple cipher governs DNA recognition by TAL effectors. *Science,* 326**,** 1501-1501.

MOWA, M. B., CROWTHER, C., ELY, A. & ARBUTHNOT, P. 2014. Inhibition of hepatitis B virus replication by helper dependent adenoviral vectors expressing artificial anti-HBV pri-miRs from a liver-specific promoter. *BioMed research international,* 2014.

MUSSOLINO, C., ALZUBI, J., FINE, E. J., MORBITZER, R., CRADICK, T. J., LAHAYE, T., BAO, G. & CATHOMEN, T. 2014. TALENs facilitate targeted genome editing in human cells with high specificity and low cytotoxicity. *Nucleic acids research,* 42**,** 6762-6773.

MUSSOLINO, C., MORBITZER, R., LÜTGE, F., DANNEMANN, N., LAHAYE, T. & CATHOMEN, T. 2011. A novel TALE nuclease scaffold enables high genome editing activity in combination with low toxicity. *Nucleic acids research,* 39**,** 9283-9293.

NAKABORI, T., HIKITA, H., MURAI, K., NOZAKI, Y., KAI, Y., MAKINO, Y., SAITO, Y., TANAKA, S., WADA, H. & EGUCHI, H. 2016. Sodium taurocholate

cotransporting polypeptide inhibition efficiently blocks hepatitis B virus spread in mice with a humanized liver. *Scientific reports,* 6**,** 27782.

NASSAL, M. 2008. Hepatitis B viruses: reverse transcription a different way. *Virus research,* 134**,** 235-249.

NASSAL, M., JUNKER-NIEPMANN, M. & SCHALLER, H. 1990. Translational inactivation of RNA function: discrimination against a subset of genomic transcripts during HBV nucleocapsid assembly. *Cell,* 63**,** 1357-1363.

NAYEROSSADAT, N., MAEDEH, T. & ALI, P. A. 2012. Viral and nonviral delivery systems for gene delivery. *Advanced biomedical research,* 1.

NEMUDRYI, A., VALETDINOVA, K., MEDVEDEV, S. & ZAKIAN, S. 2014. TALEN and CRISPR/Cas genome editing systems: tools of discovery. *Acta Naturae (англоязычная версия),* 6.

NEWBOLD, J. E., XIN, H., TENCZA, M., SHERMAN, G., DEAN, J., BOWDEN, S. & LOCARNINI, S. 1995. The covalently closed duplex form of the hepadnavirus genome exists in situ as a heterogeneous population of viral minichromosomes. *Journal of virology,* 69**,** 3350-3357.

OZKAL-BAYDIN, P. 2014. How did hepatitis B virus effect the host genome in the last decade? *World journal of hepatology,* 6**,** 851.

PATTANAYAK, V., GUILINGER, J. P. & LIU, D. R. 2014. Determining the specificities of TALENs, Cas9, and other genome editing enzymes. *Methods in enzymology,* 546**,** 47.

PATTANAYAK, V., RAMIREZ, C. L., JOUNG, J. K. & LIU, D. R. 2011. Revealing off-target cleavage specificities of zinc-finger nucleases by in vitro selection. *Nature methods,* 8**,** 765-770.

PLATANIAS, L. C. 2005. Mechanisms of type-I-and type-II-interferon-mediated signalling. *Nature Reviews Immunology,* 5**,** 375-386.

PROVASI, E., GENOVESE, P., LOMBARDO, A., MAGNANI, Z., LIU, P.-Q., REIK, A., CHU, V., PASCHON, D. E., ZHANG, L. & KUBALL, J. 2012. Editing T cell specificity towards leukemia by zinc finger nucleases and lentiviral gene transfer. *Nature medicine,* 18**,** 807-815.

RABE, B., GLEBE, D. & KANN, M. 2006. Lipid-mediated introduction of hepatitis B virus capsids into nonsusceptible cells allows highly efficient replication and facilitates the study of early infection events. *Journal of virology,* 80**,** 5465-5473.

RAMAMOORTH, M. & NARVEKAR, A. 2015. Non viral vectors in gene therapy-an overview. *Journal of clinical and diagnostic research: JCDR,* 9**,** GE01.

RAMIREZ, C. L., FOLEY, J. E., WRIGHT, D. A., MÜLLER-LERCH, F., RAHMAN, S. H., CORNU, T. I., WINFREY, R. J., SANDER, J. D., FU, F. & TOWNSEND, J. A. 2008. Unexpected failure rates for modular assembly of engineered zinc fingers. *Nature methods,* 5**,** 374.

REHERMANN, B., FERRARI, C., PASQUINELLI, C. & CHISARI, F. V. 1996. The hepatitis B virus persists for decades after patients' recovery from acute viral hepatitis despite active maintenance of a cytotoxic T–lymphocyte response. *Nature medicine,* 2**,** 1104.

REHMAN, Z., FAHIM, A. & SADIA, H. 2015. Deciphering the mystery of hepatitis B virus receptors: A historical perspective. *Virusdisease,* 26**,** 97-104.

REVILL, P. & LOCARNINI, S. 2016. Antiviral strategies to eliminate hepatitis B virus covalently closed circular DNA (cccDNA). *Current opinion in pharmacology,* 30**,** 144-150.

REYON, D., TSAI, S. Q., KHAYTER, C., FODEN, J. A., SANDER, J. D. & JOUNG, J. K. 2012. FLASH assembly of TALENs for high-throughput genome editing. *Nature biotechnology,* 30**,** 460-465.

References

RIEGER, A. & NASSAL, M. 1996. Specific hepatitis B virus minus-strand DNA synthesis requires only the 5'encapsidation signal and the 3'-proximal direct repeat DR1. *Journal of virology,* 70**,** 585-589.

ROGERS, J. M., BARRERA, L. A., REYON, D., SANDER, J. D., KELLIS, M., JOUNG, J. K. & BULYK, M. L. 2015. Context influences on TALE–DNA binding revealed by quantitative profiling. *Nature communications,* 6**,** 7440.

SANDER, J. D. & JOUNG, J. K. 2014. CRISPR-Cas systems for editing, regulating and targeting genomes. *Nature biotechnology,* 32**,** 347-355.

SCHMITZ, A., SCHWARZ, A., FOSS, M., ZHOU, L., RABE, B., HOELLENRIEGEL, J., STOEBER, M., PANTÉ, N. & KANN, M. 2010. Nucleoporin 153 arrests the nuclear import of hepatitis B virus capsids in the nuclear basket. *PLoS pathogens,* 6**,** e1000741.

SCHREIER, H. 1994. The new frontier: gene and oligonucleotide therapy. *Pharmaceutica Acta Helvetiae,* 68**,** 145-159.

SCHREINER, S. & NASSAL, M. 2017. A Role for the Host DNA Damage Response in Hepatitis B Virus cccDNA Formation—and Beyond? *Viruses,* 9**,** 125.

SEEGER, C. & MASON, W. S. 2000. Hepatitis B virus biology. *Microbiology and Molecular Biology Reviews,* 64**,** 51-68.

SEEGER, C. & MASON, W. S. 2015. Molecular biology of hepatitis B virus infection. *Virology,* 479**,** 672-686.

SHMAKOV, S., ABUDAYYEH, O. O., MAKAROVA, K. S., WOLF, Y. I., GOOTENBERG, J. S., SEMENOVA, E., MINAKHIN, L., JOUNG, J., KONERMANN, S. & SEVERINOV, K. 2015. Discovery and functional characterization of diverse class 2 CRISPR-Cas systems. *Molecular cell,* 60**,** 385-397.

SM WOLD, W. & TOTH, K. 2013. Adenovirus vectors for gene therapy, vaccination and cancer gene therapy. *Current gene therapy,* 13**,** 421-433.

SPEARMAN, C. & SONDERUP, M. W. 2014. Preventing hepatitis B and hepatocellular carcinoma in South Africa: The case for a birth-dose vaccine. *SAMJ: South African Medical Journal,* 104**,** 610-612.

SUHAIL, M., ABDEL-HAFIZ, H., ALI, A., FATIMA, K., DAMANHOURI, G. A., AZHAR, E., CHAUDHARY, A. G. & QADRI, I. 2014. Potential mechanisms of hepatitis B virus induced liver injury. *World Journal of Gastroenterology: WJG,* 20**,** 12462.

SUNBUL, M. 2014. Hepatitis B virus genotypes: global distribution and clinical importance. *World journal of gastroenterology: WJG,* 20**,** 5427.

SZCZEPEK, M., BRONDANI, V., BÜCHEL, J., SERRANO, L., SEGAL, D. J. & CATHOMEN, T. 2007. Structure-based redesign of the dimerization interface reduces the toxicity of zinc-finger nucleases. *Nature biotechnology,* 25**,** 786-793.

SZMUNESS, W., STEVENS, C. E., HARLEY, E. J., ZANG, E. A., OLESZKO, W. R., WILLIAM, D. C., SADOVSKY, R., MORRISON, J. M. & KELLNER, A. 1980. Hepatitis B vaccine: demonstration of efficacy in a controlled clinical trial in a high-risk population in the United States. *New England Journal of Medicine,* 303**,** 833-841.

THOMSSEN, R., GERLICH, W., BÖTTCHER, U., STIBBE, W., LEGLER, K., WEINMANN, E., KLINGE, O. & PFEIFER, U. 1982. Preparation and testing of a hepatitis B vaccine (author's transl). *Deutsche medizinische Wochenschrift (1946),* 107**,** 125-131.

TUR-KASPA, R., SHAUL, Y., MOORE, D. D., BURK, R. D., OKRET, S., POELLINGER, L. & SHAFRITZ, D. A. 1988. The glucocorticoid receptor recognizes a specific nucleotide sequence in hepatitis B virus DNA causing increased activity of the HBV enhancer. *Virology,* 167**,** 630-633.

VOLZ, T., ALLWEISS, L., ḾBAREK, M. B., WARLICH, M., LOHSE, A. W., POLLOK, J. M., ALEXANDROV, A., URBAN, S., PETERSEN, J. & LÜTGEHETMANN, M. 2013. The entry inhibitor Myrcludex-B efficiently blocks intrahepatic virus spreading

in humanized mice previously infected with hepatitis B virus. *Journal of hepatology,* 58**,** 861-867.

VON DEGENFELD, G., WEHRMAN, T. S. & BLAU, H. M. 2009. Imaging β-galactosidase activity in vivo using sequential reporter-enzyme luminescence. *Bioluminescence: Methods and Protocols***,** 249-259.

VOUILLOT, L., THÉLIE, A. & POLLET, N. 2015. Comparison of T7E1 and surveyor mismatch cleavage assays to detect mutations triggered by engineered nucleases. *G3: Genes, Genomes, Genetics,* 5**,** 407-415.

WAH, D. A., HIRSCH, J. A., DORNER, L. F., SCHILDKRAUT, I. & AGGARWAL, A. K. 1997. Structure of the multimodular endonuclease FokI bound to DNA. *Nature,* 388**,** 97-100.

WALTER, I., FLEISCHMANN, M., KLEIN, D., MÜLLER, M., SALMONS, B., GÜNZBURG, W. H., RENNER, M. & GELBMANN, W. 2000. Rapid and sensitive detection of enhanced green fluorescent protein expression in paraffin sections by confocal laser scanning microscopy. *The Histochemical Journal,* 32**,** 99-103.

WANG, J. C.-Y., NICKENS, D. G., LENTZ, T. B., LOEB, D. D. & ZLOTNICK, A. 2014. Encapsidated hepatitis B virus reverse transcriptase is poised on an ordered RNA lattice. *Proceedings of the National Academy of Sciences,* 111**,** 11329-11334.

WEBER, N. D., STONE, D., SEDLAK, R. H., FEELIXGE, H. S. D. S., ROYCHOUDHURY, P., SCHIFFER, J. T., AUBERT, M. & JEROME, K. R. 2014. AAV-mediated delivery of zinc finger nucleases targeting hepatitis B virus inhibits active replication. *PloS one,* 9**,** e97579.

WEEKS, D. P., SPALDING, M. H. & YANG, B. 2016. Use of designer nucleases for targeted gene and genome editing in plants. *Plant biotechnology journal,* 14**,** 483-495.

WERLE–LAPOSTOLLE, B., BOWDEN, S., LOCARNINI, S., WURSTHORN, K., PETERSEN, J., LAU, G., TREPO, C., MARCELLIN, P., GOODMAN, Z. & DELANEY, W. E. 2004. Persistence of cccDNA during the natural history of chronic hepatitis B and decline during adefovir dipivoxil therapy. *Gastroenterology,* 126**,** 1750-1758.

WIEDMANN, M., LIEBERT, U. G., OESEN, U., PORST, H., WIESE, M., SCHROEDER, S., HALM, U., MÖSSNER, J. & BERR, F. 2000. Decreased immunogenicity of recombinant hepatitis B vaccine in chronic hepatitis C. *Hepatology,* 31**,** 230-234.

WU, X., KRIZ, A. J. & SHARP, P. A. 2014. Target specificity of the CRISPR-Cas9 system. *Quantitative biology,* 2**,** 59-70.

YAN, H., ZHONG, G., XU, G., HE, W., JING, Z., GAO, Z., HUANG, Y., QI, Y., PENG, B. & WANG, H. 2012. Sodium taurocholate cotransporting polypeptide is a functional receptor for human hepatitis B and D virus. *elife,* 1.

YAN, W., SMITH, C. & CHENG, L. 2013. Expanded activity of dimer nucleases by combining ZFN and TALEN for genome editing. *Scientific reports,* 3.

YANG, F., YIN, Y., WANG, F., ZHANG, L., WANG, Y. & SUN, S. 2009. An altered pattern of liver apolipoprotein AI isoforms is implicated in male chronic hepatitis B progression. *Journal of proteome research,* 9**,** 134-143.

YANG, P. L., ALTHAGE, A., CHUNG, J. & CHISARI, F. V. 2002. Hydrodynamic injection of viral DNA: a mouse model of acute hepatitis B virus infection. *Proceedings of the National Academy of Sciences,* 99**,** 13825-13830.

YI, P., CHEN, R., HUANG, Y., ZHOU, R.-R. & FAN, X.-G. 2016. Management of mother-to-child transmission of hepatitis B virus: Propositions and challenges. *Journal of Clinical Virology,* 77**,** 32-39.

YOUN, H. & CHUNG, J.-K. 2015. Modified mRNA as an alternative to plasmid DNA (pDNA) for transcript replacement and vaccination therapy. *Expert opinion on biological therapy,* 15**,** 1337-1348.

References

YU, X., JIN, L., JIH, J., SHIH, C. & ZHOU, Z. H. 2013. 3.5 Å cryoEM structure of hepatitis B virus core assembled from full-length core protein. *PLoS One,* 8**,** e69729.

YUH, C. & TING, L. 1990. The genome of hepatitis B virus contains a second enhancer: cooperation of two elements within this enhancer is required for its function. *Journal of virology,* 64**,** 4281-4287.

ZABOIKIN, M., ZABOIKINA, T., FRETER, C. & SRINIVASAKUMAR, N. 2017. Non-Homologous End Joining and Homology Directed DNA Repair Frequency of Double-Stranded Breaks Introduced by Genome Editing Reagents. *PloS one,* 12**,** e0169931.

ZHANG, M., WANG, F., LI, S., WANG, Y., BAI, Y. & XU, X. 2014. TALE: a tale of genome editing. *Progress in biophysics and molecular biology,* 114**,** 25-32.

ZHANG, Y.-Y., ZHANG, B.-H., THEELE, D., LITWIN, S., TOLL, E. & SUMMERS, J. 2003. Single-cell analysis of covalently closed circular DNA copy numbers in a hepadnavirus-infected liver. *Proceedings of the National Academy of Sciences,* 100**,** 12372-12377.